

1992

Mineralogy, geochemistry, and dispersal of opaque oxides on the continental shelf of the Cascadia margin

Kommajosyula Subramanya Ravi
Portland State University

Follow this and additional works at: https://pdxscholar.library.pdx.edu/open_access_etds



Part of the [Geochemistry Commons](#), [Geology Commons](#), and the [Mineral Physics Commons](#)

Let us know how access to this document benefits you.

Recommended Citation

Ravi, Kommajosyula Subramanya, "Mineralogy, geochemistry, and dispersal of opaque oxides on the continental shelf of the Cascadia margin" (1992). *Dissertations and Theses*. Paper 4363.
<https://doi.org/10.15760/etd.6219>

This Thesis is brought to you for free and open access. It has been accepted for inclusion in Dissertations and Theses by an authorized administrator of PDXScholar. Please contact us if we can make this document more accessible: pdxscholar@pdx.edu.

AN ABSTRACT OF THE THESIS OF Kommajosyula Subramanya Ravi
for the Master of Science in Geology presented May 26, 1992.

Title: Mineralogy, Geochemistry, and Dispersal of Opaque
Oxides on the Continental Shelf of the Cascadia
Margin.

APPROVED BY THE MEMBERS OF THE THESIS COMMITTEE:


Curt D. Peterson, Chair


Marvin H. Beeson


Ansel G. Johnson


Raymond P. Lutz

Opaque oxide minerals (ilmenite, chromite, and magnetite) in sands from the Oregon continental shelf have been studied to establish the provenance, dispersal, and grade of potential shelf placer deposits. The study area extends southward from offshore of the Columbia River in northern Oregon to the Klamath River in northern California. The opaque mineral compositions were determined by instrumental neutron activation analysis (INAA), electron microprobe and standard petrographic microscope. The

contrasting distributions of chromium-rich oxides (south of 43°) and titanium-rich oxides (north of 43°) source rocks from the Klamath Mountains (south) and the Coast Range (north) respectively. Linear regressions of specific major and trace element pairs (Co-Cr, Ta-Ti, Hf-Ti, Sc-Ti and V-Fe) demonstrate trace element partitioning into the dominant opaque mineral phases (Cr-rich chromite, Ti-rich ilmenite and the Fe-oxide magnetite). The trace element partitioning is based on valence and ionic radii constraints. Factor analysis of combined shelf-beach-river geochemical data yield distinct factors which correspond with onshore provenances. Four principal opaque mineral sources that are identified by factor analysis include: (1) a Klamath Mountain terrain in the southern shelf, (2) a Coast Range terrain in the northern shelf, (3) a north Klamath source terrain and (4) a Columbia River source, the four factors accounting for over 95% of the data variance. Contour maps containing opaque- and non-opaque mineral chemistry and Fourier grain-shape analysis of quartz grains establish contrasting dispersal patterns on the shelf. The shelf opaque- and non-opaque oxide mineral geochemistry demonstrate dominantly west-east and south-north dispersal patterns respectively. The results from grain-mineral and grain-size distributions from six samples off Cape Blanco suggest the potential for a shelf winnowing process of heavy mineral concentration, supporting an offshore origin for the

shelf heavy mineral (HM) concentrations. The shelf winnowing process, possibly forced by focusing of storm geostrophic currents around headlands could account for the association of shelf HM concentrations around major headlands.

MINERALOGY, GEOCHEMISTRY, AND DISPERSAL OF OPAQUE OXIDES
ON THE CONTINENTAL SHELF OF THE CASCADIA MARGIN

by

KOMMAJOSYULA SUBRAMANYA RAVI

A thesis submitted in partial fulfillment of the
requirements for the degree of

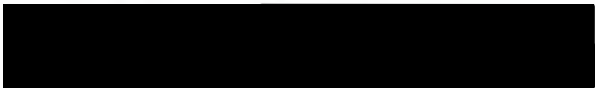
MASTER OF SCIENCE
in
GEOLOGY

Portland State University

1992

TO THE OFFICE OF GRADUATE STUDIES:

The members of the Committee approve the thesis of
Kommajosyula Subramanya Ravi presented May 26, 1992.


Curt D. Peterson, Chair


Maryin H. Beeson


Ansel G. Johnson


Raymond P. Lutz

APPROVED: 


Ansel G. Johnson, Chair, Department of Geology


C. William Savery, Vice Provost for Graduate Studies and
Research

ACKNOWLEDGEMENTS

I would like to express my sincere gratitude to Dr. Curt D. Peterson for his support, guidance and patience throughout this study. I would also like to thank his wife, Carolyn Peterson for accepting me as part of their family.

Thanks to Dr. Marvin H. Beeson, who taught me trace-element geochemistry and provided advice and encouragement on numerous occasions. I would like to thank Dr. Ansel G. Johnson who introduced me to mathematical and statistical geology. I thank Drs. M.L.Cummings, R.E.Thoms, P.E.Hammond and S.F.Burns for their enthusiasm and dedication, which have been a constant inspiration to me.

I thank Margaret Mumford and Dr. Roger Nielson of Oregon State University's College of Oceanography for providing me with bulk opaque oxide splits and for helping me with the electron microprobe techniques.

Special thanks to Drs. Dreisen, Michael Bower, Eric Freidman, Gilbert Lipschutz, Janet Murphy and Ronald Dworkin of Providence Medical Center for treating me for the tuberculosis and pulmonary embulus. Without their incredible efforts and humanitarian concerns, my life would not have been the same.

I would like to thank my parents Dr. K.V.N. Rao and Latha and to my family members DR. N. Rao and S. Ram, for their unending support and love, without which I would not have had the opportunity to pursue this degree. And lastly, I would like to thank Charles Clough for assisting with the figure drafting.

TABLE OF CONTENTS

	PAGE
ACKNOWLEDGEMENTS.....	iii
LIST OF TABLES.....	vii
LIST OF FIGURES.....	ix
CHAPTER	
I INTRODUCTION	1
II STUDY AREA	5
III REGIONAL GEOLOGY	8
Klamath Mountains.....	11
IV PREVIOUS WORK ON MARINE PLACERS	17
V METHODS	20
Sample Description	20
Sample Separation	23
Sample Encapsulation	27
Instrumental Neutron Activation-	
Analysis (INAA)	28
Electron Microprobe	30
VI RESULTS	34
INAA of Continental Shelf Deposits	34
Mineral-Grain Hydrodynamic Relations	69

	Microprobe Analysis of Shelf	
	Opaque Minerals	76
VII	DISCUSSION	87
	Shelf Opaque Dispersal Patterns (Q-mode Factor Analysis)	87
	Contour Maps Comprising Dispersal of Opaque Oxide-, Non-Opaque Minerals and Quartz Grain Rounding	98
	Relationships of the Various Hydrodynamic Models	101
	Mineral Economic Grade and Silicate Contaminants	106
VIII	CONCLUSIONS	109
	REFERENCES	113
	APPENDICES	
	A ELEMENTAL COMPOSITIONS OF BULK OPAQUE MINERAL SPLITS FROM THE SHELF BY INSTRUMENTAL NEUTRON ACTIVATION ANALYSIS.....	119
	B DETAILED FACTOR LOADINGS.....	128
	C CONTOUR MAPS	136

LIST OF TABLES

TABLE		PAGE
I	Heavy Minerals and Metals in Marine Placers of the Pacific Northwest USA	22
II	Radionuclides and INAA Parameters	31
III	Elemental Correlation Coefficients for Opaque Mineral Fraction of River, Beach, and Shelf Sands in Oregon and Northern California, 40.5-46.5 Degrees Latitude ..	47
IV	Preliminary Grain Size Frequencies of Opaque Mineral Distributions in the Sixes River, Oregon	70
V	Calculated Statistical Parameters for Magnetite, Quartz, and Bulk Samples from the Cape Blanco Shelf	74
VI	Microprobe Analysis of Averaged Elemental Compositions of Ilmenite from the selected Shelf Placer Minerals	78
VII	Microprobe Analysis of Averaged Elemental Compositions of Chromite from the selected Shelf Placer Samples	82

VIII	Microprobe Analysis of Averaged Elemental Compositions of Magnetite from the selected Shelf Placer Samples	85
IX	General Statistics for Element Abundances in Shelf Opaque Separates	88
X	Element Factor Scores for the Combined River, Beach, and Shelf Sample Set	90
XI	Factors Loadings for Four Factors of Elemental Composition	93
XII	Summary of Average Shelf Microprobe Analysis..	108

LIST OF FIGURES

FIGURE		PAGE
1.	Area of Investigation in Relation to Northwestern United States and Northeastern Pacific Ocean	6
2.	General Tectonic Map for the Subduction Regime and Geologic Provinces in the Study Area	9
3.	Potential Source Rocks of the Continental Shelf Sediments from Coastal Drainages and Interior Continental Regions of the Pacific Northwest, including the Klamath-Mountain provenance in southern Oregon and northern California and the northern Oregon Coast Ranges (Modified from Wells et al., 1984)...	10
4.	Geologic Map of Klamath Mountain Province in North western California and Southwestern Oregon (From Irvin, 1966).....	12
5.	Physiographic Divisions of western Oregon ...	15
6.	Location Map of Shelf Samples used in INAA and Electron Microprobe analysis	21
7.	Sample Separation Scheme: Preliminary sieving (250 mm) was used to screen off the rock fragments and multimineralic aggregates ...	25

8. Plot of the Major Element Chromium of Bulk Opaque Mineral Separates from the Continental Shelf as a Function of Latitude 36
9. Plot of the Major Element Titanium of Opaque Mineral Separates from the Continental Shelf as a Function of Degrees Latitude 37
10. Across-shelf Transect of Chromium and Titanium Elemental Abundance for the Samples from 41-42 Degrees Latitude 38
11. Across-shelf Transect of Chromium and Titanium Elemental Abundance for the Samples from 42-43 Degrees Latitude 39
12. Across-shelf Transect of Chromium and Titanium Elemental Abundance for the Samples from 43-44 Degrees Latitude 40
13. Across-shelf Transect of Chromium and Titanium Elemental Abundance for the Samples from 44-45 Degrees Latitude 41
14. Across-shelf Transect of Chromium and Titanium Elemental Abundance for the Samples from 45-46 Degrees Latitude 42
15. Plots of the Major Element (Fe, Cr, and Ti) Abundances as a Function of Latitude are shown for the opaque mineral separates from the shelf of placers..... 44

16.	Plots of Chromium and Cobalt Elemental Values of Opaque Mineral Oxides from the Continental Shelf	46
17.	Plots of Titanium and Hafnium Elemental Values of Opaque Mineral Oxides from the Continental Shelf	50
18.	Plots of Titanium and Scandium Elemental Values of Opaque Mineral Oxides from the Continental Shelf	51
19.	Plots of Iron and Vanadium Elemental Values of Opaque Mineral Oxides from the Continental Shelf	52
20.	Plot of Lanthanum Elemental Abundance as a Function of Degrees Latitude.....	54
21.	Plot of Cerium Elemental Abundance as a Function of Degrees Latitude	55
22.	Plot of Samarium Elemental Abundance as a Function of Degrees Latitude	56
23.	Plot of Europium Elemental Abundance as a Function of Degrees Latitude	57
24.	Plot of Ytterbium Elemental Abundance as a Function of Degrees Latitude	58
25.	Plot of Lutecium Elemental Abundance as a Function of Degrees Latitude	59
26.	Plot of Hafnium Elemental Abundance as a Function of Degrees Latitude	60

27.	Plot of Tantalum Elemental Abundance as a Function of Degrees Latitude	61
28.	Chondrite-Normalized REE Distributions in Shelf Opaque Oxide Minerals Derived from Klamath Mountain Provenance (north of 41-42 degrees latitude)	63
29.	Chondrite-Normalized REE Distributions in Shelf Opaque Oxide Minerals Derived from Coast Range Provenance (north of 43-44 degrees latitude)	64
30.	Chondrite-Normalized REE Distributions in Shelf Opaque Oxide Minerals Derived from Columbia River Provenance (north of 45-46 latitude)	65
31.	Distributions of Shelf Opaque Oxide Minerals on a La/Sm Ratio vs Latitude Diagram	66
32.	Distributions of Shelf Opaque Oxide Minerals on a La/Yb Ratio vs Latitude Diagram	67
33.	Distributions of Shelf Opaque Oxide Minerals on a Ce/Yb Ratio vs Latitude Diagram	68
34.	Location Map and Heavy Mineral Concentrations in Short Box Cores used in Mineral Grain-Size Statistics (Modified from Kulm, 1988)	73
35.	Major Elemental (Ti, Fe) Distributions in the Ilmenite Phase as a Function of Latitude...	79

36. Trace Element Contaminants in the Shelf
 Ilmenite Grains as a Function of Latitude.. 80
37. Major Elemental (Cr, Fe) Distributions in the
 Chromite Phase as a Function of Latitude... 83
38. Trace Element Contaminants in the Shelf
 Chromite Grains as a Function of Latitude.. 84
39. Major Elemental (Fe, Ti), Distributions in the
 Magnetite Phase as a Function of Latitude.. 86
40. Plot of Combined Shelf and Onshore Factor 1
 Loadings as a Function of Latitude 94
41. Plot of Combined Shelf and Onshore Factor 2
 Loadings as a Function of Latitude 95
42. Plot of Combined Shelf and Onshore Factor 3
 Loadings as a Function of Latitude 96
43. Plot of Combined Shelf and Onshore Factor 4
 Loadings as a Function of Latitude 97
44. Hydraulic Settling Equivalence Model (Komar and
 Wang, 1984; Komar, 1988) for the formation of
 heavy minerals involves process of selective
 entrainment and sorting according to their
 contrasting grain densities and sizes. The
 opaque- and non-opaque minerals are denoted by
 closed and open circles respectively 102

45. Kulm's hypothesis (1988) and Phillip's hypothesis (1979) relating to the formation of beach placers..... 104

CHAPTER I

INTRODUCTION

Heavy mineral concentrations in marine deposits, i.e., marine placers, are of interest to geologists as sources of economic minerals, and as distinct indicators of specific transport mechanisms and depositional environments. Marine placers have been investigated in beaches and continental shelves of Africa (Beiersdorf et al., 1980), India (Mallik, 1986), Australia (Kudrass, 1987), and the Atlantic (Darby, 1984) and Pacific coast (Kulm et al., 1968; Peterson and Binney, 1988) of the United States, among other regions. Heavy mineral enrichment in onshore environments can occur from a variety of potential sorting mechanisms (Rubey, 1933; Slingerland, 1977; Sallenger, 1979; Komar and Wang, 1984). However the relative importances of these sorting mechanisms in offshore environments are generally not known.

A renewed interest in the formation and economic potential of marine placers in the U.S. Pacific Northwest (PNW) region has followed recent reports of abundant ilmenite, a titanium-iron oxide, in onshore placer deposits (Peterson et al., 1987). Historically, the onshore marine placers from southern Oregon and northernmost California were mined for gold and chromite (Pardee, 1934; Twenhofel,

1943; Griggs, 1945). Preliminary analyses of selected sand samples from the Oregon shelf also indicate the presence of ilmenite in variable ratios to the remaining two oxide phases, chromite and magnetite (Kulm and Peterson, 1989). However, the aerial distribution, economic grade and origin of potential offshore marine placers from this area have yet to be fully evaluated.

Petrographic studies of the non-opaque, heavy mineral fractions of PNW shelf sands have indicated a general northward littoral transport in Late Quaternary time (Scheidegger et al., 1971; Venkatarathnam and McManus, 1973). Unfortunately, the specific sources and dispersal patterns of the opaque oxide minerals cannot be similarly studied by transmission petrography. However, geochemical analyses of ilmenite and chromite from onshore placers in southern Oregon confirm both local sources, Klamath and Coast Range terrains, and a net northward transport of these minerals during successive transgressions (Lupeke, 1980; Peterson et al., 1986). Such analyses have not yet been performed on equivalent oxide minerals from adjacent shelf deposits in the region.

Heavy minerals, i.e., mineral grain densities greater than 2.9 g cm^3 , in concentrations of 10 to 50% by weight have been identified in surface deposits of the continental shelf offshore Oregon, Washington, and northernmost California (Kulm et al., 1968; Moore and Silver, 1968;

Venkatarathnam and McManus, 1973). Several different origins have been proposed for these shelf heavy-mineral anomalies including mineral entrapment in embayments (Twenhofel, 1943), reworking of shoreline placers during successive transgressions (Chambers, 1969; Kulm, 1988), winnowing of shelf deposits by offshore currents (Phillips, 1979), and selective mineral entrainment by longshore currents (Peterson et al., 1986).

Recent work by Kulm (1988) suggested that shelf HM concentrations offshore of southern Oregon might be derived from (1) placer mineral accumulations on the beach faces with, (2) the subsequent reworking of the beach face placers during a marine transgression. He found downcore transitions from deep-water to shallow water foraminiferal assemblages, downcore increases in heavy mineral abundances, and early Holocene C^{14} dates from the shallow box cores (0.4 m penetration). Alternatively, the shelf HM accumulations might have formed from the winnowing of fine grained shelf deposits by offshore currents (Phillips, 1979). Significantly, the first of these two models for offshore placer development implies heavy mineral concentration in beach deposits with subsequent reworking during transgression. It is presently not known whether basal transgressive lag deposits, enriched in beach placer minerals, underly the offshore heavy mineral anomalies reported from the Oregon continental shelf.

The goal of the study presented here is to develop mineralogical and geochemical exploration models for potential titanium- and chromium-rich oxide placers in the continental shelf sands of an active margin. The study objectives are (1) establish the opaque mineral economic grade; (2) constrain the possible models of regional opaque mineral dispersal; (3) evaluate potential mechanisms of origins of marine placers, and (4) decipher the provenance of heavy opaque minerals. These objectives are accomplished by analysis of shelf bulk opaque oxide compositions, by instrumental neutron activation analysis (INAA), electron microprobe, and petrographic grain size statistics.

CHAPTER II

STUDY AREA

The area under investigation includes the inner- and middle-continental shelf offshore of Oregon and northernmost California, extending from 46.25° to 40.62° latitude (Figure 1). This study area represents an open coastline distance of 800 km and a continental shelf area of approximately 4×10^4 km². The shelf break at 200 m water depth varies from 80 to 120 km distance from the coastline (shelf-width). The northern Oregon Coastline is relatively straight with the few exceptions of resistant headlands and the local indentations of small bays and estuaries. By comparison the southern part of the coast is dominated by rocky headlands and short beach-fronted embayments. The continental shelf off the coast of Oregon is an active and complex sedimentary environment. New sediment is presently being reworked and deposited on the inner portions of the continental shelf while the outer shelf deposits appear to be palimpsest (Kulm et al., 1975). Kulm et al. (1975) have classified the unconsolidated sediments deposited on the Oregon continental

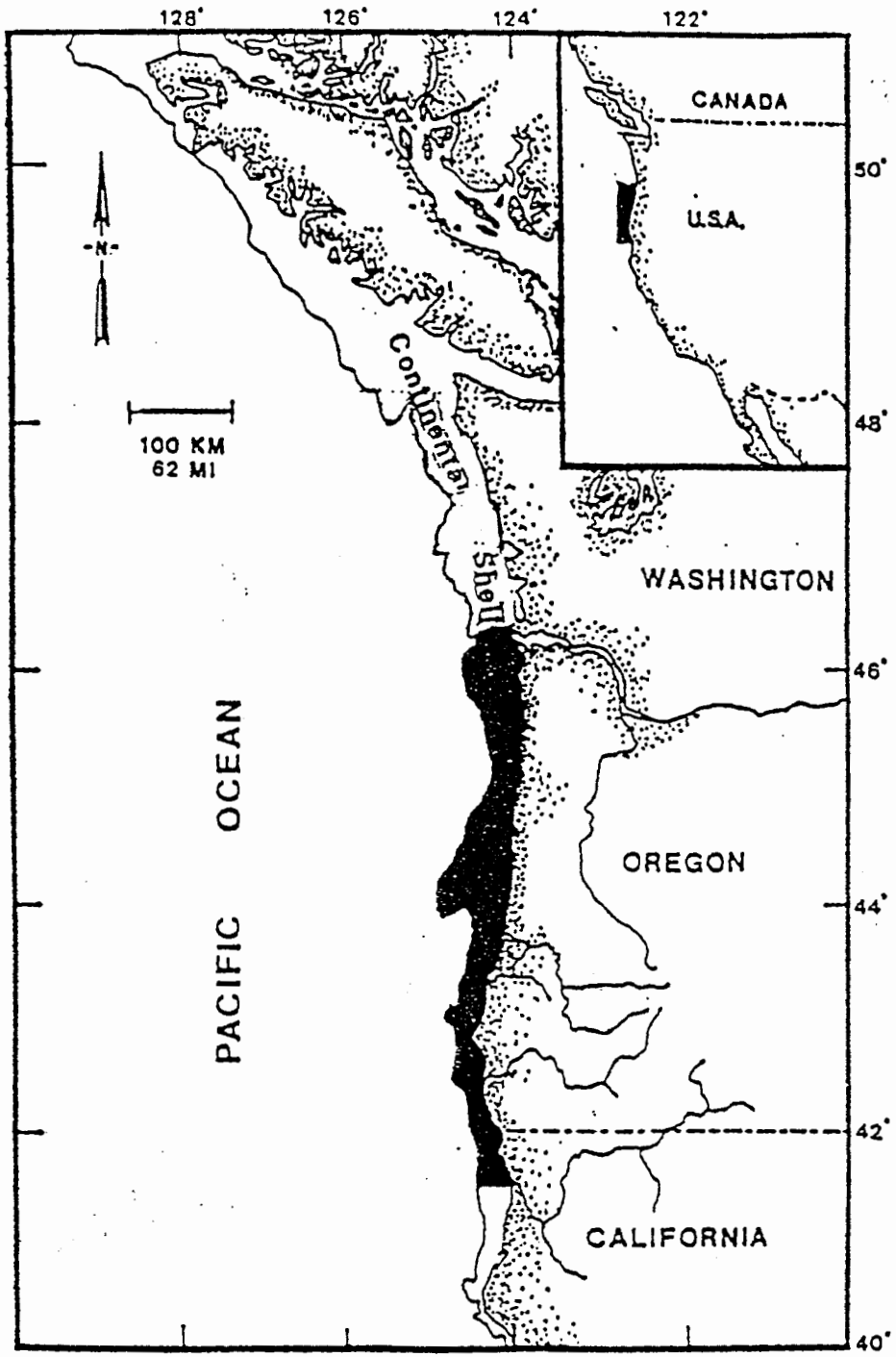


Figure 1. Area of Investigation in Relation to Northwestern United States and Northeastern Pacific Ocean.

shelf into distinct sedimentary facies: (1) a transgressive sand facies, composed of well sorted fine sand; (2) a modern mud facies consisting of silt and clay; and (3) a mixed facies of sand and mud. The surface shelf currents generally flow northward during the winter months; while bottom currents appear to move northward for most of the year (Gross and Nelson, 1966). Smith and Hopkins (1972) have measured current velocities up to 70 cm/sec at 80 m depths.

CHAPTER III

REGIONAL GEOLOGY

The tectonic setting of the Pacific Coastal States can be divided into two different active plate margins on either side of a triple junction at Cape Mendocino, California. These margins include the southern transform plate boundary of the San Andreas fault system, and the northern subduction boundary where the Gorda and Juan de Fuca plates are being subducted beneath the North American plate in the Cascadia subduction zone (Figure 2; Mooney and Weaver, 1989). Emplacements of oceanic crusts into the Cascadia continental margin occurred between 160 and 40 million years ago, and they produced north-south linear terrains comprising much of the coastal drainages.

The source rock lithology in the southern Cascadia margin is strongly controlled by convergent plate tectonics (as noted above). A variety of accretion, subduction, and obduction events since Cretaceous time has yielded a complex assortment of accreted source rock terrains (Figure 3). These terrains include the Coast Ranges (northern

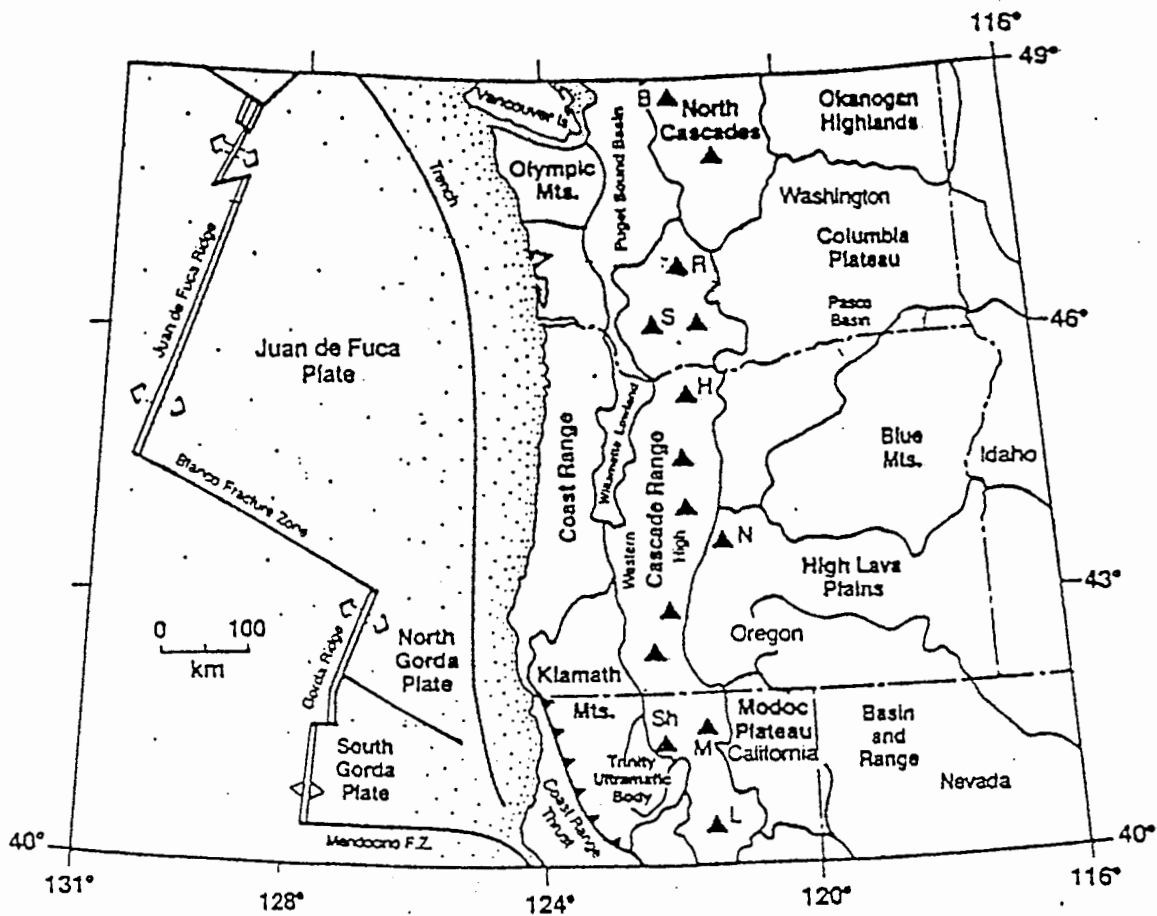


Figure 2. General Tectonic Map for the Subduction Regime and Geologic Provinces in the Study Area.

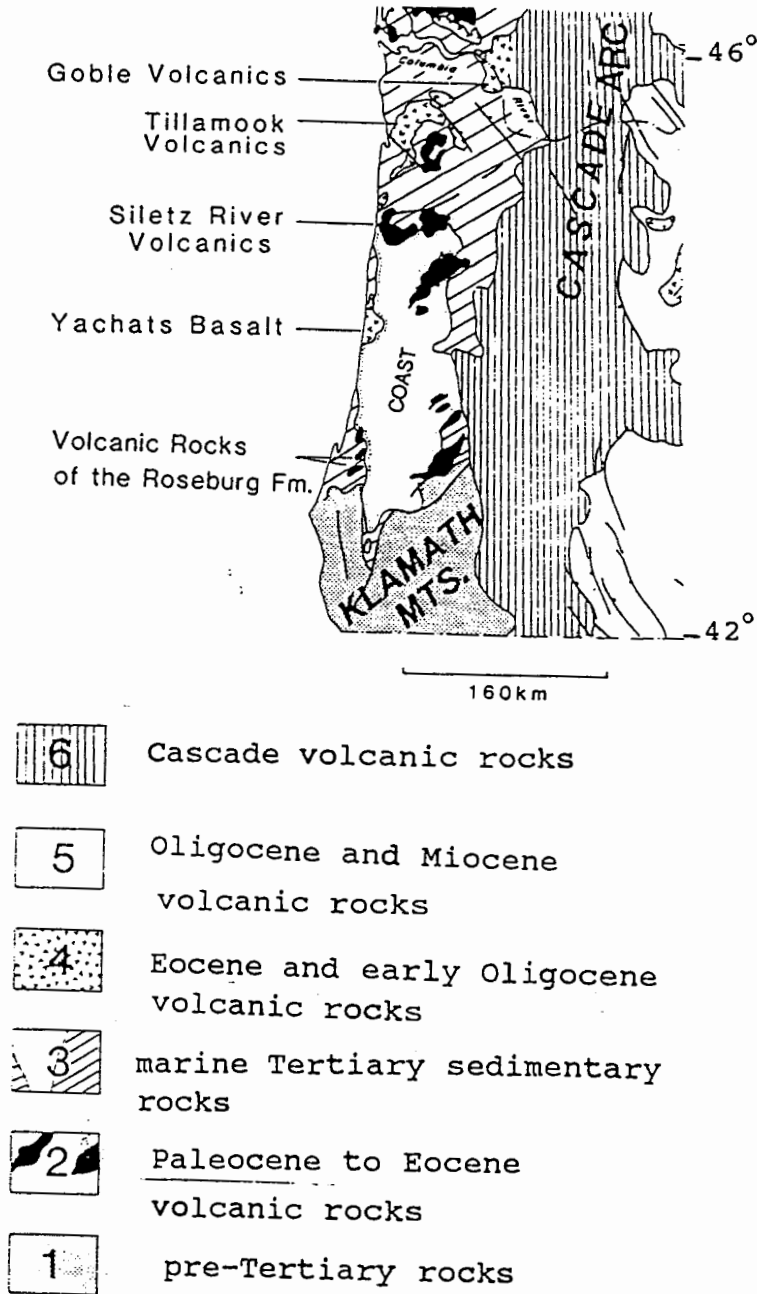


Figure 3. Potential Source Rocks of the Continental Shelf Sediments from Coastal Drainages and Interior Continental Regions of the Pacific Northwest, including the Klamath-Mountain provenance in southern Oregon and northern California and the northern Oregon Coast Ranges (Modified from Wells et al., 1984).

California, Oregon, and Washington), and the Klamath Mountains (southwestern Oregon). These 'accreted' terrains are rich in intermediate and mafic rocks, containing the opaque oxide minerals (Ramp, 1961; and Wells et al., 1984). Both river sediments and the recycling of uplifted Pleistocene marine deposits are the likely sources of these minerals to the modern marine placer deposits of the study area (Komar and Clemens, 1986).

KLAMATH MOUNTAINS

The Klamath Mountains were produced from the accretion of Mesozoic oceanic crust and the island arc fragments, emplaced via imbricate east-dipping thrust faults (Irwin, 1981). The Klamath terrain is a complex assortment of metamorphic source rocks containing Paleozoic and Mesozoic metasedimentary, metavolcanic, ultramafic, and sedimentary rocks which have been intruded by granitoid melts (Baldwin, 1964). The areal distribution of lithologies in the Klamath Mountains, define concentric and arcuate belts. These belts include the following lithologic units: the eastern Klamath, central metamorphic, western Paleozoic and Triassic, and western Jurassic (Figure 4). The early Paleozoic Trinity (ophiolite) ultramafic sheet overlies Paleozoic and Triassic metamorphic rocks in association with sedimentary and volcanic rocks of fore arc origin (Irwin, 1966).

The juxtaposed metamorphic, ultramafics, and granitic intrusions are likely to yield a complex assortment of opaque minerals.

Coast Ranges

The northern California Coast Range contains many coalescing mountains and major structural valleys, yielding high relief and sediments (Spigai, 1971). This coast range consists of two different core complexes, one composed of Franciscan rocks which are a complex Jurassic-Cretaceous eugeosynclinal assemblage, and the other composed of Early Cretaceous granitic intrusions and older metamorphic rocks (Page, 1966). These two core complexes are overlain by thick sequences of Cenozoic shelf and slope deposits which conceal most of the underlying core complexes.

The Oregon Coast Range includes both accreted volcanic rocks of probable seamount origin and post-accretion volcanic rocks. The Siletz River (Snively et al., 1968), and Tillamook Volcanics respectively, are dominantly tholeiitic and alkalic basalts, and they might reach thicknesses of 15-20 km. These evolved (differentiated) basement rocks are potentially important sources of ilmenite. Whole rock chemistries of Tillamook Highland Volcanics and Siletz River Volcanics reach up to 4% and 5-10% titanium oxide by weight, respectively (Mumford, 1988).

Cascade Mountain. The Cascade Mountains represent the volcanic arc east of the Coast Ranges. These mountains trend north-south for the entire length of the study area and are divided into two physiographic provinces, the Western Cascades and the High Cascades (Figure 5). The Western Cascades comprise lava flows (Eocene to Pliocene in age) of pyroxene andesite, pyroclastic debris, and localized occurrences of nonmarine and shallow-marine sediments. The Western Cascades portray a greater variety and a larger percentage of pyroclastic rocks than the High Cascades (Spigai, 1971). The High Cascades are predominantly pyroxene-rich andesites of Pliocene to Recent age.

Columbia River Drainage. The Columbia River Basin encompasses parts of seven states in the northwestern United States and the province of British Columbia in Canada. Major tributaries include the Snake, Salmon, and Willamette Rivers. From the Columbia River headwaters, in the Rocky Mountains, folded and faulted sedimentary, granitic, and coarse grained metamorphic rocks contribute sediment to the river system (Scheidegger et al., 1971). Much of the lower Columbia River drainage is in the Columbia River Basalt Province of Oregon and eastern Washington. However, Whetten et al. (1969) working on the heavy mineral analysis of lower channel samples of the Columbia River recognized the influence of andesitic detritus formed from the erosion of the Cascade Range.

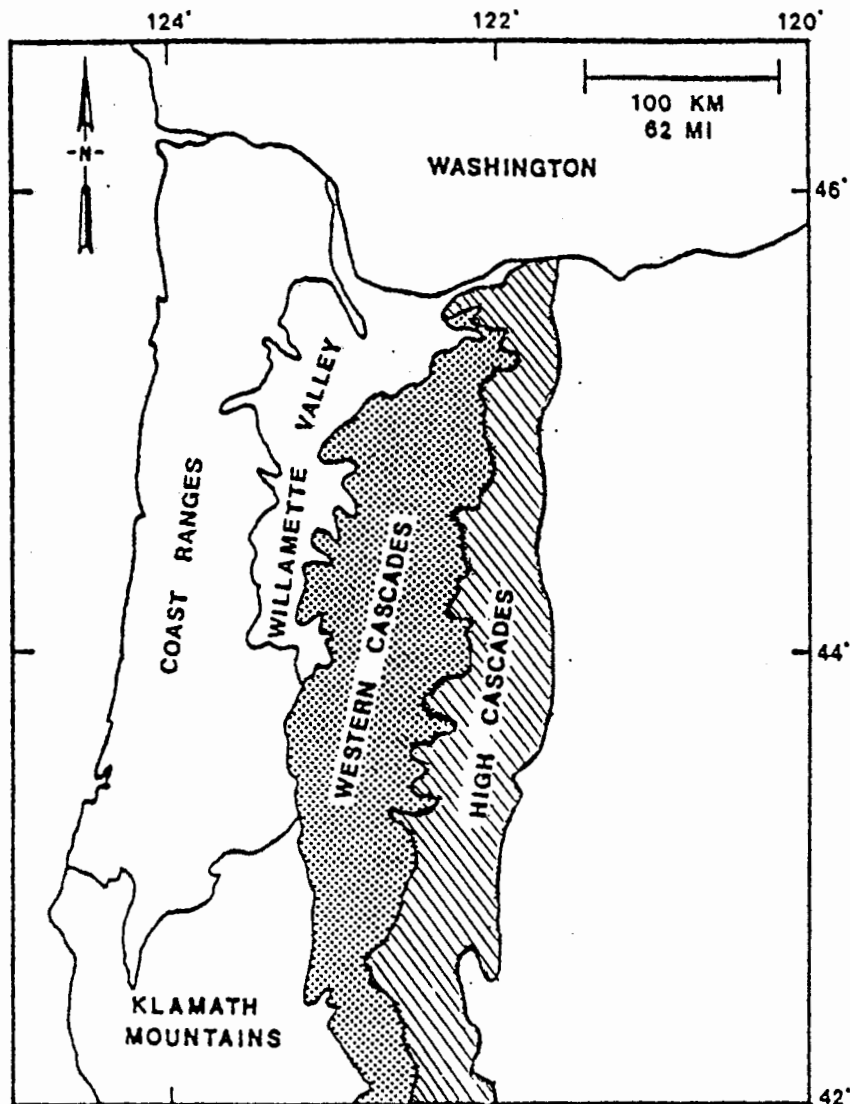


Figure 5. Physiographic Divisions of western Oregon. The Cascade volcanic range is shaded (Modified from Peck et al., 1964).

One of the most comprehensive studies on the mineralogy of sands of the Columbia River estuary was done by White (1967). He found that all of the common heavy minerals present in the Columbia River drainage were also present in the shelf sediments, although orthopyroxene from the Cascade Volcanics appeared to be particularly diagnostic of the Columbia River sediments. Later work by Scheidegger et al. (1971) showed that orthopyroxene rich shelf sands from the Umpqua River (central Oregon) could also be traced to source rocks in the Cascade volcanic arc.

CHAPTER IV

PREVIOUS WORK ON MARINE PLACERS

Rivers and beaches of southwest Oregon and northwest California have historically been mined for placer deposits containing gold and platinum (Horner, 1918). During mineral shortages of World War II, the coastal terraces of southwest Oregon and the Columbia River mouth respectively, were explored for chromite and ilmenite (Griggs, 1945; Kelly, 1947). Onshore marine placers of gold and platinum-group metals are reported to be restricted to southwest Oregon and northwest California (Pardee, 1934). Early studies indicated that these deposits are also enriched in chromite, ilmenite, garnet, and zircon (Day and Richards, 1906).

The relationship between continental shelf sediments, potential source areas, and transport mechanisms has been investigated by numerous researchers from several different perspectives. One of the earliest studies on the factors contributing to the concentration of heavy minerals on the beaches of the Pacific Northwest was that of Twenhofel (1946). He proposed that selective removal of light

minerals by winds coupled with the selective longshore transport may lead to local concentrations of heavy minerals on the southern side of headlands.

Stapor (1973) working on marine and coastal dune sands of the Atlantic coast suggested that heavy minerals were not concentrated on the beach face, but were developed offshore and formed as a slug to the beach face. However, this proposed mechanism of placer development contradicts the observation of restricted development of heavy mineral concentrations on beach faces (Everts, 1972).

Slingerland (1977) postulated that the combination of boundary flow turbulence and the ratio of grain size to bed roughness determines the entrainment and the deposition of sand size grains of different density. Bedload transport involves the rolling and saltation of grains which make repeated contacts with the bed. The larger, hydraulically equivalent quartz grains will be rolled away selectively from the relatively smooth bed formed by the finer heavy mineral grains. Sorting leading to heavy mineral deposits can occur only if there are marked differences in critical shear stress (Komar, 1986) between the heavy and light minerals. Later work by Peterson et al. (1986) focused on the distribution of maximum placer development in beach sands (Oregon coast) which occur to the south of headlands. Anomalous high concentrations of placer minerals typically occur at shoreline inflection points where convergence

(deceleration) of longshore currents apparently occurs, generally south of major headlands.

The first comprehensive work on the sediment sources and dispersal patterns of shelf sands in the study area was performed by Scheidegger et al. (1971). These researchers based their investigation on regional variations of the non-opaque heavy minerals in the shelf sands. This study is particularly interesting, because for the first time, the multivariate vector (factor) analysis approach was used to discriminate the shelf sediments into source end-members. Their work resulted in the delineation of four provenances or source areas. These researchers identified the Columbia River Basin, the Oregon Coast Range, the Klamath Mountains, and Tertiary-Pleistocene terrace deposits along the central Oregon coast as the major sand contributing provenances. Northward longshore drift during the Pleistocene sea level lowstands is suggested as a plausible mechanism for the apparent northward dispersal of Klamath terrain sediments in the continental shelf. Landward transgression of these shelf sands might supply sediment to some beaches on the Oregon coast during marine transgression (Komar and Clemens, 1986).

CHAPTER V

METHODS

SAMPLE DESCRIPTION

The samples discussed in this study were sub sampled from collections at Oregon State University (Chambers, 1969; Kulm, 1968; Runge, 1966). The samples were chosen on the basis of a wide geographic range, potentially demonstrating distinct sediment sources along the Pacific Coast. Figure 6 shows the location of the shelf sample areas in the study area. The bulk sediment samples consist of three classes of minerals:

- a. Light: quartz, feldspar, mica
- b. Heavy (Magnetic): magnetite, chromite, ilmenite, garnet, epidote, pyroxene, zoisite
- c. Heavy (Non-magnetic): zircon, rutile

Opaque oxide minerals reside in the heavy magnetic part of the bulk samples, with restricted specific gravities from 3.8 to 5.2 (Table I).

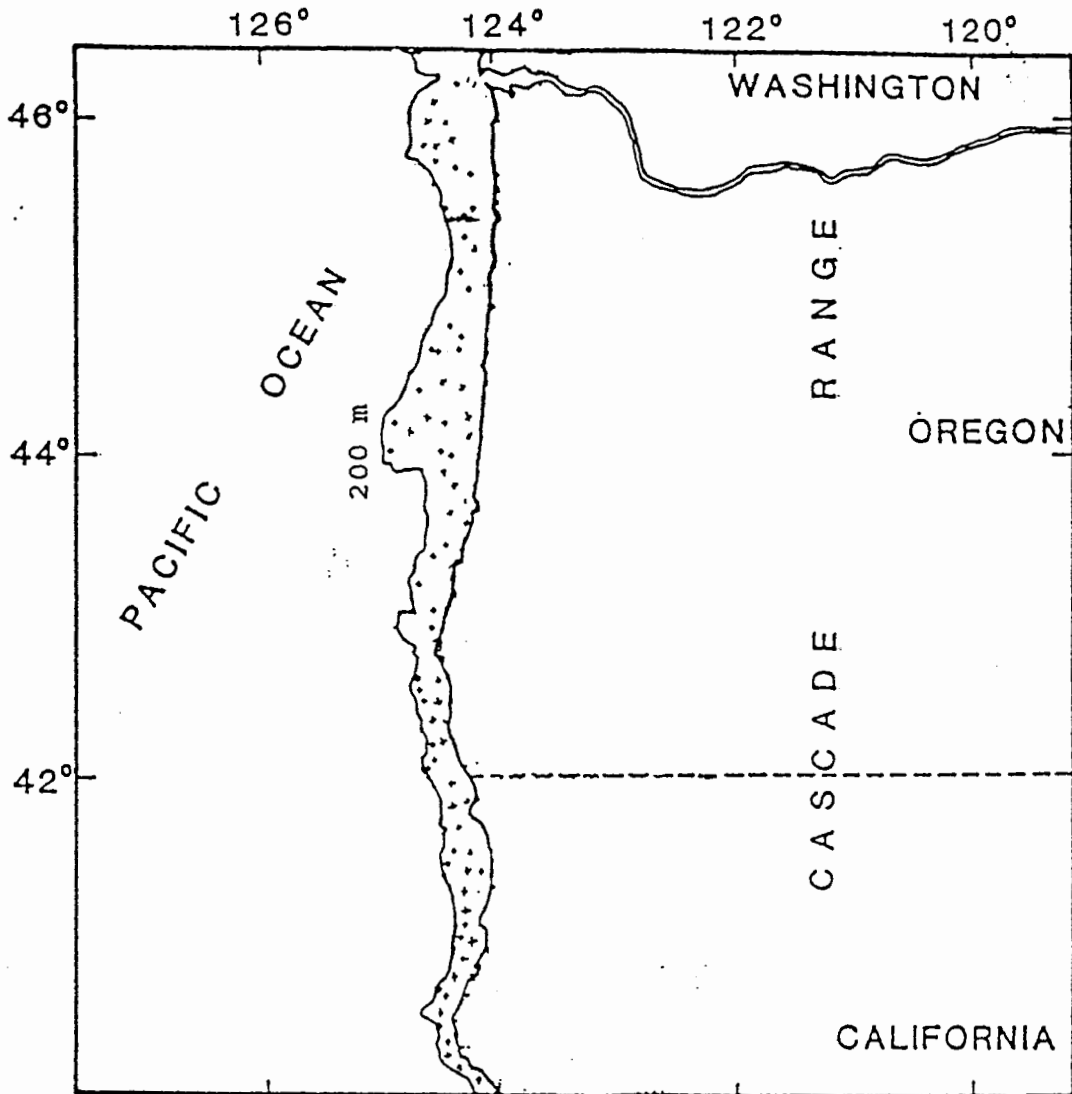


Figure 6. Location Map of Shelf Samples used in INAA and Electron Microprobe analysis.

TABLE I

HEAVY MINERALS AND METALS IN MARINE PLACERS OF THE
PACIFIC NORTHWEST USA

Native Metals	Formula	Density	Magnetic
Susceptibility			(g/cm ³)
Gold	Au (+Ag)	17-19	Non Susceptible
Platinum	Pt (+Fe)	14-19	Non Susceptible
Economic Heavy-Minerals			
Magnetite	Fe ₃ O ₄	5.0-5.2	Strong Susceptibility
Ilmenite	(Fe,Ti)O ₃	4.7-4.8	Moderate Susceptibility
Chromite	(Fe,Mg)(Cr,Al) ₂ O ₄	3.8-5.2	Moderate Susceptibility
Zircon	ZrSiO ₄	4.6-4.7	Low Susceptibility
Garnet	(Fe,Mg,Ca,Al) ₅ (SiO ₄) ₃	3.6-4.3	Moderate Susceptibility

SAMPLE SEPARATION

The sample preparation steps used at Oregon State University, College of Oceanography are outlined below. All sample processing, instrumental neutron activation analysis, and electron microprobe analysis was performed by Mumford. Raw analytical data was sent to Portland State University for analysis by this author. The separation of the mineral phases is as follows: (1) separation of heavy minerals from light ones at a specific gravity of 3.0, (2) separation of the heavy minerals into magnetic and non-magnetic minerals, and (3) a separation of the magnetic minerals at a specific gravity > 3.8 . Heavy mineral (HM) separation techniques (Figure 7) involved the use of sodium polytungstate with a specific gravity of 3.0, and tungsten carbide (WC) mixed with the sodium polytungstate to make a colloidal solution of specific gravity (4.2).

Sieving was carried out mainly to separate out rock fragments and other larger particles of silica and quartz which were not of interest for this analysis. The sodium polytungstate separation (specific gravity of 3.0) was used to remove the light minerals such as quartz and feldspar in the sample. This step reduced the sample mass, which speeded up the later separation steps. Sample grains were added to 20 ml of sodium polytungstate solution. The sample was centrifuged for about 15 minutes. The grains of greater

than 3.0 specific gravity settled down in the bottom, while the lighter grains floated on the top.

Once the separation was accomplished, liquid nitrogen was used to isolate the light and heavy minerals. Liquid nitrogen was poured into a large beaker and the test tubes containing the separated portions of the sample in the sodium polytungstate was placed carefully into the liquid nitrogen without disturbing the contents. The bottom part of the solution, where the heavier particles were settled, was frozen completely. The lighter particles, which floated at the top, were then washed off with distilled water into a funnel lined with filter paper. The heavier particles thawed after several minutes and were washed off into a different funnel. The samples in their respective funnels were thoroughly rinsed to wash off the sodium polytungstate. The light minerals for selected river (Sixes River) and shelf sites (10) were grain mounted for petrographic size analysis.

The heavy mineral fractions of all samples underwent additional separation steps as outlined below (Figure 7). The main object of this separation process was to retrieve the heavy opaque magnetic fraction of the sample (magnetic minerals such as magnetite, chromite, and ilmenite). A hand magnet was used first for the removal of strongly magnetic substances (magnetite). This method was efficient and it averted magnetite clogging in the Frantz separator. In the Frantz isodynamic magnetic separator, a series of current

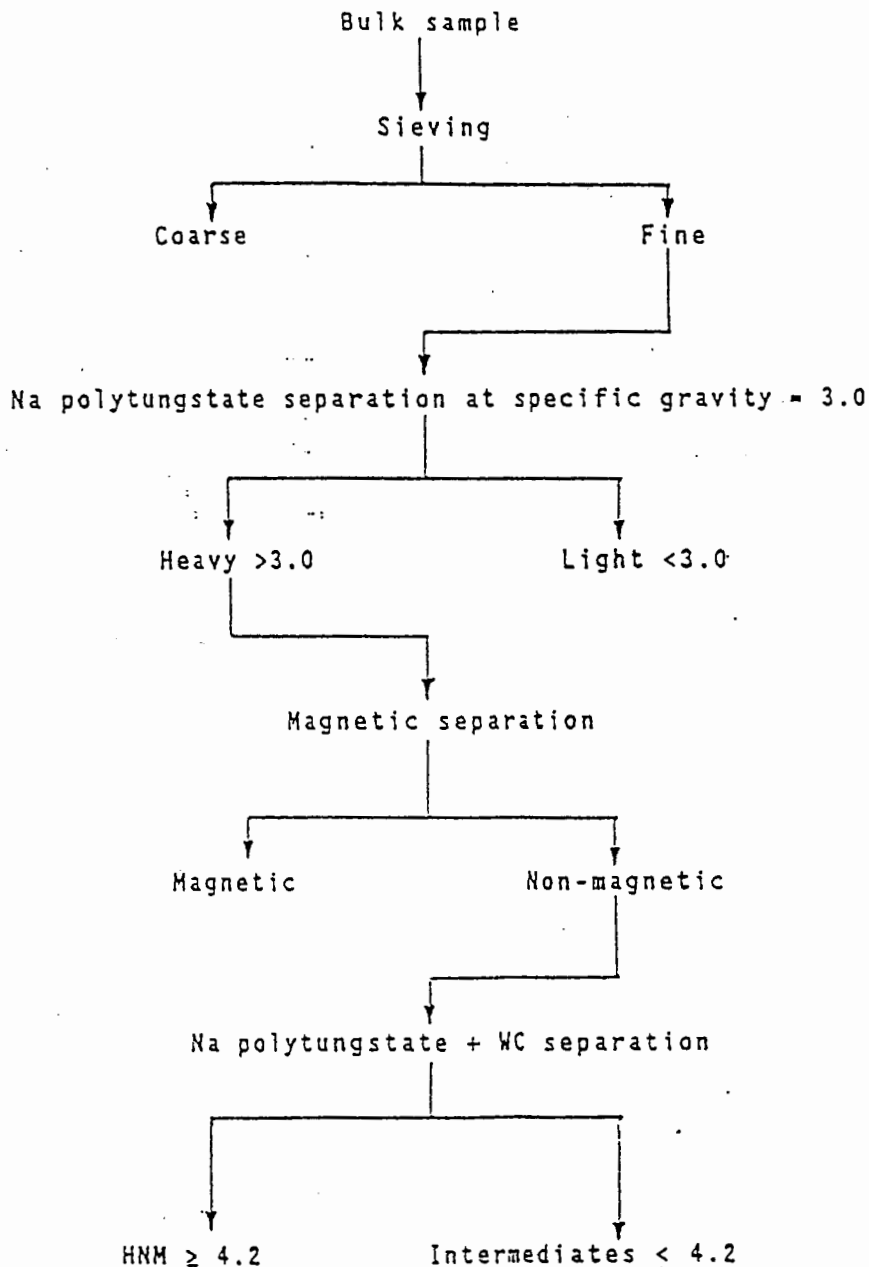


Figure 7. Sample Separation Scheme:
 Preliminary sieving (250 mm) was used to screen off the rock fragments and multiminerale aggregates.

settings were required to separate out the heavy magnetic minerals. Initially the current was set at 0.1 A and the tilt angle was set at 20°. The sample was run through the separator once to remove the most magnetically susceptible particles. Next the current was increased to 0.4 A and the non-magnetic portion of the sample was run through at least three times again to remove the ilmenite, chromite and their associated silicate contaminants. At each setting the portion of the sample retained as non-magnetic was run through the Frantz separator to clean the sample of magnetic minerals. The magnetic and the non-magnetic portions were weighed, and the masses were registered.

The mineral separation experiments utilizing magnetic-susceptibility and density have clearly demonstrated, an inability to separate the pure opaque phases (chromite, ilmenite, and magnetite) due to the presence of inclusions and exsolution lamellae of different opaque minerals within the mineral grains. The inclusions might also result in some cross contamination of trace elements (Ca, Al, Mn, Mg, Co, Sc, and V) in the mineral separates. Minor intergrowths of ilmenite/magnetite, chromite/magnetite, and incorporation of pyroxene and amphibole make geochemically pure mineral separations unattainable.

SAMPLE ENCAPSULATION

Encapsulation for irradiation was the final step in sample preparation for the neutron activation analysis (INAA). After the opaques (magnetite, chromite and ilmenite) had been separated, they were triply encapsulated in polyethylene polyvials for the purpose of safeguarding against the accidental spilling from the breakage of polyvials after irradiation. Since the mass of the sample was not to exceed 160 mg (this upper limit for mass is determined on the basis of activity produced in the sample), 2/27 dram polyvials were appropriate for the inner sample encapsulation.

Sample Mounting and Polishing for Microprobe work

To establish the grain size distributions of the opaque oxide minerals (chromite, ilmenite, and magnetite) in river sources, composite sampling was done for the Sixes River in southern Oregon. Opaque mineral grains (at least 100 per sample) were mounted in epoxy and polished for energy dispersive x-ray analysis (electron microprobe) of relative abundance of ilmenite, chromite, and magnetite grains for different grain size distributions.

INSTRUMENTAL NEUTRON ACTIVATION ANALYSIS (INAA)

Neutron activation analysis is based on the identification of elements present in a sample after it has been irradiated by a neutron source, such as a nuclear reactor. The energy of the emitted gamma ray and the area of the associated photopeak are used to determine the amount of that particular element in the sample (Knoll, 1979). The potential use of neutron activation for chemical analysis was realized as early as 1936 (Hevesy and Levi). With advances in technology including more efficient and higher resolution detectors, INAA has become a powerful method for trace element analysis of geologic samples.

INAA Parameters

In this project the comparative method for sequential neutron activation analysis was used to determine the elemental concentrations of major and trace elements in bulk oxide splits (chromite, magnetite and ilmenite). The standards used for the Rabbit Analyses (OSU nuclear reactor was used; Mumford, 1991; personal communication) include Spex Oxides (Al_2O_3 , TiO_2 and CaCO_3) liquid V and Mn standards, NBS STDS (SRM-1571-leaves, -1632-coal and -688-silicate rock) and USGS STD BCR-1. Standards used for the long-lived Analyses include, in-house liquid REE STD, USGS BCR-1, USGS DTS-1 and NBS STD SRM 1633-Fly Ash. These

standards were chosen because they contain a wide variety of elements expected to be present in the opaque oxides.

Neutron Flux. The samples and the standards are generally irradiated under identical neutron flux conditions for INAA. In this project the Oregon State University (OSU) nuclear reactor was used for irradiating the samples. For both long and short irradiations the reactor was operated at a power level of 1 MW, which gave a flux of 9×10^{12} n/cm²-s in the pneumatic transfer system, and a flux level of 3×10^{12} n/cm²-s at the rotating rack. The mass of the samples combined with this flux level gave a count rate which produced satisfactory statistics for most of the nuclides of interest.

Irradiation, decay and counting times. Irradiation, decay and counting times are important factors in sequential NAA (Laul, 1979). Sequential neutron activation analysis follows the procedure of counting the short-lived radionuclides first, followed by a decay period and subsequent counting of the longer lived radionuclides.

For short irradiations the samples were irradiated in the pneumatic transfer facility for 2 minutes and then allowed to decay for 10 minutes (an average time of 10 minutes was required to transfer the samples to clean polyvials and transport them to the counting room). The short-lived radionuclides (representative of the elements Ti, Al, V, Mg and Ca) which have a half life in the range of

2-10 minutes were counted first. The first counting time was of 5 minutes duration. The samples and the standards were then allowed to decay for 3 hours in order to reduce the activity level of the short-lived radionuclides. The decay of these short-lived nuclides reduced the Compton continuum for the photopeaks of the longer-lived radionuclides. These samples were then counted for 10 minutes for the elements Na, K and Mn.

For the long irradiations, the samples and the standards were irradiated for 7 hours in the rotating rack (Lazy Susan). The samples were allowed to decay for 7 days which was sufficient for the short-lived radionuclides to decay completely. The samples were then counted for 3 hours for the elements Fe, Co, As, Sb, Rb, Ba, La, Nd, Sm, Yb and Lu. The radionuclides associated with these elements were allowed to decay for 30 days and then the radionuclides associated with the elements Sc, Cr, Co, Zn, Sr, Sb, Cs, Ce, Eu, Tb, Zr, Hf, and Ta were counted for 6 hours.

Table II gives properties of the radioisotopes measured along with some other parameters of this analysis (Laul, 1979).

ELECTRON MICROPROBE

In order to establish the elemental compositions and size distributions of the specific mineral phases (chromite, ilmenite and magnetite), splits of opaque minerals from

TABLE II
 RADIONUCLIDES AND INAA PARAMETERS

Element Isotope Half life gamma ray energy

		Group A	(keV)
Ti	⁵¹ Ti	5.79 min	320
Mg	²⁷ Mg	9.46 min	1014
V	⁵² V	3.75 min	1434
Al	²⁸ Al	2.32 min	1779
Ca	⁴⁹ Ca	8.80 min	3084
		Group B	
Mn	⁵⁶ Mn	2.58 hr	847, 1811
Na	²⁴ Na	15.0 hr	1369
K	⁴² K	12.4 hr	1524
		Group C	
Fe	⁵⁹ Fe	44.5 day	1099, 1292
Co	⁵⁸ Ni (⁵⁸ Co)	71.3 day	811
La	¹⁴⁰ La	40.2 hr	816, 1597
			(keV)
Sm	¹⁵³ Sm	46.8 hr	103
Yb	¹⁷⁵ Yb	4.21 day	283, 396
Lu	¹⁷⁷ Lu	6.74 day	208

TABLE II
 RADIONUCLIDES AND INAA PARAMETERS
 (continued)

Element	Isotope	Half life	gamma ray energy
Group D			
Sc	⁴⁶ Sc	83.85 day	889, 112
Cr	⁵¹ Cr	27.8 day	320
Sb	¹²⁴ Sb	60.3 day	564, 169
Ce	¹⁴¹ Ce	32.5 day	146
Eu	¹⁵² Eu	12.7 day	122, 1408
Hf	¹⁸¹ Hf	42.5 day	482

selected river samples (23) were mounted in epoxy and polished for analysis by electron microprobe. Microprobe analyses of individual mineral grains provides accurate elemental compositions of specific mineral phases. A Cameca SX50 microprobe and scanning electron microscope system (Oregon State University) was used for the analysis. Specimen counting times ranged from 10 seconds (major and minor elements) to 100 seconds (trace and rare earth-elements), with a beam (2-5 micron width) generated at 15 kv and 20 na. Beam positions within specimen grains were located (under reflected light) to avoid (1) multimineralic phase boundaries, (2) inclusions, and (3) cracks or dissolution embayments. At least 100 randomly picked opaque grains per sample were analyzed for elemental composition (Mumford, 1991; personal communication).

Preliminary microprobe analysis of the opaque oxide splits based on density and magnetic susceptibility experiments demonstrated minor mineral cross contamination (Peterson and Binney, 1988). The contamination occurs due to the presence of magnetite and ilmenite intergrowths, rare magnetite rims around chromite grains, and magnetite inclusions in chromite grains (Peterson, 1991; personal communication).

CHAPTER VI

RESULTS

INAA OF CONTINENTAL SHELF DEPOSITS

Elemental analysis of bulk opaque mineral fractions was performed on surface sediments from the continental shelf off Oregon and northwest California, in order to compare the relative abundances of iron, titanium, and chromium, and to establish associated trace elements in the opaque mineral fractions. Elemental analysis of the opaque mineral fractions was performed by Instrumental Neutron Activation Analysis (INAA). Some 87 surface and near-surface samples (S1 - OR-16) were selected from existing grab samples, short box cores (<45 cm), and short piston or gravity cores (<60 cm; see the Appendix A for cross reference of sample numbers) from Oregon State University core archives (Mumford, 1991; personal communication). The sediment samples were selected based on the following criteria: (1) geographical distribution relative to known coastal placer deposits containing economic minerals, (2)

landward fluvial sources of economic minerals, and (3) high heavy-mineral content of shelf deposits. Samples analyzed in this study range in water depths from 17 to about 200 meters on the shelf.

A full suite of 21 elements (Appendix A) was run on 87 samples. Figure 8 and 9 show the variation of Cr and Ti respectively as a function of latitude in the bulk opaque mineral fractions. High values of Ti (exceeding 20 wt%) are found in the northern shelf between latitudes 42.5° and 46.0°. In contrast, the elevated Cr values (4-6 wt%) are restricted to the southern shelf at latitudes 40.5° and 42.5°. These relative trends of Ti and Cr abundance in shelf bulk opaque mineral splits are very similar to the results found in onshore river and beach deposits (Peterson et al., 1988). Across-shelf transects (Figures 10-14) of Cr and Ti from the opaque fraction of shelf sands generally reflect the regional variability associated with the onshore source rocks. However, the plots of samples from 44-45, and 45-46 degrees latitude (Figures 13 and 14) do show slight decreases in titanium with increased distance offshore. Whereas, elemental chromium values slightly increase towards the offshore.

The latitudinal distribution of high chromium abundance in shelf sands corresponds to source rocks associated with the Klamath Mountains (Figure 8). In contrast, high titanium abundance is restricted to the shelf

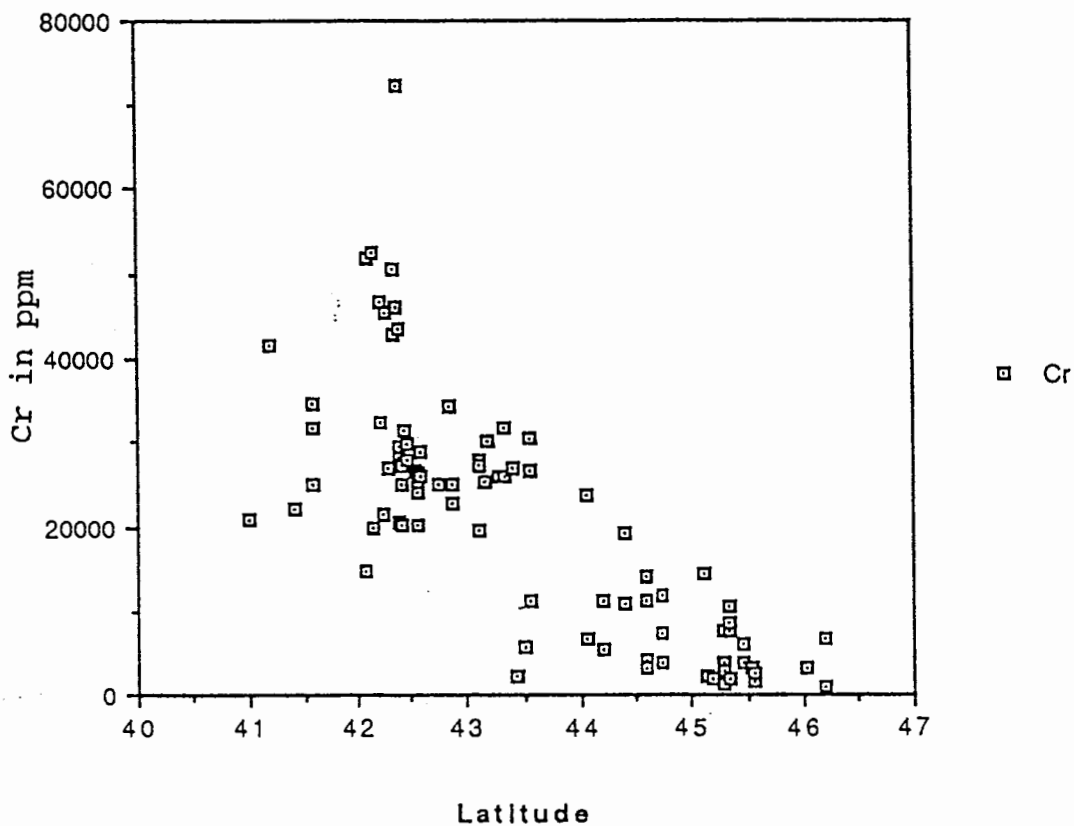


Figure 8. Plot of the Major Element Chromium of Bulk Opaque Mineral Separates from the Continental Shelf as a Function of Latitude.

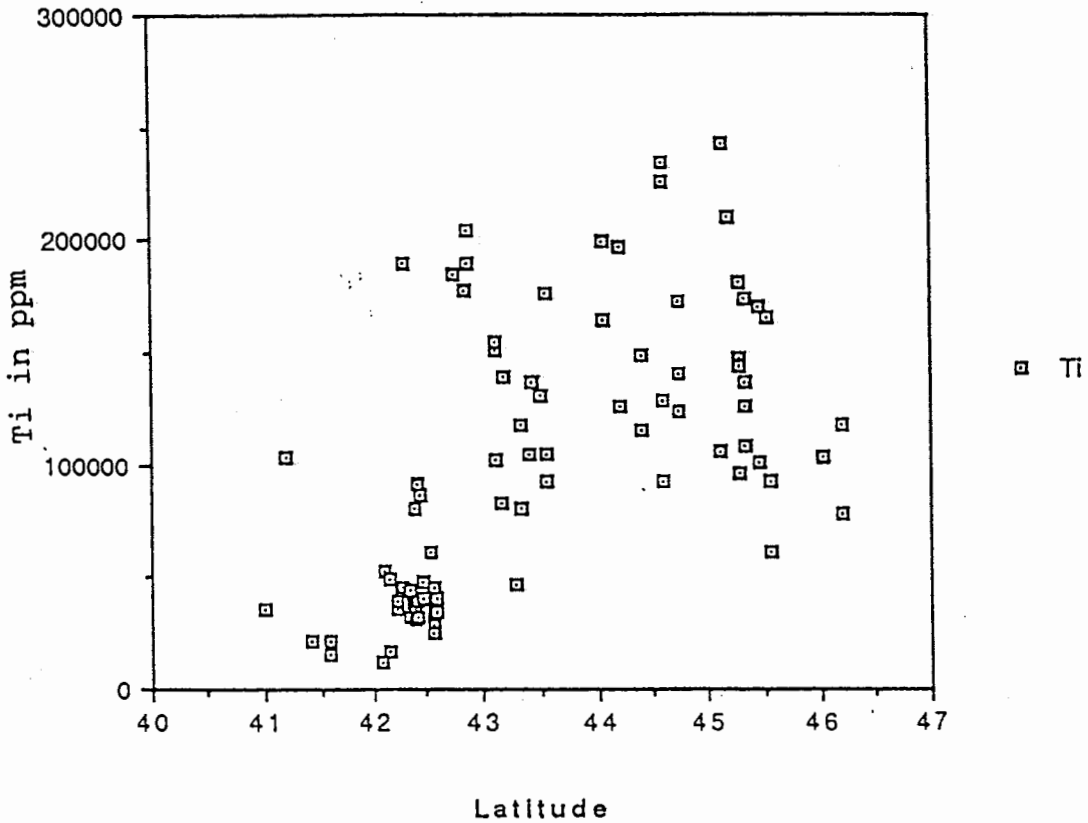


Figure 9. Plot of the Major Element Titanium of Opaque Mineral Separates from the Continental Shelf as a Function of Degrees Latitude.

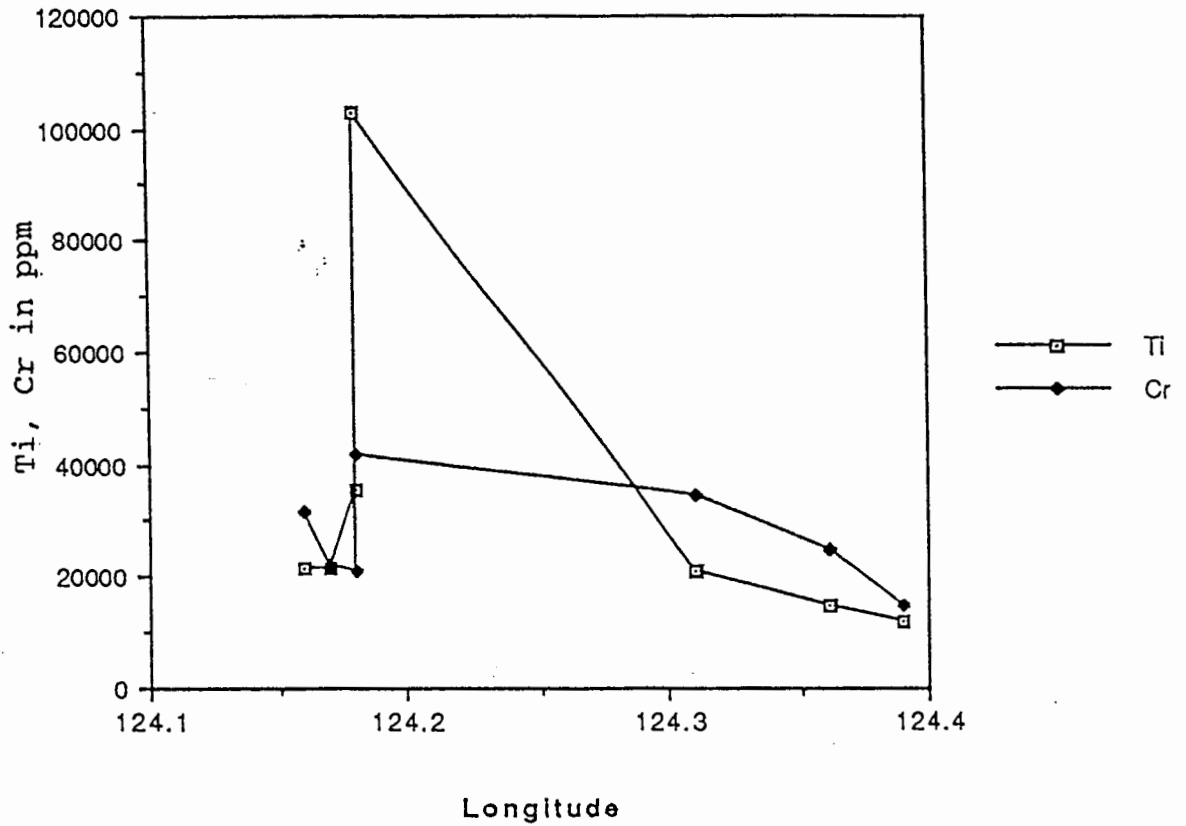


Figure 10. Across-shelf Transect of Chromium and Titanium Elemental Abundance for the Samples from 41-42 Degrees Latitude.

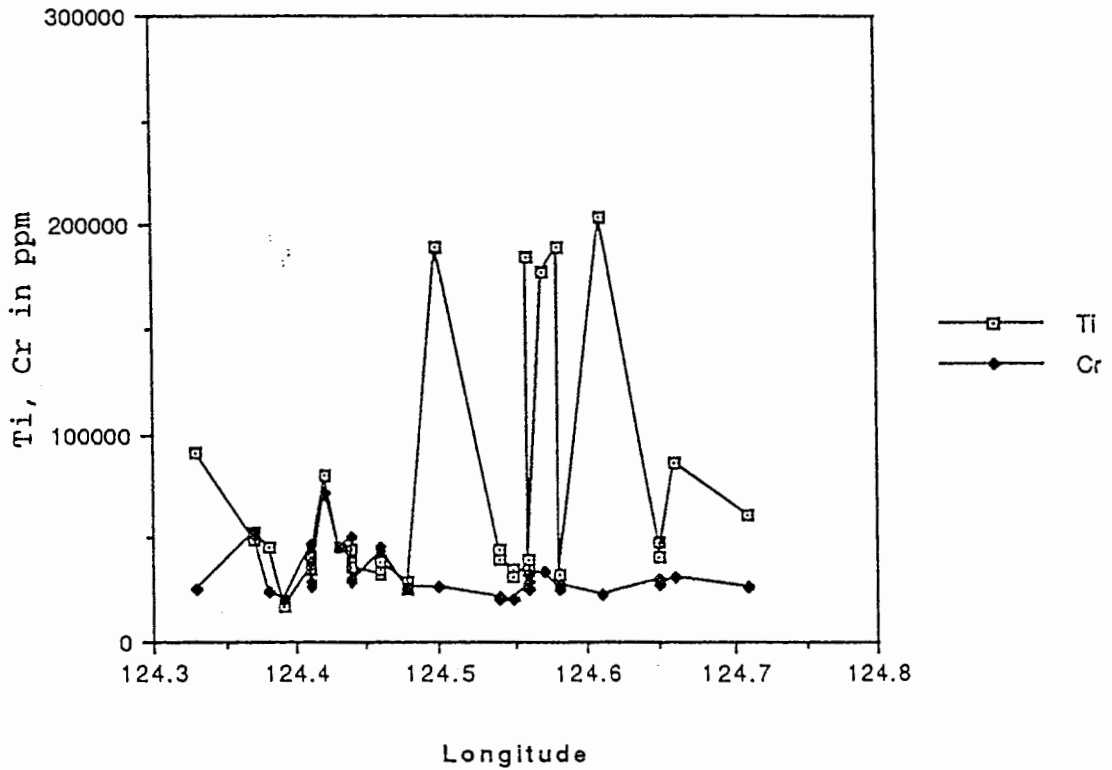


Figure 11. Across-shelf Transect of Chromium and Titanium Elemental Abundance for the Samples from 42-43 Degrees Latitude.

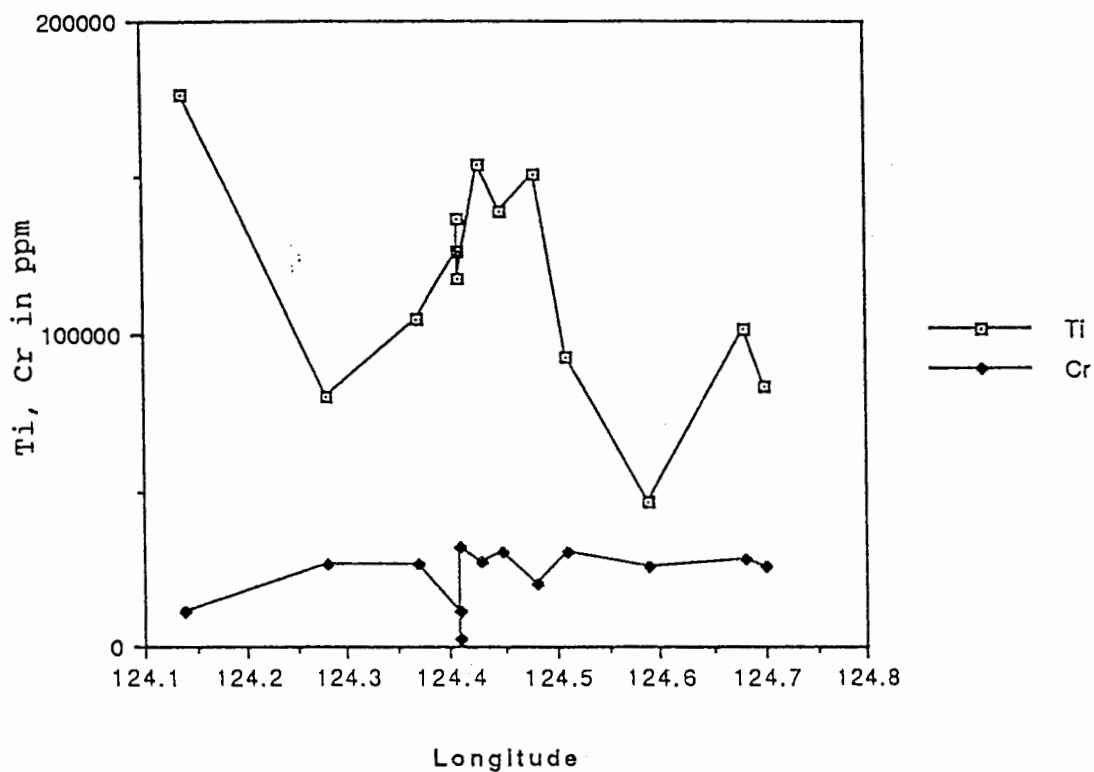


Figure 12. Across-shelf Transect of Chromium and Titanium Elemental Abundance for the Samples from 43-44 Degrees Latitude.

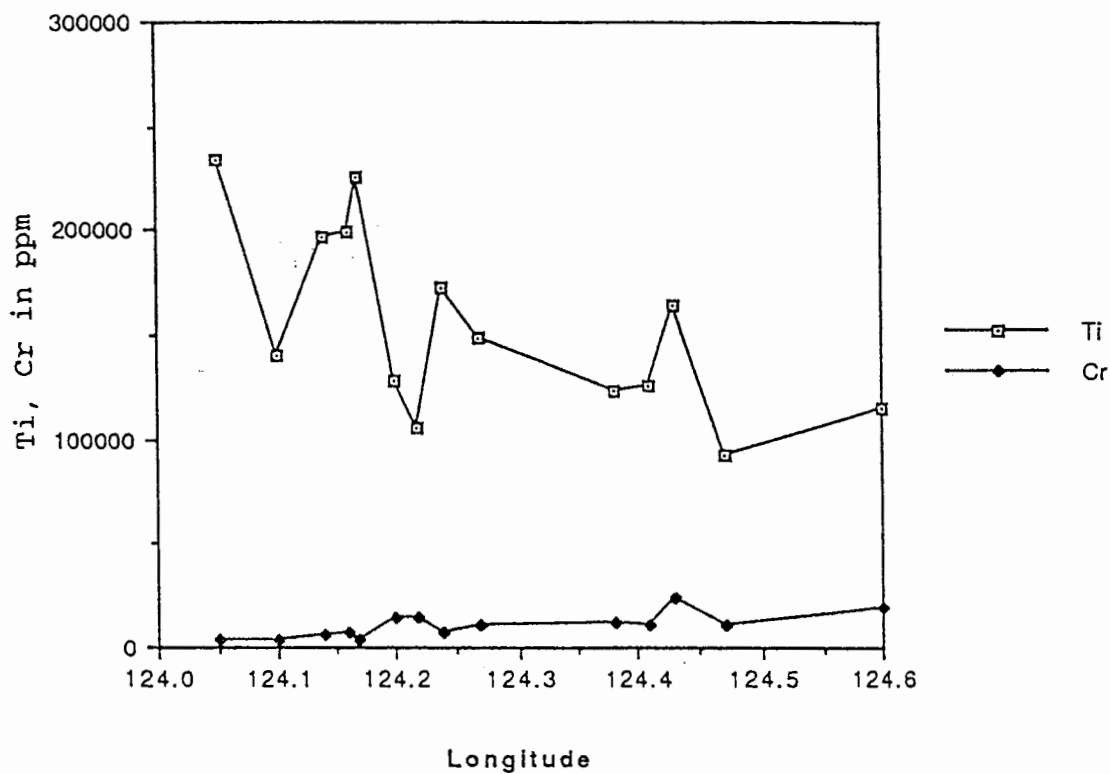


Figure 13. Across-shelf Transect of Chromium and Titanium Elemental Abundance for the Samples from 44-45 Degrees Latitude.

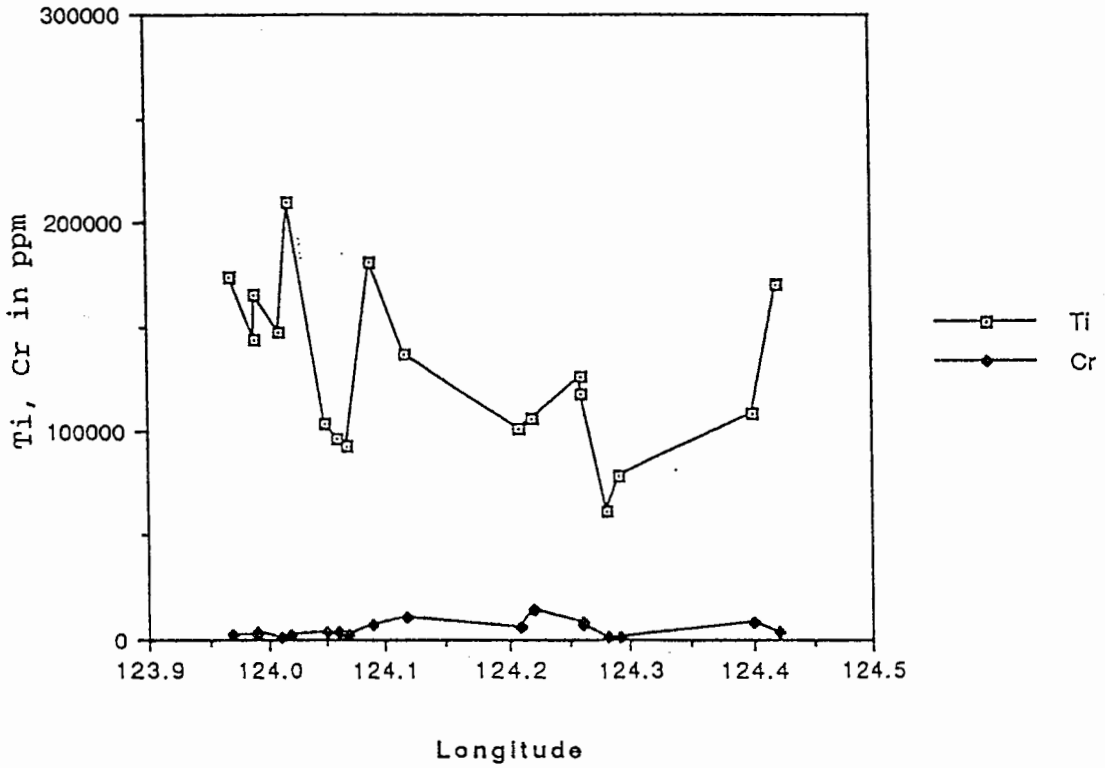


Figure 14. Across-shelf Transect of Chromium and Titanium Elemental Abundance for the Samples from 45-46 Degrees Latitude.

sediments derived from drainages of Oregon Coast Range (Figure 9). Maximum values of titanium (exceeding 20 wt%) are found in the northern shelf between latitudes 43° and 45.5° . Figure 11 indicates the titanium and chromium variability might also be due to crossing of north-south (along-shelf) boundary rather than a across-shelf dispersal phenomena. The shelf opaque mineral geochemistry generally demonstrates an across-shelf mineral dispersal pattern, with the possible exception of the most seaward samples on the shelf (Figure 12 and 13).

Total iron abundances are shown in Figure 15 for the shelf samples. Iron in the opaque mineral separates demonstrates significant local variability (20-51 wt%) over length scales of 10-100 km. It does not define any consistent regional trend. Maximum iron values (40-51 wt%) occur at about 42.5° and 44.5° latitude. In contrast to the iron, both chromium and titanium indicate significant regional changes in element abundance along the shelf. The contrasting distributions of chromium-rich oxides (south of 43°) and titanium-rich oxides (north of 43°) delineate distinctly different source rocks from the Klamath Mountains (south) and the Coast Range (north).

Linear regressions of specific major and trace element pairs can be used to establish trace element partitioning into the dominant opaque oxide phases. From the microprobe data discussed below, it is known that chromium is present

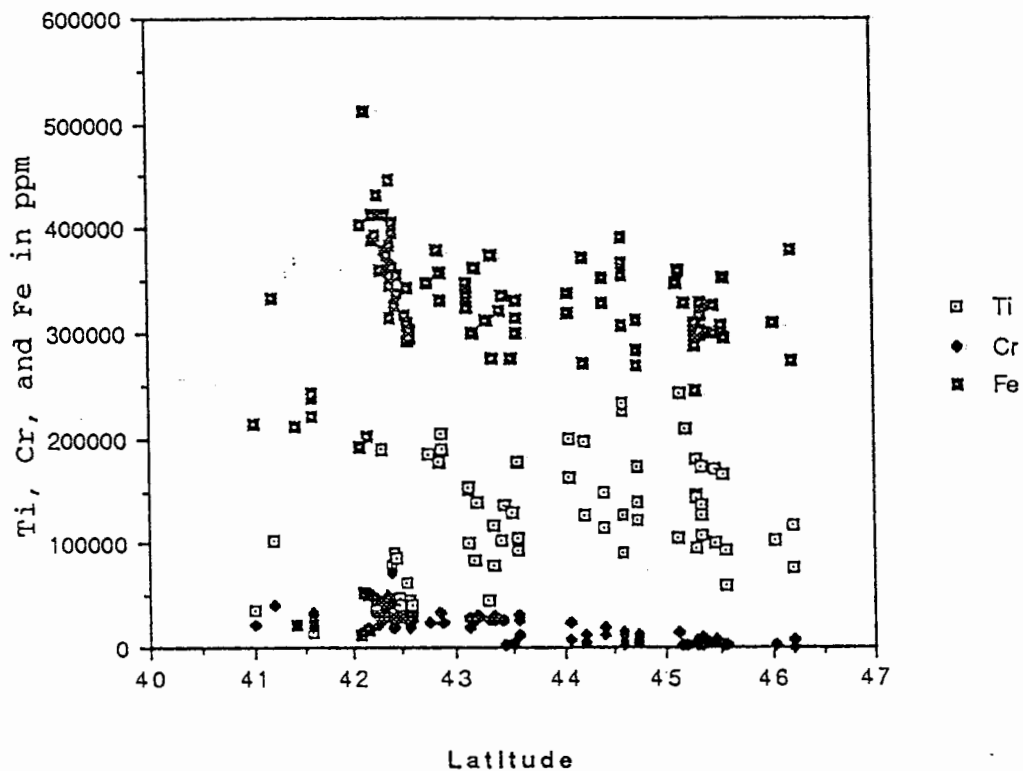


Figure 15. Plots of the Major Element (Fe, Cr, and Ti) Abundances as a Function of Latitude are shown for the opaque mineral separates from the shelf of placers.

exclusively in the chromite mineral grains. A high positive correlation between cobalt and chromium (Co-Cr, correlation coefficient $r=0.92$; Figure 16) indicates efficient trace element (cobalt) partitioning into chromite. However, a lack of high correlation between nickel and chromium suggests that Ni is not entirely partitioned into chromite (see correlation matrix Table IV). The major and trace elements partitioned into chromite (Mg, Al, Co, and Ni) are characterized by +2 or +3 valence states and intermediate to large ionic-radii (0.2-0.4 in octahedral coordination). The high positive correlations between trace (Hf, Sc) and titanium (Hf-Ti, $r=0.90$; Figure 17 and Sc-Ti, $r=0.70$; Figure 18) indicate that these trace elements are partitioned into ilmenite, and possibly to some extent, into titaniferous magnetite. The trace elements (Hf, Sc, Ta) partitioned into ilmenite, are characterized by their +3, +4 valence states and small ionic radii. The elements Mg, Ca and Mn, which are not selectively partitioned into ilmenite, are distinguished by their +2 valence states and large ionic radii. Figure 19 shows that the only trace element correlated with the iron, is vanadium (V-Fe, $r=0.74$). Presumably, the vanadium is largely partitioned into magnetite, as it is not correlated with either the chromium or titanium metals in chromite and ilmenite respectively. The relatively moderate correlation between vanadium and iron, likely results from the distribution of some of the

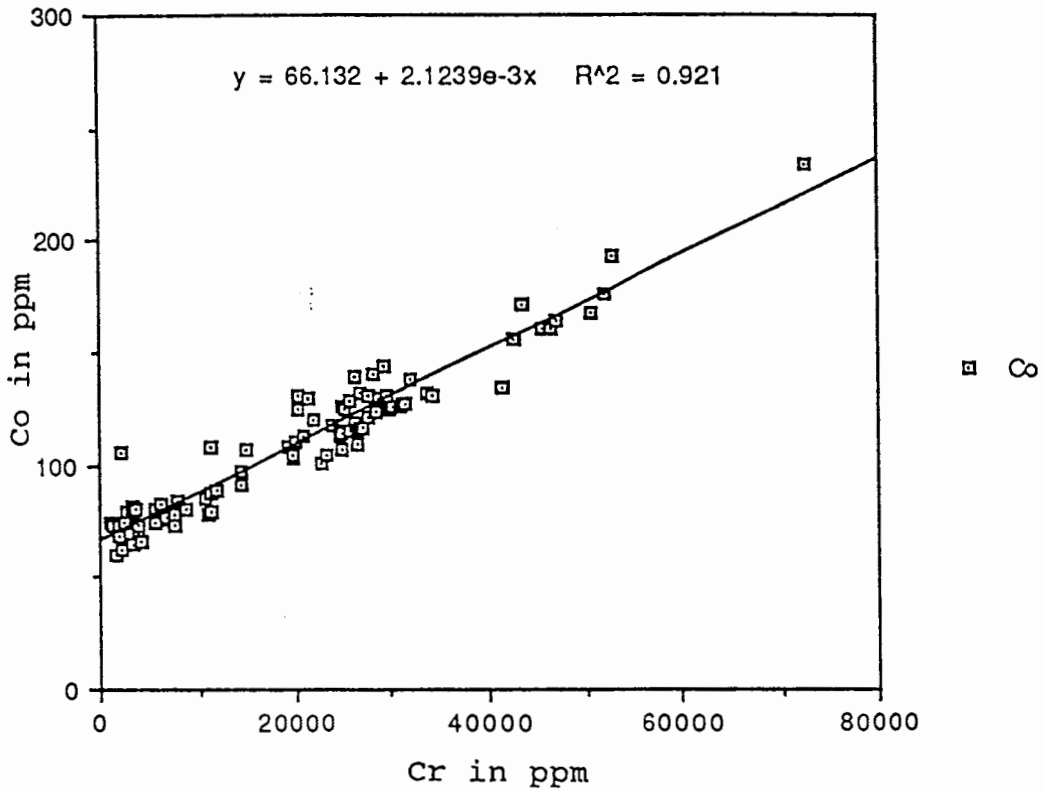


Figure 16. Plots of Chromium and Cobalt Elemental Values of Opaque Mineral Oxides from the Continental Shelf.

TABLE III

ELEMENTAL CORRELATION COEFFICIENTS FOR OPAQUE MINERAL FRACTION OF RIVER, BEACH, AND SHELF SANDS IN OREGON AND NORTHERN CALIFORNIA, 40.5-46.5 DEGREES LATITUDE

	1	2	3	4	5	6	7
1	1.000	0.374	0.210	0.631	0.054	-0.278	-0.083
2	0.374	1.000	0.580	0.780	-0.269	-0.679	-0.100
3	0.210	0.580	1.000	0.457	-0.550	-0.791	-0.009
4	0.631	0.780	0.457	1.000	-0.071	-0.515	-0.122
5	0.054	-0.269	-0.550	-0.071	1.000	0.793	-0.159
6	-0.278	-0.679	-0.791	-0.515	0.793	1.000	-0.078
7	-0.083	-0.100	-0.009	-0.122	-0.159	-0.078	1.000
8	-0.438	0.119	0.654	-0.140	-0.618	-0.513	0.036
9	-0.376	-0.502	-0.335	-0.443	0.593	0.669	-0.109
10	-0.514	-0.563	-0.304	-0.739	-0.364	0.073	0.291
11	-0.378	0.155	0.654	-0.128	-0.705	-0.585	0.064
12	0.406	0.363	0.284	0.490	-0.060	-0.252	-0.098
13	0.327	0.235	0.178	0.309	0.178	-0.024	-0.111
14	0.439	-0.243	-0.219	0.009	0.471	0.339	-0.110
15	0.497	-0.147	-0.119	0.090	0.384	0.217	-0.113
16	0.689	-0.039	-0.048	0.251	0.351	0.143	-0.130
17	0.748	0.089	0.123	0.421	0.179	-0.028	-0.107
18	-0.180	-0.401	-0.426	-0.297	0.678	0.684	-0.138
19	0.022	-0.281	-0.330	-0.246	0.407	0.417	-0.077
20	-0.277	-0.669	-0.689	-0.526	0.675	0.886	-0.078
21	-0.231	-0.626	-0.726	-0.451	0.833	0.969	-0.111

TABLE III

ELEMENTAL CORRELATION COEFFICIENTS FOR OPAQUE MINERAL
 FRACTION OF RIVER, BEACH, AND SHELF SANDS IN OREGON AND
 NORTHERN CALIFORNIA, 40.5-46.5 DEGREES LATITUDE
 (Continued)

	8	9	10	11	12	13	14
1	-0.438	-0.376	-0.514	-0.378	0.406	0.327	0.439
2	0.119	-0.502	-0.563	0.155	0.363	0.235	-0.243
3	0.654	-0.335	-0.304	0.654	0.284	0.178	-0.219
4	-0.140	-0.443	-0.739	-0.128	0.490	0.309	0.009
5	-0.618	0.593	-0.364	-0.705	-0.060	0.178	0.471
6	-0.513	0.669	0.073	-0.585	-0.252	-0.024	0.339
7	0.036	-0.109	0.291	0.064	-0.098	-0.111	-0.110
8	1.000	-0.096	0.200	0.965	-0.051	-0.100	-0.469
9	-0.096	1.000	-0.019	-0.206	-0.111	0.207	0.284
10	0.200	-0.019	1.000	0.254	-0.402	-0.385	-0.261
11	0.965	-0.206	0.254	1.000	-0.044	-0.133	-0.477
12	-0.051	-0.111	-0.402	-0.044	1.000	0.650	0.215
13	-0.100	0.207	-0.385	-0.133	0.650	1.000	0.311
14	-0.469	0.284	-0.261	-0.477	0.215	0.311	1.000
15	-0.399	0.181	-0.276	-0.411	0.289	0.428	0.951
16	-0.470	0.126	-0.425	-0.457	0.378	0.446	0.909
17	-0.333	-0.007	-0.480	-0.297	0.481	0.489	0.715
18	-0.353	0.861	-0.170	-0.441	-0.040	0.161	0.427
19	-0.312	0.469	-0.053	-0.329	-0.127	-0.012	0.354
20	-0.385	0.602	0.105	-0.458	-0.206	-0.070	0.375
21	-0.504	0.695	-0.028	-0.589	-0.199	0.022	0.408

TABLE III

ELEMENTAL CORRELATION COEFFICIENTS FOR OPAQUE MINERAL
 FRACTION OF RIVER, BEACH, AND SHELF SANDS IN OREGON AND
 NORTHERN CALIFORNIA, 40.5-46.5 DEGREES LATITUDE
 (Continued)

	15	16	17	18	19	20	21
1	0.497	0.689	0.748	-0.180	0.022	-0.277	-0.231
2	-0.147	-0.039	0.089	-0.401	-0.281	-0.669	-0.626
3	-0.119	-0.048	0.123	-0.426	-0.330	-0.689	-0.726
4	0.090	0.251	0.421	-0.297	-0.246	-0.526	-0.451
5	0.384	0.351	0.179	0.678	0.407	0.675	0.833
6	0.217	0.143	-0.028	0.684	0.417	0.886	0.969
7	-0.113	-0.130	-0.107	-0.138	-0.077	-0.078	-0.111
8	-0.399	-0.470	-0.333	-0.353	-0.312	-0.385	-0.504
9	0.181	0.126	-0.007	0.861	0.469	0.602	0.695
10	-0.276	-0.425	-0.480	-0.170	-0.053	0.105	-0.028
11	-0.411	-0.457	-0.297	-0.441	-0.329	-0.458	-0.589
12	0.289	0.378	0.481	-0.040	-0.127	-0.206	-0.199
13	0.428	0.446	0.489	0.161	-0.012	-0.070	0.022
14	0.951	0.909	0.715	0.427	0.354	0.375	0.408
15	1.000	0.906	0.738	0.308	0.221	0.260	0.288
16	0.906	1.000	0.888	0.282	0.263	0.143	0.220
17	0.738	0.888	1.000	0.101	0.076	-0.031	0.030
18	0.308	0.282	0.101	1.000	0.536	0.659	0.738
19	0.221	0.263	0.076	0.536	1.000	0.387	0.428
20	0.260	0.143	-0.031	0.659	0.387	1.000	0.863
21	0.288	0.220	0.030	0.738	0.428	0.863	1.000

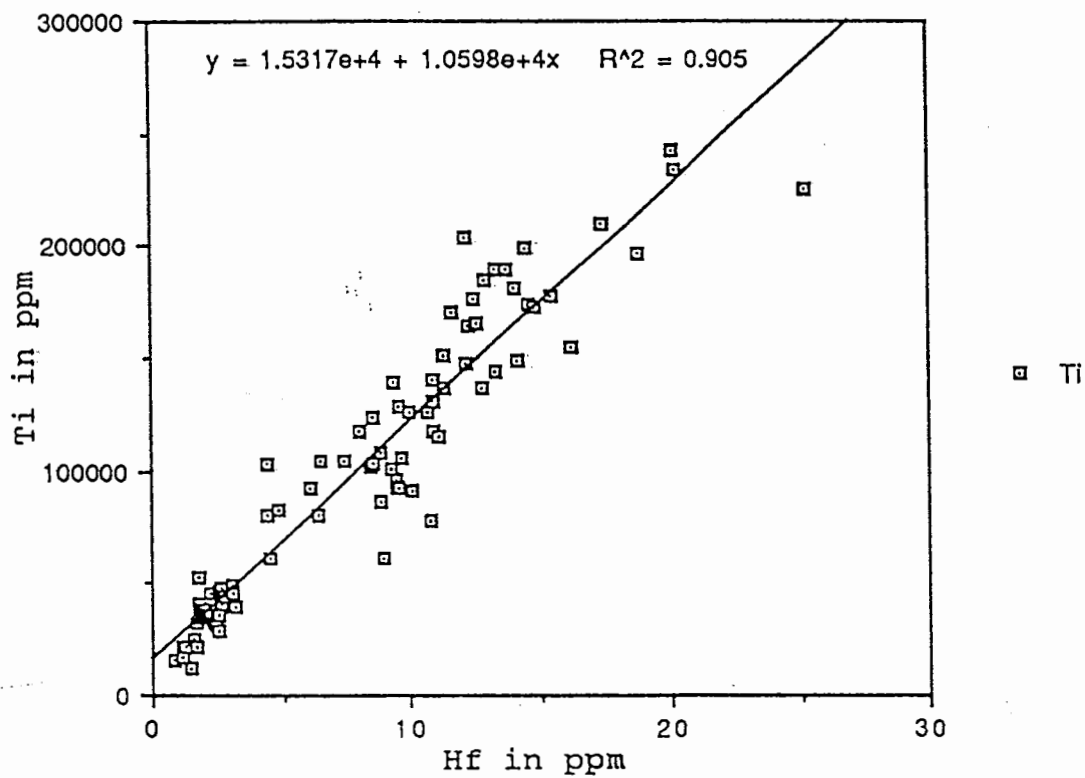


Figure 17. Plots of Titanium and Hafnium Elemental Values of Opaque Mineral Oxides from the Continental Shelf.

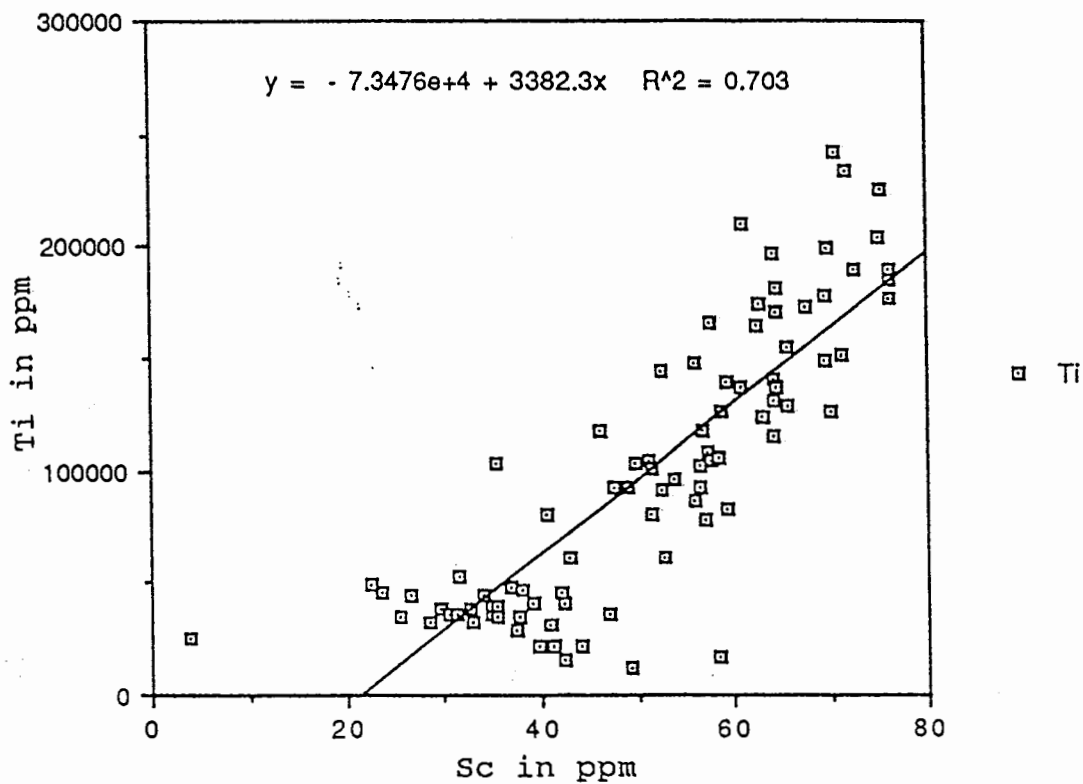


Figure 18. Plots of Titanium and Scandium Elemental Values of Opaque Mineral Oxides from the Continental Shelf.

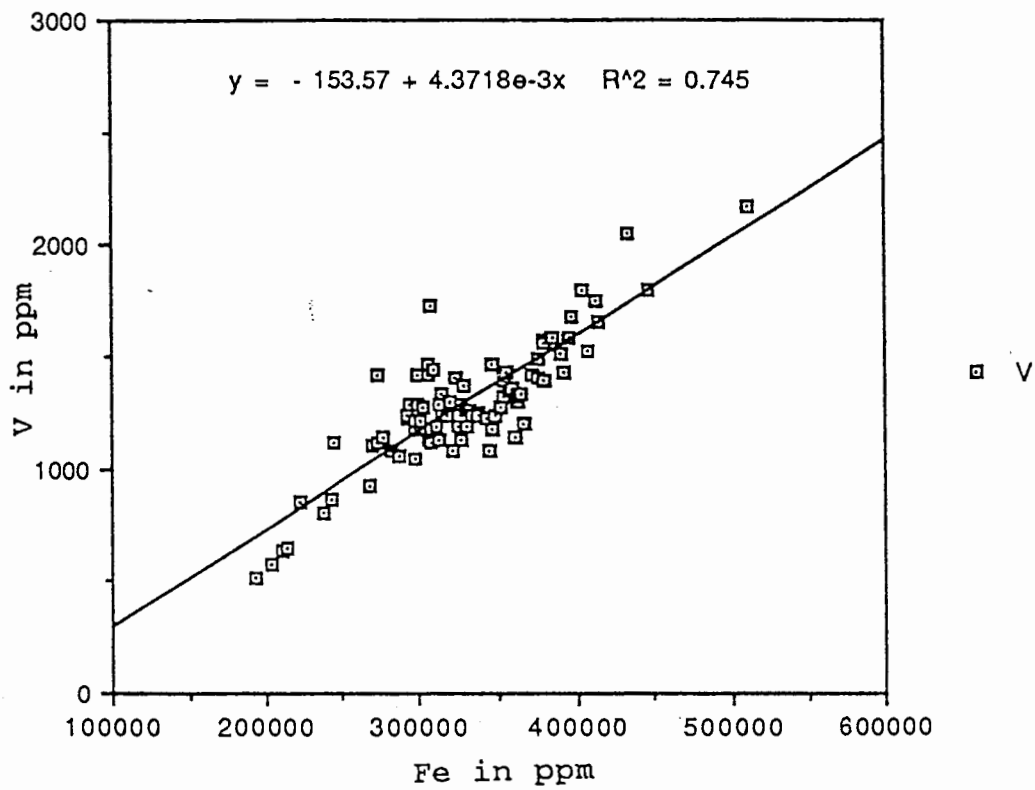


Figure 19. Plots of Iron and Vanadium Elemental Values of Opaque Mineral Oxides from the Continental Shelf.

iron in the non-magnetite phases i.e., chromite and ilmenite (see Table I).

In the lanthanide group the following trace elements were detected: La (3-56 ppm), Ce (112-7 ppm), Sm (10-1 ppm), Eu (< 1.0-1.8 ppm) and Lu (< 1.0-2.4 ppm; refer to Appendix A). La, Hf, and Ce in the lanthanide group show similar abundance trends as a function of latitude i.e., increasing to the north (Figures 20-22). The remaining rare earth elements show only weak or no increases from south to north in the study area (refer to Figures 20-27).

The light rare earth element (LREE) abundances are generally incompatible with the oxide minerals, and their variable abundances might reflect distinct source areas. Plots of the LREE (La-Sm) abundances as a function of latitude (Figures 20, 21, and 22) can be used to discriminate distinct geochemical source terranes. Low values of La, Ce, and Sm generally reflect the Klamath Mountain source (42-43°), slightly higher values (La, Ce, and Sm) occur to the south around 41° possibly reflecting the Eel River draining the California Coast range. Maximum values of La (56 ppm), Ce (112 ppm), and Sm (9 ppm) are associated with a sample collected offshore of the Columbia River (46°). Figures 23-27 show the variation of Eu and Yb, Hf, and Ta-HREE (heavy rare earth element) respectively as a function of latitude. The high values of Eu (1.4-1.8 ppm, Figure 23) clearly define the opaque oxides derived from the

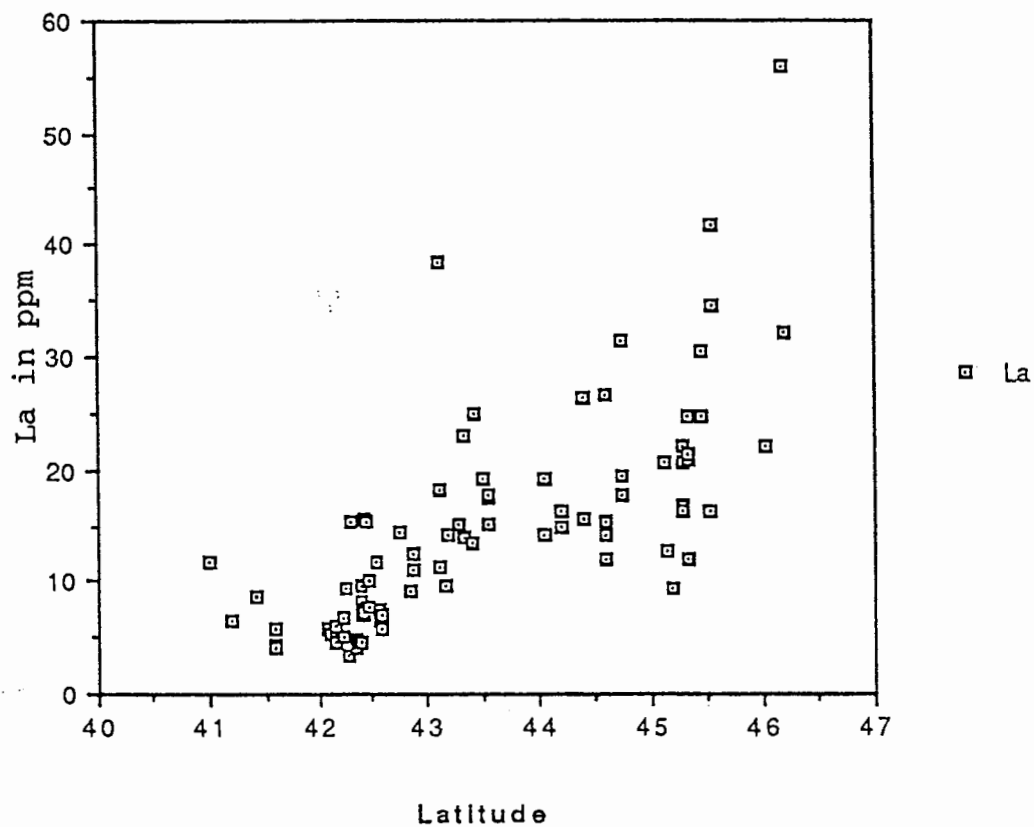


Figure 20. Plot of Lanthanum Elemental Abundance as a Function of Degrees Latitude.

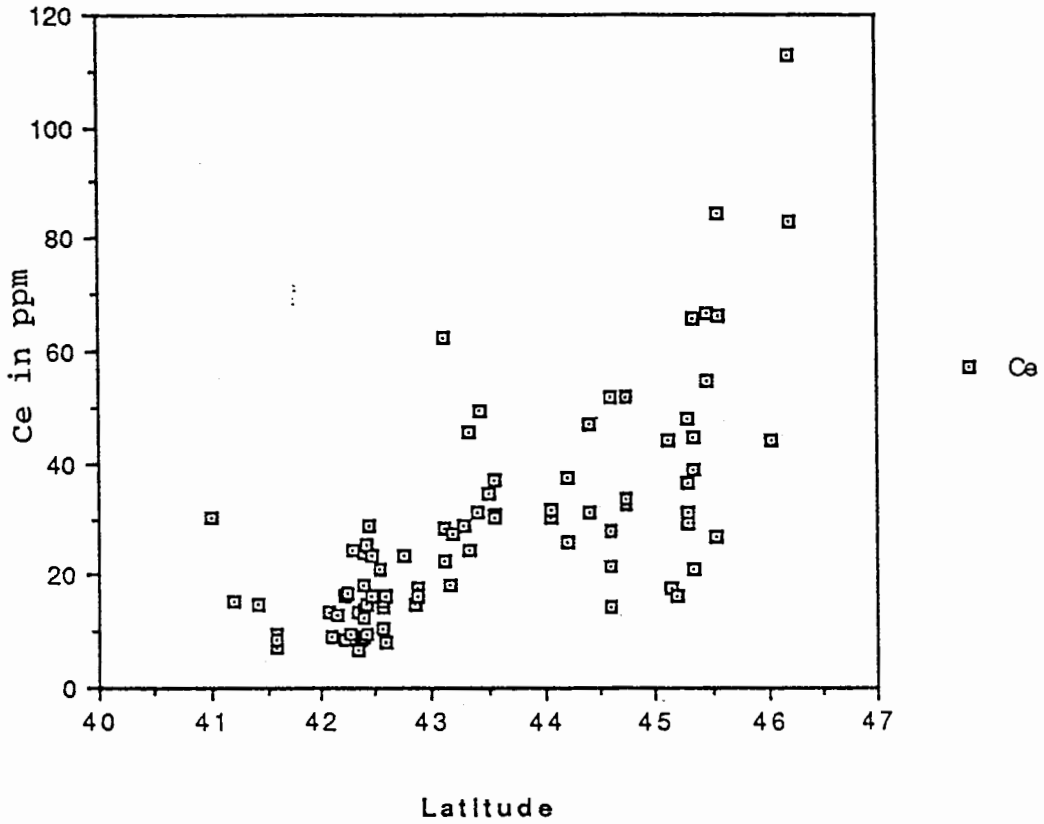


Figure 21. Plot of Cerium Elemental Abundance as a Function of Degrees Latitude.

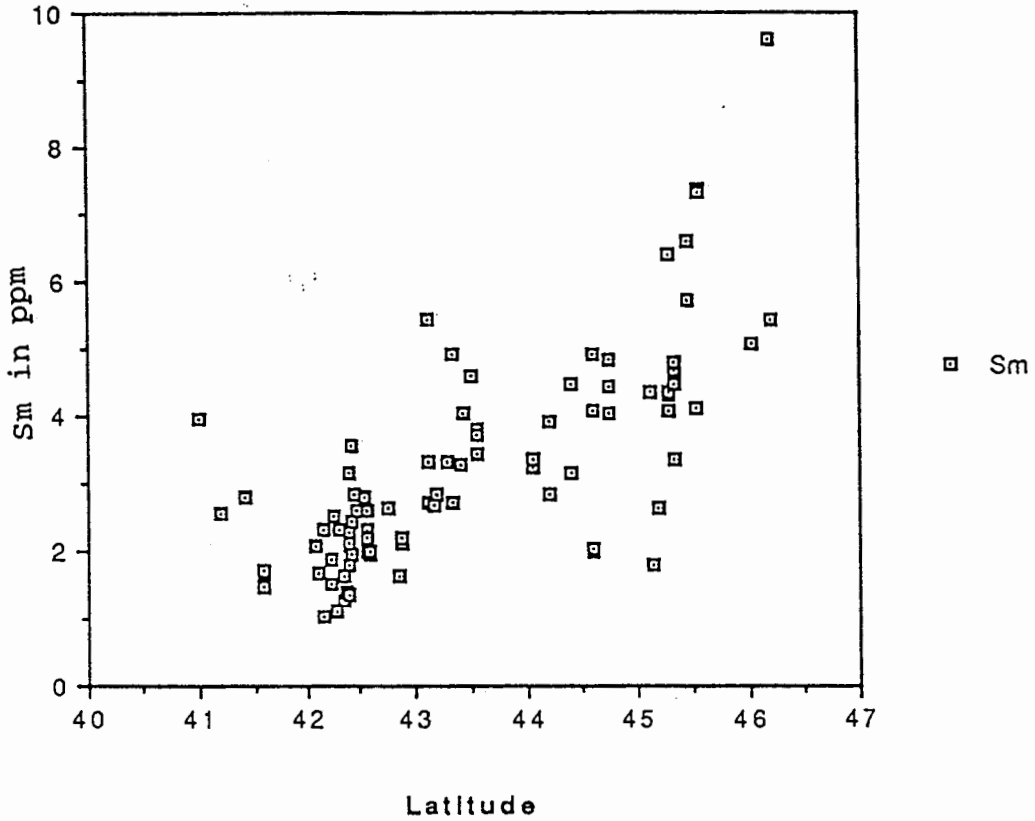


Figure 22. Plot of Samarium Elemental Abundance as a Function of Degrees Latitude.

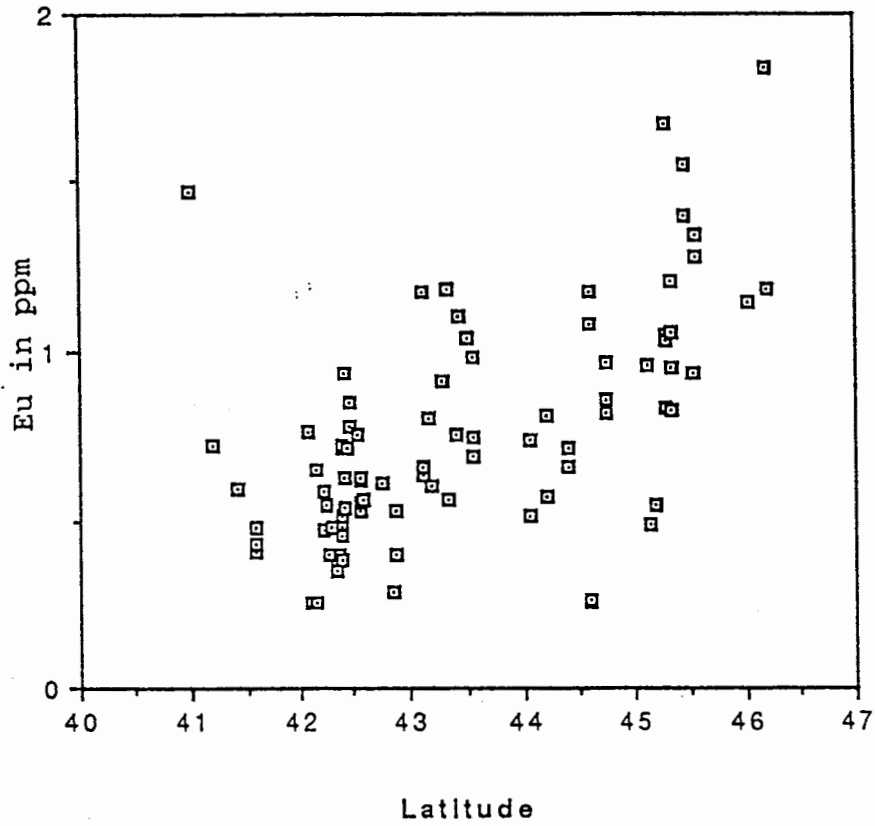


Figure 23. Plot of Europium Elemental Abundance as a Function of Degrees Latitude.

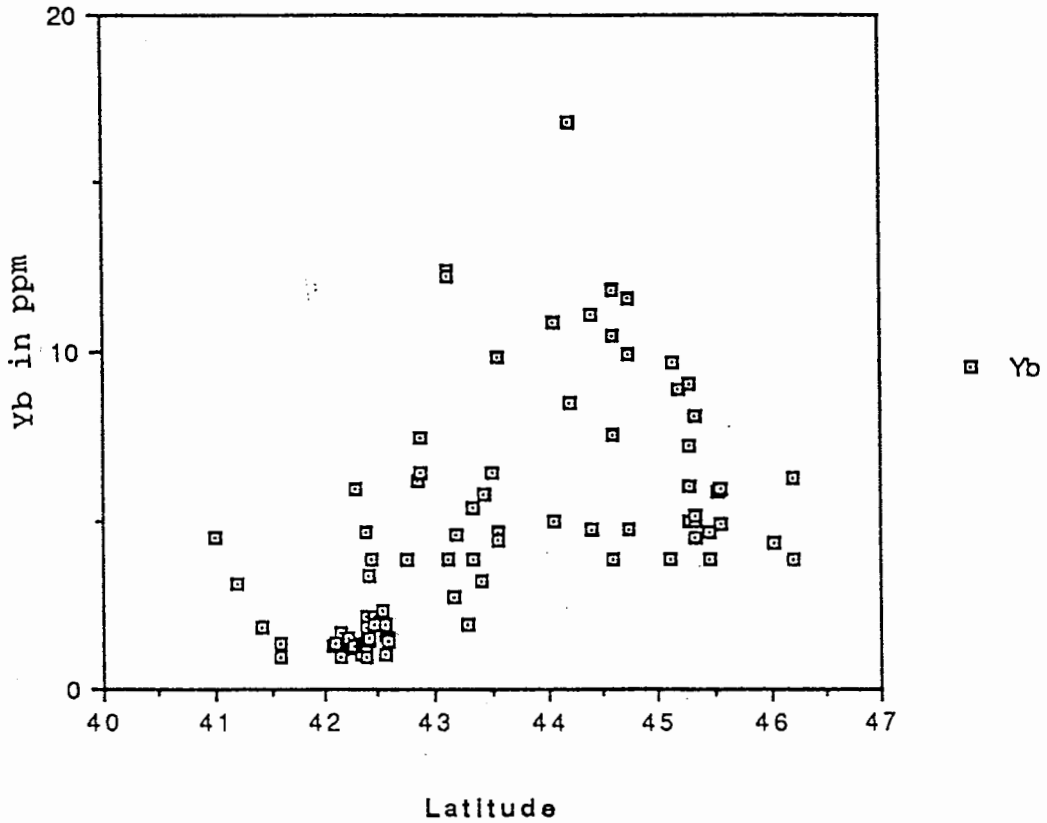


Figure 24. Plot of Ytterbium Elemental Abundance as a Function of Degrees Latitude.

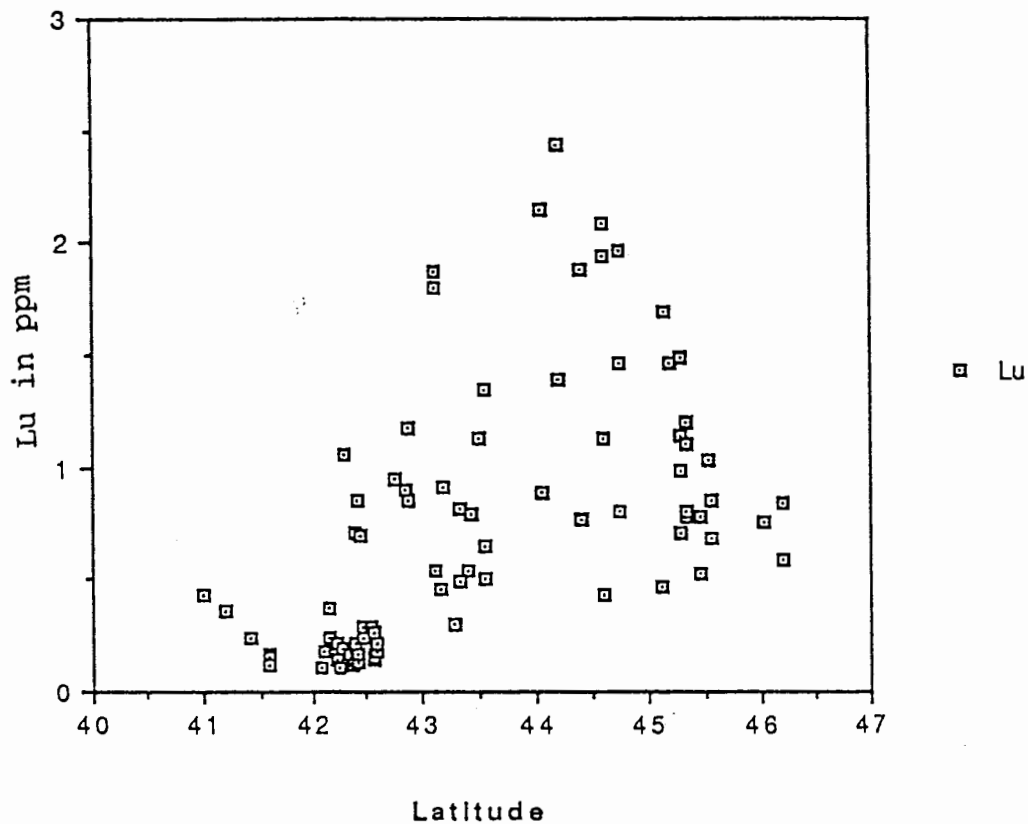


Figure 25. Plot of Lutecium Elemental Abundance as a Function of Degrees Latitude.

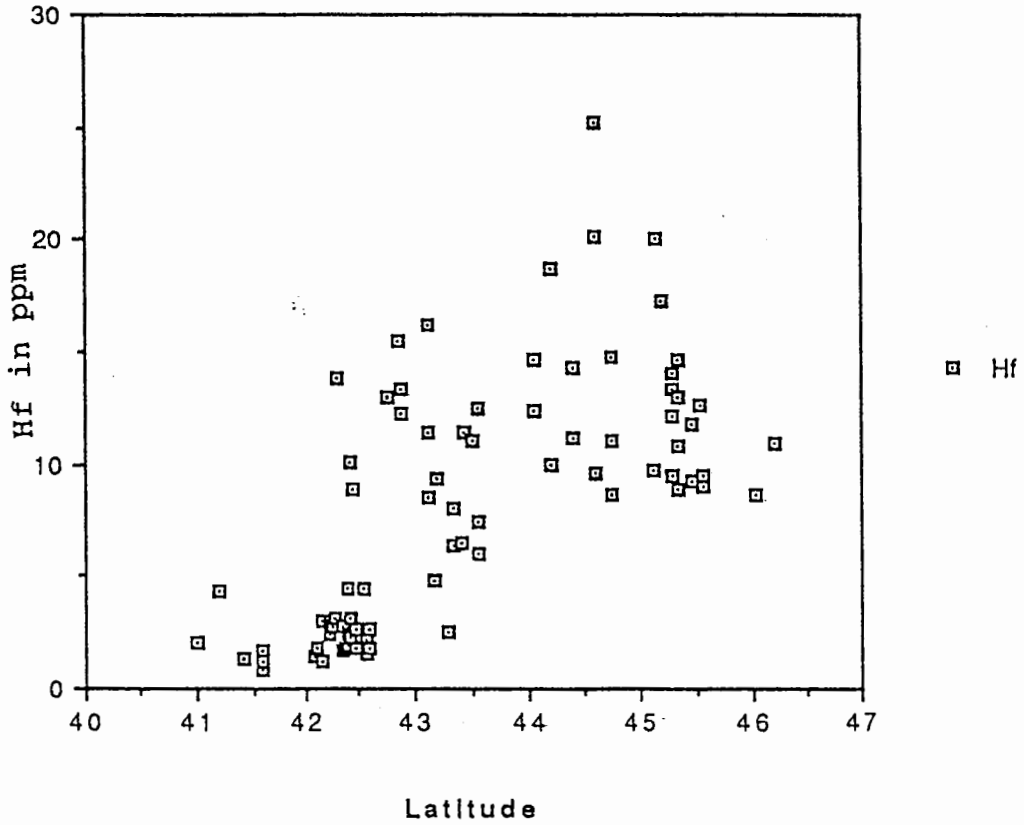


Figure 26. Plot of Hafnium Elemental Abundance as a Function of Degrees Latitude.

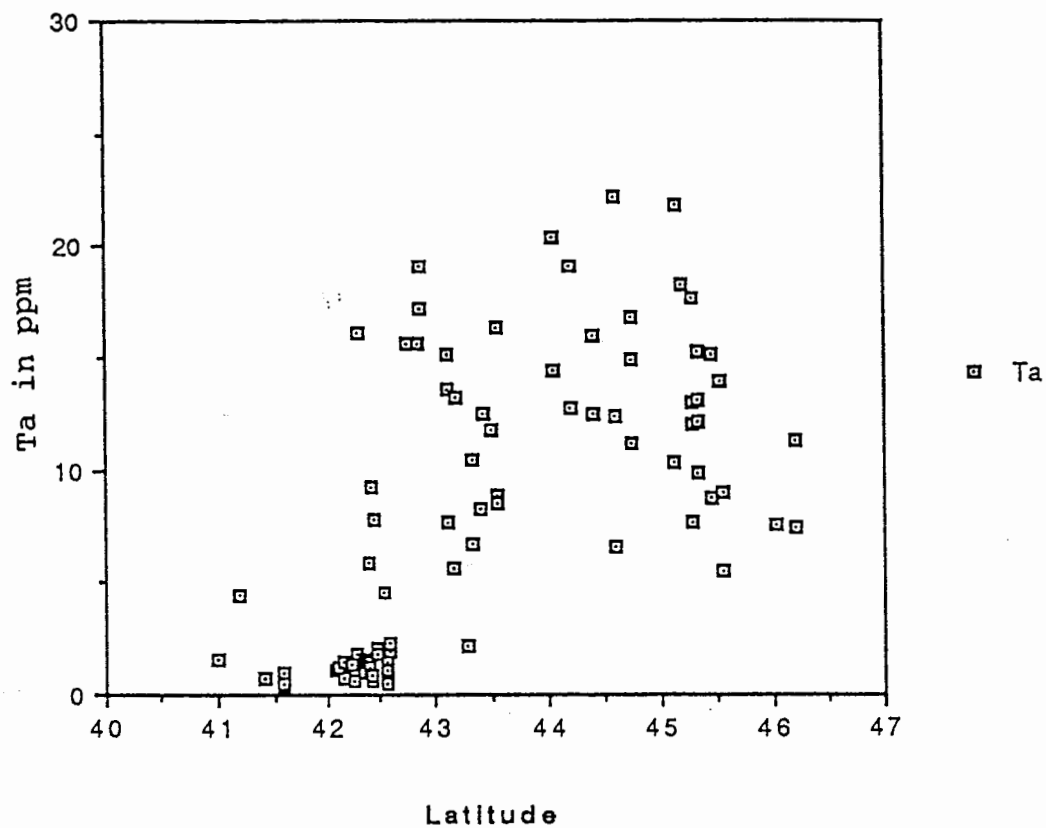


Figure 27. Plot of Tantalum Elemental Abundance as a Function of Degrees Latitude.

most southern drainage (south of 41°) and from the Columbia-River source north of 46°. In contrast, maximum values of Yb, Lu, and Hf-HREE (Figures 24-27) reflect the northern Coast Range basalts, and not the Columbia River source. The Ta-HFSE (high field strength element) follows the high ilmenite abundance from the Oregon coast range as noted previously.

The chondrite-normalized REE distribution patterns for shelf opaque oxides are shown in Figures 28-30. The chondritic values used are those determined by Taylor and McLennan, 1985. The chondrite-normalized REE distribution patterns for shelf opaque oxide minerals derived from discrete source provinces i.e., Klamath Mountain, Coast Range and Columbia River respectively, demonstrate (Figures 28-30) generally similar fractional crystallization and differentiation processes. Although, the LREE distributions are very slightly enriched for Coast Range and Columbia River provinces relative to the Klamath provenance.

Since, the REE's have not fractionated relative to each other, REE ratios (La/Sm, La/Yb and Ce/Yb) are used to trace the source of opaque oxides. High values of (> 7.0) of La/Sm ratio (Figure 31) indicate the greatest degree of LREE enrichment. High values of La/Yb and Ce/Yb ratios (Figures 32-33) for bulk opaque oxides reflect the accreted source terrains associated with Klamath and Coast Range basalts.

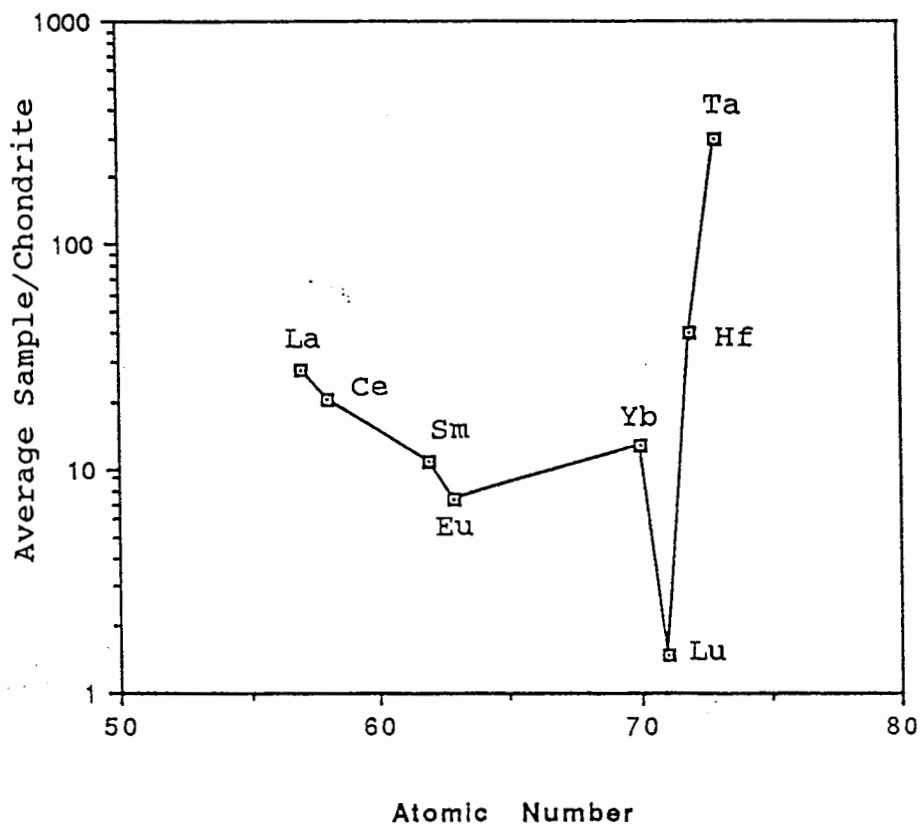


Figure 28. Chondrite-Normalized REE Distributions in Shelf Opaque Oxide Minerals Derived from Klamath Mountain Provenance (north of 41-42 degrees latitude).

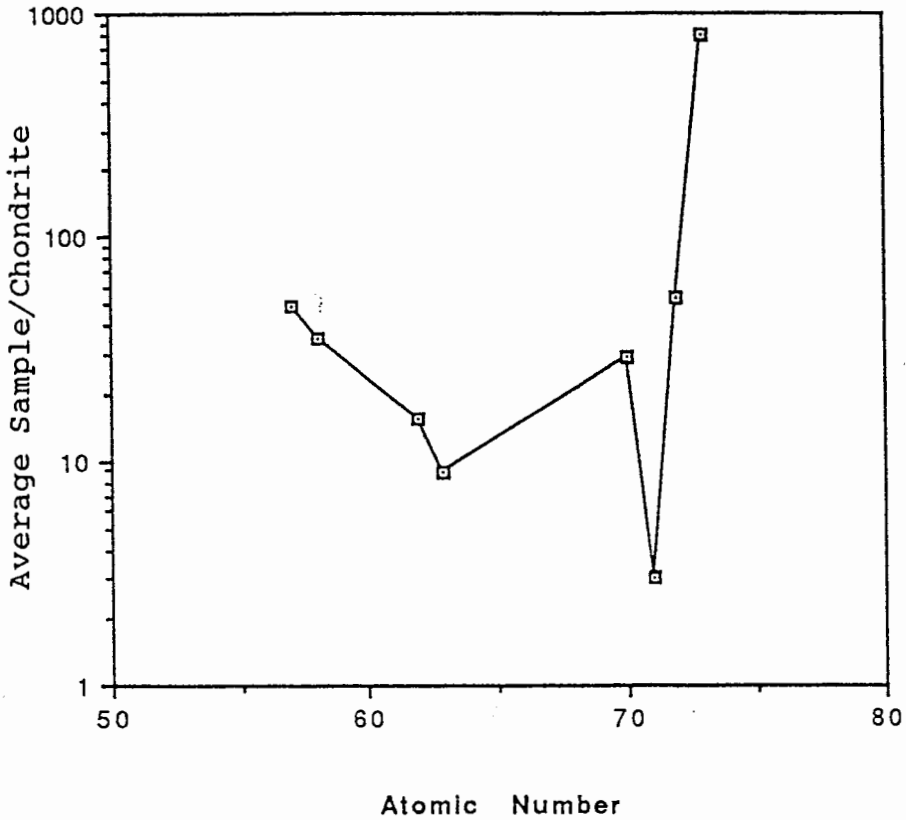


Figure 29. Chondrite-Normalized REE Distributions in Shelf Opaque Oxide Minerals Derived from Coast Range Provenance (north of 43-44 degrees latitude).

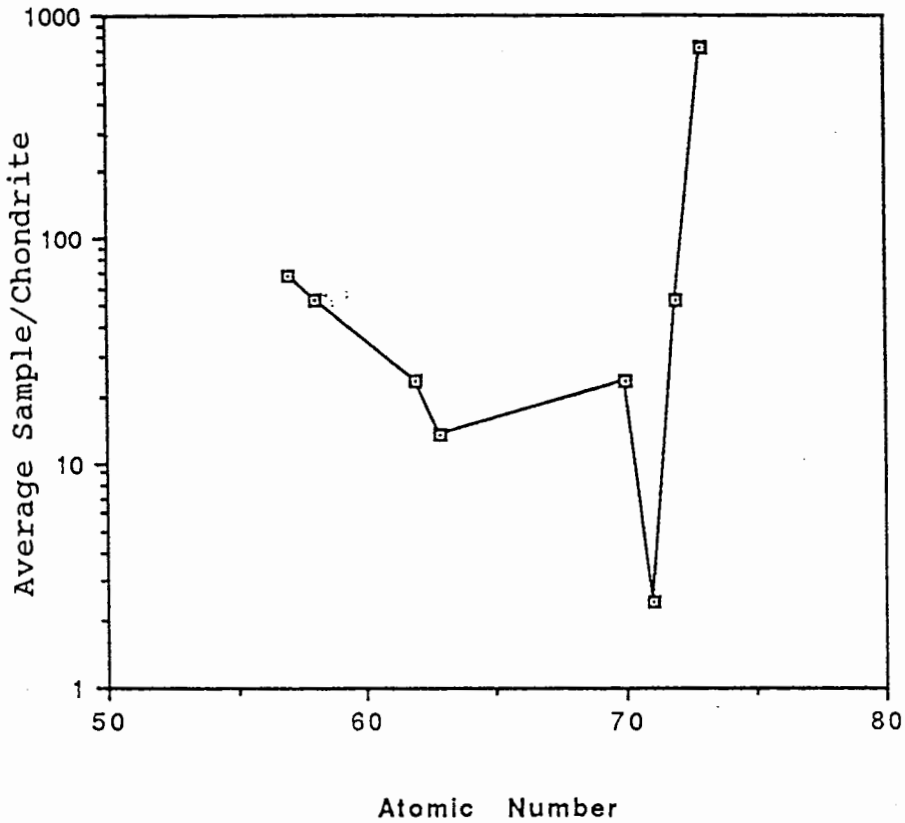


Figure 30. Chondrite-Normalized REE Distributions in Shelf Opaque Oxide Minerals Derived from Columbia River Provenance (north of 45-46 latitude).

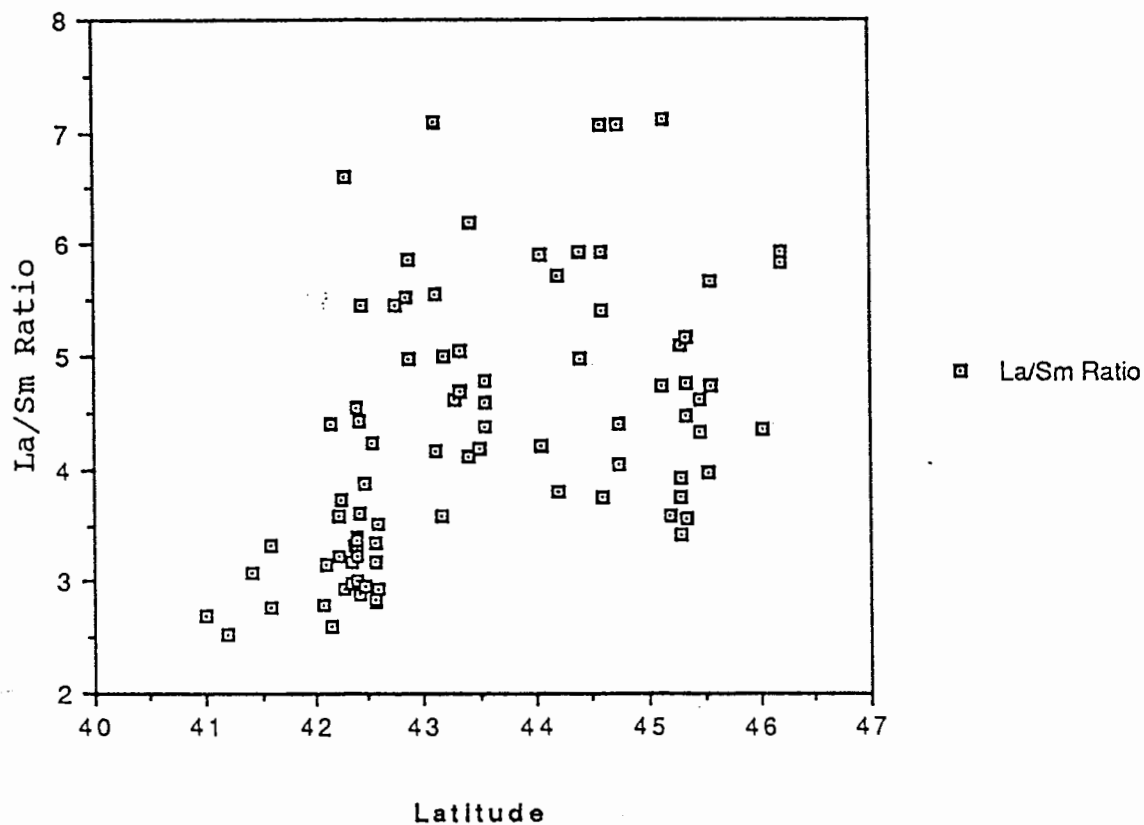


Figure 31. Distributions of Shelf Opaque Oxide Minerals on a La/Sm Ratio vs Latitude Diagram.

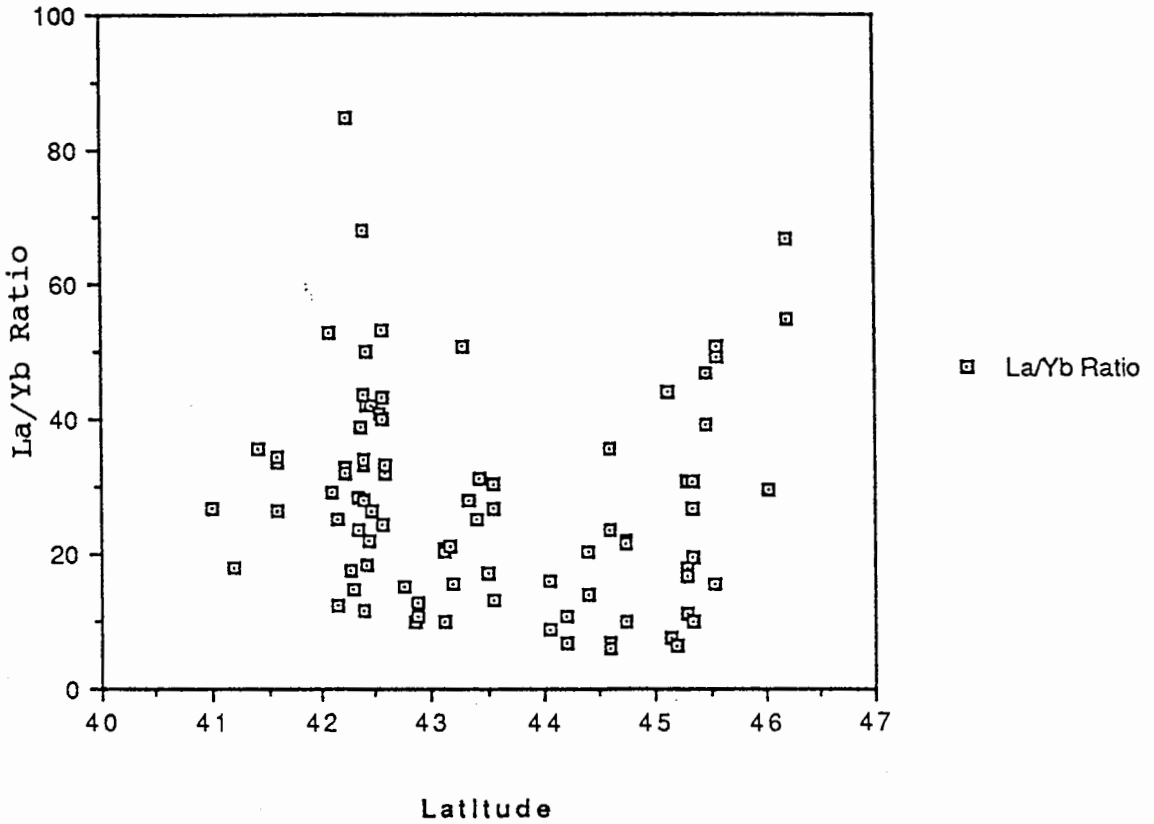


Figure 32. Distributions of Shelf Opaque Oxide Minerals on a La/Yb Ratio vs Latitude Diagram.

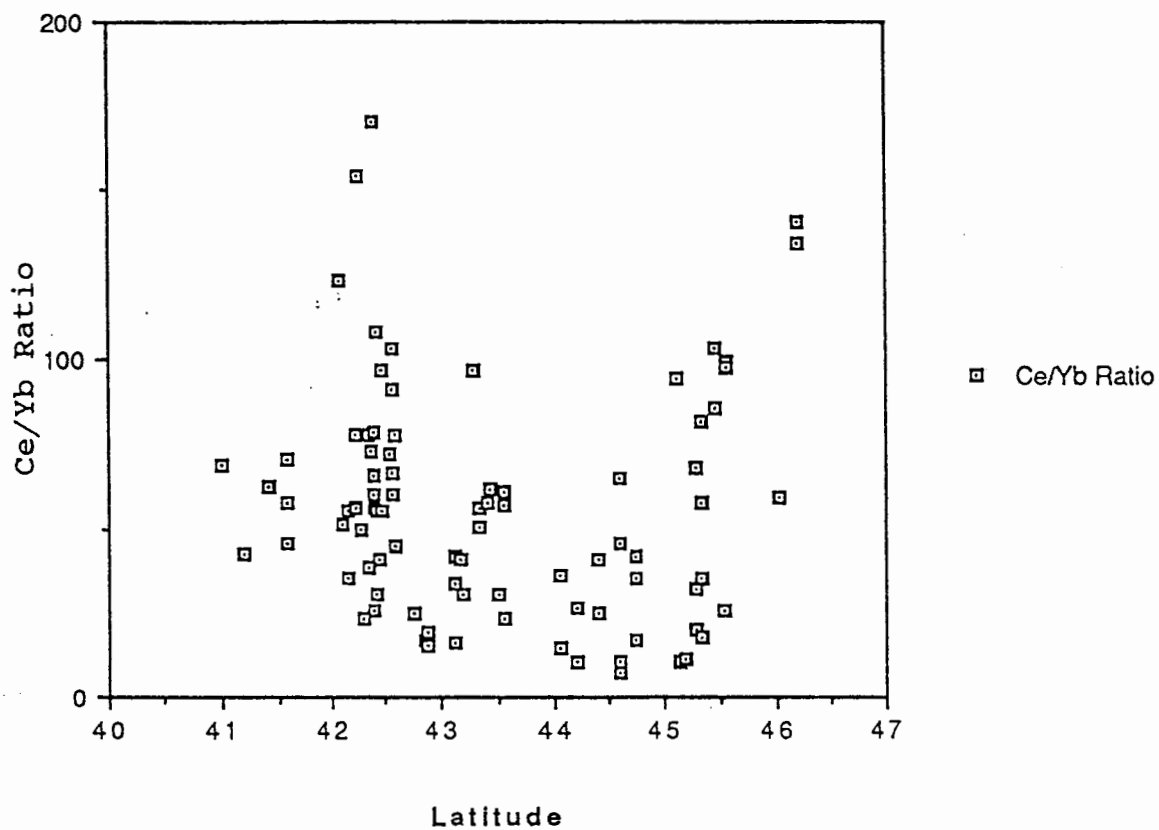


Figure 33. Distributions of Shelf Opaque Oxide Minerals on a Ce/Yb Ratio vs Latitude Diagram.

MINERAL-GRAIN HYDRODYNAMIC RELATIONS

An understanding of the relative abundances of opaque minerals in different grain size distributions is needed to evaluate potential mineral sorting mechanisms across the river-beach-shelf environments of the continental margin.

One river (Sixes) of the south-central Oregon coast was sampled for detailed analysis of mineral-grain size relations. Composite samples include fine to coarse sediments from channel axis, point bar and flood over-bank deposits. The composite river sample (1 kg) was sieved for three representative grain size ranges, 300-250 microns, 175-125 microns and less than 75 microns. The sample splits were processed for opaque mineral splits in Sodium Polytungstate solution (refer to Sample Preparation) and were mounted and polished for mineral-size analysis by SEM/microprobe EDX. Initial results from the Sixes River are shown in Table IV. Chromite rather than ilmenite seems to be preferentially concentrated in the finer grain size fractions for this river. The hypothesis that coarse grained chromite from coarse grained source rocks would be selectively deposited in beach deposits at the expense of fine grained ilmenite (Peterson and Binney, 1988) is not supported by these results. Relatively high ilmenite values in shelf sediments must reflect shelf dispersal patterns

TABLE IV

PRELIMINARY GRAIN SIZE FREQUENCIES OF OPAQUE MINERAL
DISTRIBUTIONS IN THE SIXES RIVER, OREGON

Grain Size (microns)	Magnetite	Ilmenite	Chromite
300 - 250	45%	45%	10%
175 - 125	19%	31%	50%
< 75	33%	-	66%

patterns that differ from those of modern beach deposits.

High concentrations of heavy minerals occur as isolated placer deposits on modern beaches and in Pleistocene beach terraces of the Pacific Northwest (PNW). The top, bottom and middle of six box cores (maximum penetration of 40 cm; Figure 34) showing increasing heavy mineral content with depth are chosen to calculate grain size statistics of quartz and magnetite grains. These results are used to evaluate settling velocity equivalence and critical shear stress values of the light and heavy minerals. The results from this analysis should help to test the onshore versus offshore origins of the shelf placers.

The modified Gibb's equation (Komar, 1981) for the grain settling velocities was used to calculate hydrodynamic settling velocities for quartz and magnetite respectively. The analysis of the quartz-density grains have yielded an average $R_v = 1.0269$. Average R_v values for a range of grain densities provided by Komar (1981), were used in equation (1) to reduce systematic errors in the evaluation of grain settling rates in water,

$$W_g = \frac{-3\mu + \sqrt{9\mu^2 + gr^2\rho(\rho_s - \rho)(0.015476 + 0.19841r)}}{\rho(0.011607 + 0.14881r)} \quad (1)$$

where W_n (cm/sec) is the settling velocity, r (cm) is the sphere radius, u (poise) is the water dynamic viscosity, g (cm/sec²) is the acceleration of gravity, and ρ_s and ρ (g/cm³) are the grain and water densities respectively.

Entrainment Shear stress of measured quartz and magnetite mineral grains (Komar and Wang, 1984) is used to establish potential winnowing effects from offshore currents.

$$T_x = 0.00515g(\rho_s - \rho)Db^{0.668}[\tan(61.5(Db/ks)^{-0.3})] \quad (2)$$

where T_x is critical shear stress, g is gravitational force, Db is grain intermediate diameter, ρ is fluid density, ρ_s is grain- density, and ks is bed roughness or mean size of bed particles (Komar and Wang, 1984).

Six box core samples (6708-62B, 6708-62T, 6708-67B, 6708-67T, 6708-70B, and 6708-70T) from the inner-shelf off Cape Blanco, southern Oregon (Figure 34), were selected for analysis of heavy-mineral sorting mechanisms. Each of the six samples were split for light-, heavy-, and magnetic mineral separation. Three mineral splits, including (1) magnetite, (2) quartz, and (3) bulk, were analyzed for intermediate grain diameter (Db), based on optical micrometer measurements of at least 100 grains per sample. Magnetite grains were separated by using a hand magnet. The sample grain size distributions are shown in Table V.

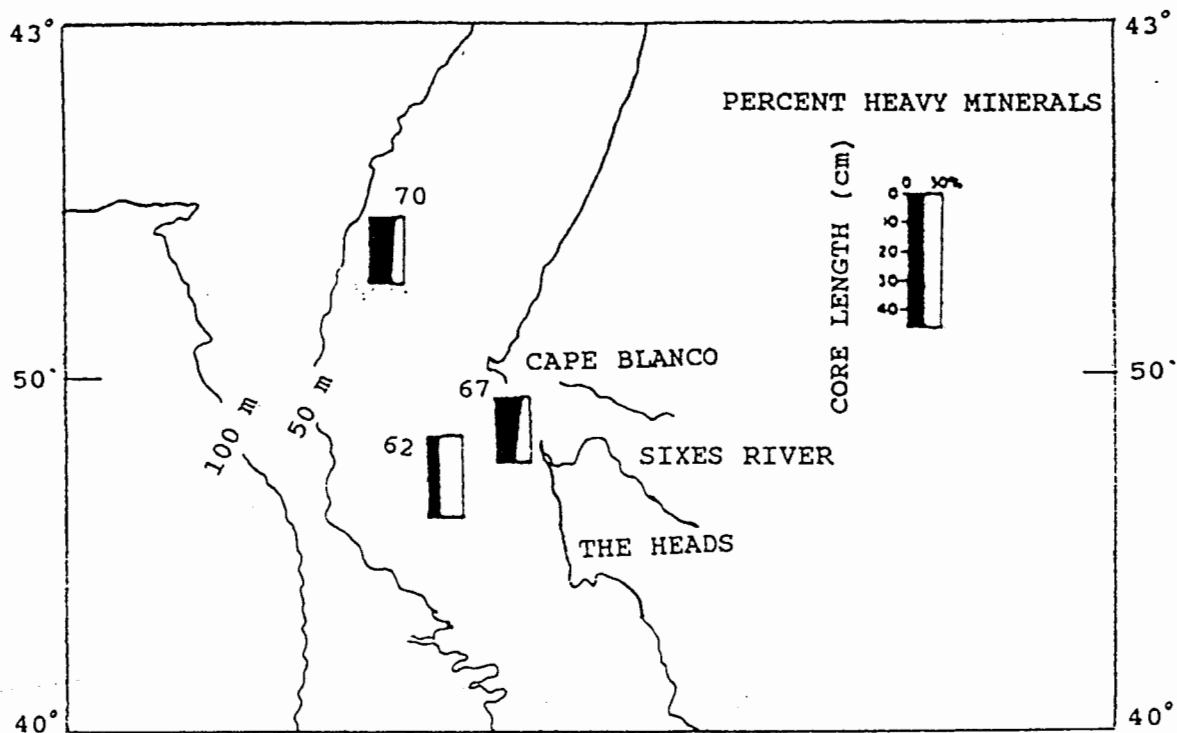


Figure 34. Location Map and Heavy Mineral Concentrations in Short Box Cores used in Mineral Grain-Size Statistics (Modified from Kulm, 1988).

TABLE V

CALCULATED STATISTICAL PARAMETERS FOR MAGNETITE, QUARTZ, AND
BULK SAMPLES FROM THE CAPE BLANCO SHELF

Magnetite

Sample number	Db	SD	Vx	Tx
6708-62B	108.20	27.721	2.06	4.17
6708-62T	108.20	29.072	2.06	4.89
6708-67B	111.60	29.910	2.18	4.26
6708-67T	103.60	25.920	1.95	3.96
6708-70B	127.30	39.870	2.67	4.13
6708-70T	127.92	34.330	2.67	3.64

Quartz

Sample number	Db	SD	Vx	Tx
6708-62B	192.70	58.532	1.64	1.40
6708-62T	244.20	65.000	3.21	1.50
6708-67B	190.40	55.470	2.24	1.43
6708-67T	190.82	44.070	2.24	1.34
6708-70B	191.30	49.455	2.23	1.46
6708-70T	219.30	53.772	2.74	1.32

TABLE V

CALCULATED STATISTICAL PARAMETERS FOR MAGNETITE, QUARTZ, AND
BULK SAMPLES FROM CAPE BLANCO SHELF
(continued)

Bulk (Opagues and Non-opagues)

Sample number	Db	SD
6708-62B	157.80	45.230
6708-62T	180.82	58.415
6708-67B	162.50	37.534
6708-67T	146.80	32.410
6708-70B	167.96	43.840
6708-70T	145.70	30.625

In addition, both grain settling velocity (V_x) and critical entrainment shear stress (T_x) are calculated (refer to Table V). The results demonstrate approximate settling velocity (V_x) equivalence, but widely different shear stress values. These results suggest the potential for a shelf winnowing process (Phillips, 1979), accompanied by local entrainment shear stress, rather than a vertical mixing of a coarser basal placer. The results from the mineral grain-size statistics are important in terms of establishing the possible origins of the continental shelf placers (see discussion).

MICROPROBE ANALYSIS OF SHELF OPAQUE MINERALS

In order to establish mineral economic grade, bulk opaque oxide splits were analyzed using the electron microprobe for approximate relative abundance of the chromium- and titanium-bearing iron oxides. The microprobe analyses of the opaque minerals included the following elements Mg, Al, Cr, Si, Ca, Ti, Mn, Fe, Zn, Co, Ni, Zr, Mo, V and Cu. Elemental compositions of separate oxide mineral phases, ilmenite, chromite and magnetite from the shelf placers; Mumford, 1991; personal communication). A total of 20 shelf samples were analyzed for opaque oxide chemistry by microprobe. Opaque mineral grains (at least 25 grains per sample) are mounted in epoxy and polished for wave length

dispersive x-ray analysis of quantitative elemental composition.

Average titanium oxide values of the ilmenite (defined as grains with >20% Ti) for the shelf samples range from 25.08 to 27.47% Ti (Table VI). The highest and lowest mean values of titanium oxide are present in the samples derived from the inner-shelf and mid-shelf areas offshore of the Rogue River. Figure 29 shows the distribution of titanium and iron concentration phases within the ilmenite (averaged) grains as a function of latitude. Trace element contaminants (Ca, Mg and Mn; Figure 30) in the shelf ilmenite grains generally totalled less than 3%. Vanadium elemental concentrations were between 1 and 2%.

The average chromium oxide values of chromite (defined as >5% Cr) from the shelf samples range from 18 to 29% Cr based on the averaged 8 chromite analyses (Table VII). The grains with 10% chromium oxide are still considered as chromites, although the low chromium grains might actually be chromiferous magnetite. Samples with significant abundances of low chromium (S48 and S51 offshore of the Rogue River) can be split into low chromium-rich oxides (<20% Cr) and high chromium oxides (>20% Cr) in Figure 31. Contaminants Al, Mg are abundant (>15%) in the analyzed chromites, while Co abundances confirm previously suggested trends of increasing Co with increasing Cr (Figure 32).

TABLE VI

MICROPROBE ANALYSIS OF AVERAGED ELEMENTAL COMPOSITIONS OF
ILMENITE FROM THE SELECTED SHELF PLACER MINERALS

	Sample	Latitude	Longitude	Mg	Al	Si	Ca
1	S68Ti	43.440	124.410	1.079	0.015	0.021	0.037
2	S16Ti	42.880	124.580	1.036	0.018	0.013	0.018
3	S17Ti	42.860	124.570	1.112	0.000	0.011	0.015
4	S56Ti	42.580	124.410	0.942	0.005	0.010	0.021
5	S51Ti	42.420	124.580	1.185	0.063	0.039	0.207
6	S48Ti	42.400	124.440	0.205	0.068	0.159	0.078
7	S39Ti	42.150	124.390	1.040	0.039	0.024	0.012
8	S5Ti	41.590	124.310	0.666	0.016	0.019	0.059

	Cu	Zn	Zr	Mo	O	Total
1	0.000	0.030	0.000	0.000	29.998	95.280
2	0.022	0.036	0.039	0.021	30.625	97.571
3	0.000	0.040	0.000	0.000	28.827	93.302
4	0.040	0.036	0.039	0.023	30.148	95.513
5	0.000	0.000	0.000	0.000	28.384	92.169
6	0.000	0.031	0.000	0.000	30.655	95.629
7	0.026	0.041	0.025	0.020	29.998	94.952
8	0.025	0.079	0.017	0.010	30.563	96.978

	Ti	V	Cr	Mn	Fe	Co	Ni
1	26.307	1.638	0.045	0.952	34.976	0.119	0.060
2	26.716	1.673	0.038	1.094	36.037	0.133	0.049
3	25.977	0.000	0.039	1.102	36.042	0.039	0.078
4	26.792	1.652	0.048	1.194	34.378	0.143	0.039
5	25.084	0.000	0.026	0.869	36.198	0.061	0.046
6	28.364	1.901	0.024	1.334	32.700	0.039	0.068
7	26.779	1.472	0.043	0.604	34.645	0.103	0.081
8	27.469	1.531	0.046	1.627	34.793	0.040	0.017

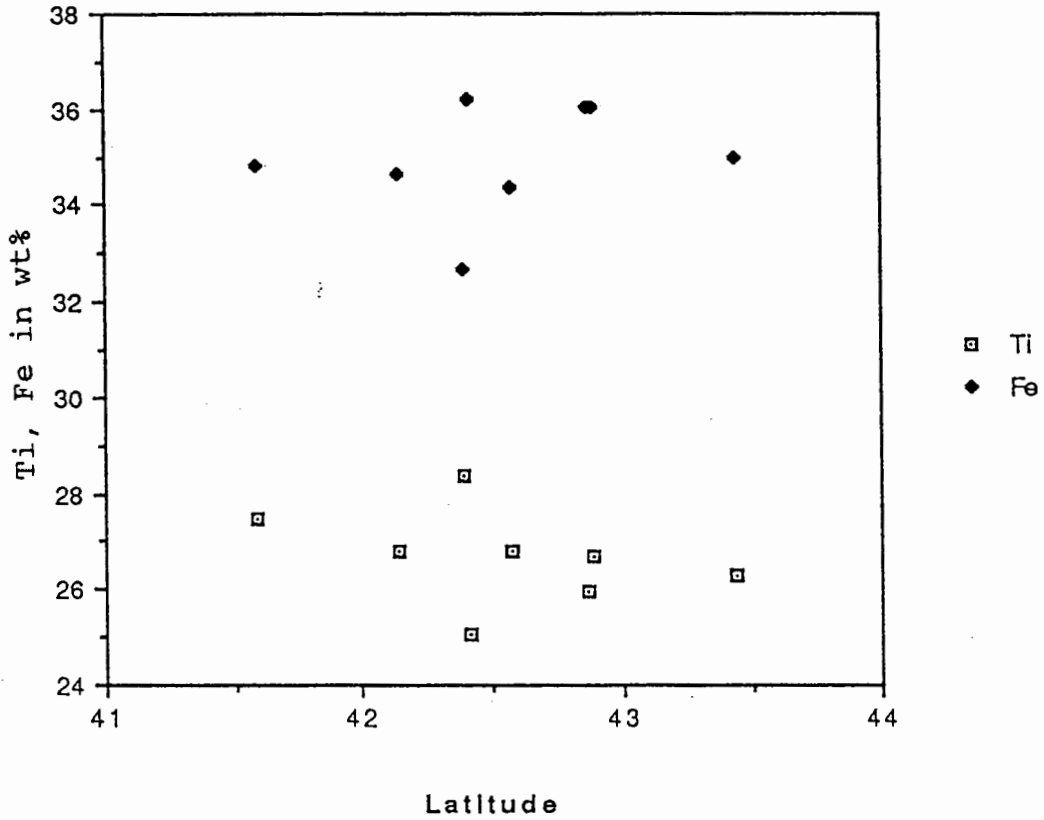


Figure 35. Major Elemental (Ti, Fe) Distributions in the Ilmenite Phase as a Function of Latitude.

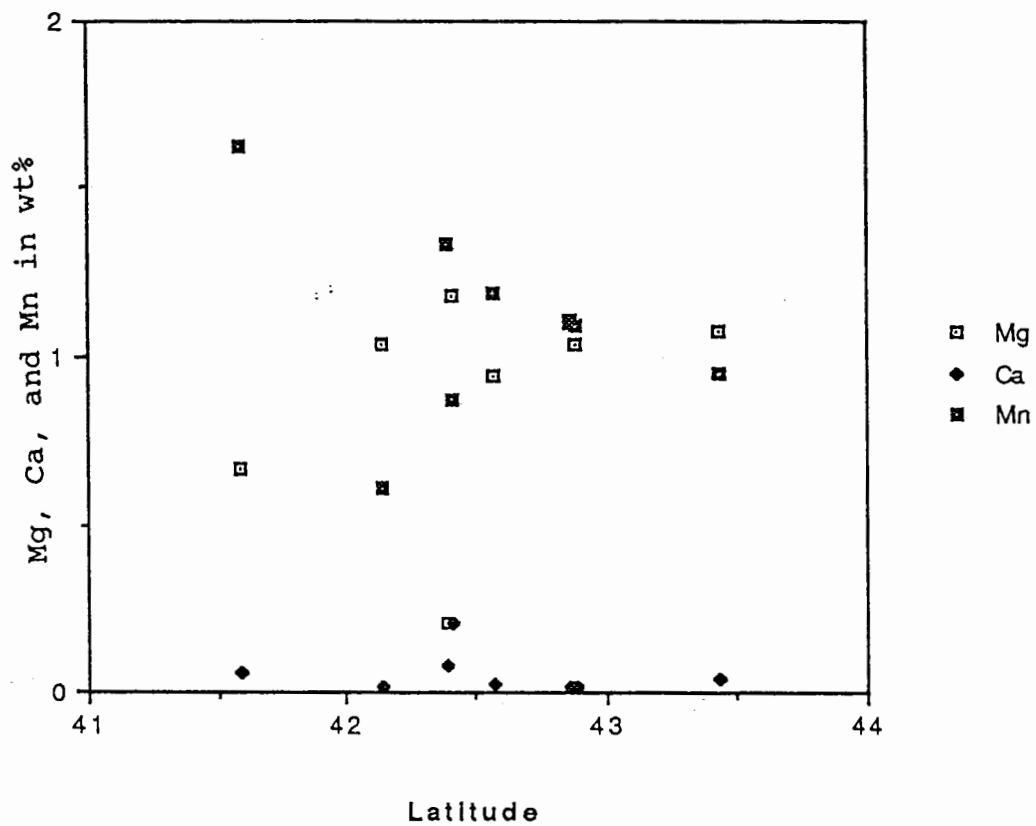


Figure 36. Trace Element Contaminants in the Shelf Ilmenite Grains as a Function of Latitude.

The average iron oxide values of magnetite from the shelf samples range from 60 to 62% (%Fe) based on 4 magnetite oxide splits (Table VIII; Figure 33 shows the distribution of Fe, Ti as a function of latitude). Relatively high titanium values (>4%) indicate the presence of magnetite/titaniferous magnetite phase transitions. Silicate contaminants V, Mn and Al in the shelf magnetite grains generally totalled less than 2%. Neither the major or minor elements in the analyzed ilmenite and chromite grains showed regional trends of abundance (north-south) associated with different source rocks over the sampled area.

TABLE VII

MICROPROBE ANALYSIS OF AVERAGED ELEMENTAL COMPOSITIONS OF CHROMITE FROM THE SELECTED SHELF PLACER MINERALS

	Sample	Latitude	Longitude	Mg	Al	Si	Ca
1	S68Cr	43.440	124.410	5.484	9.407	0.030	0.010
2	S16Cr	42.880	124.580	6.234	11.533	0.170	0.010
3	S17Cr	42.860	124.570	5.588	9.062	0.180	0.000
4	S56Cr	42.580	124.410	5.439	8.562	0.240	0.020
5	S51Cr	42.420	124.580	4.843	8.123	0.170	0.010
6	S48Cr	42.400	124.440	3.675	6.179	0.330	0.050
7	S39Cr	42.150	124.390	6.257	10.283	0.040	0.020
8	S5Cr	41.590	124.310	4.808	7.078	0.010	0.130

	Ti	V	Cr	Mn	Fe	Co	Ni
1	0.340	0.200	28.473	0.040	19.935	0.450	0.120
2	0.270	0.170	24.466	0.140	20.522	0.470	0.180
3	0.190	0.000	29.046	0.330	19.234	0.300	0.130
4	0.270	0.170	24.333	0.290	23.370	0.550	0.130
5	0.250	0.000	23.596	0.330	27.672	0.320	0.210
6	0.250	0.150	18.425	0.310	36.371	0.310	0.190
7	0.120	0.140	27.602	0.010	18.653	0.610	0.120
8	0.150	0.470	25.053	0.470	27.229	0.530	0.180

	Zn	O	Total
1	0.170	31.000	96.100
2	0.230	32.000	96.800
3	0.240	31.000	95.600
4	0.230	30.000	93.700
5	0.130	30.000	95.500
6	0.220	28.000	94.200
7	0.180	32.000	95.900
8	0.290	30.000	95.900

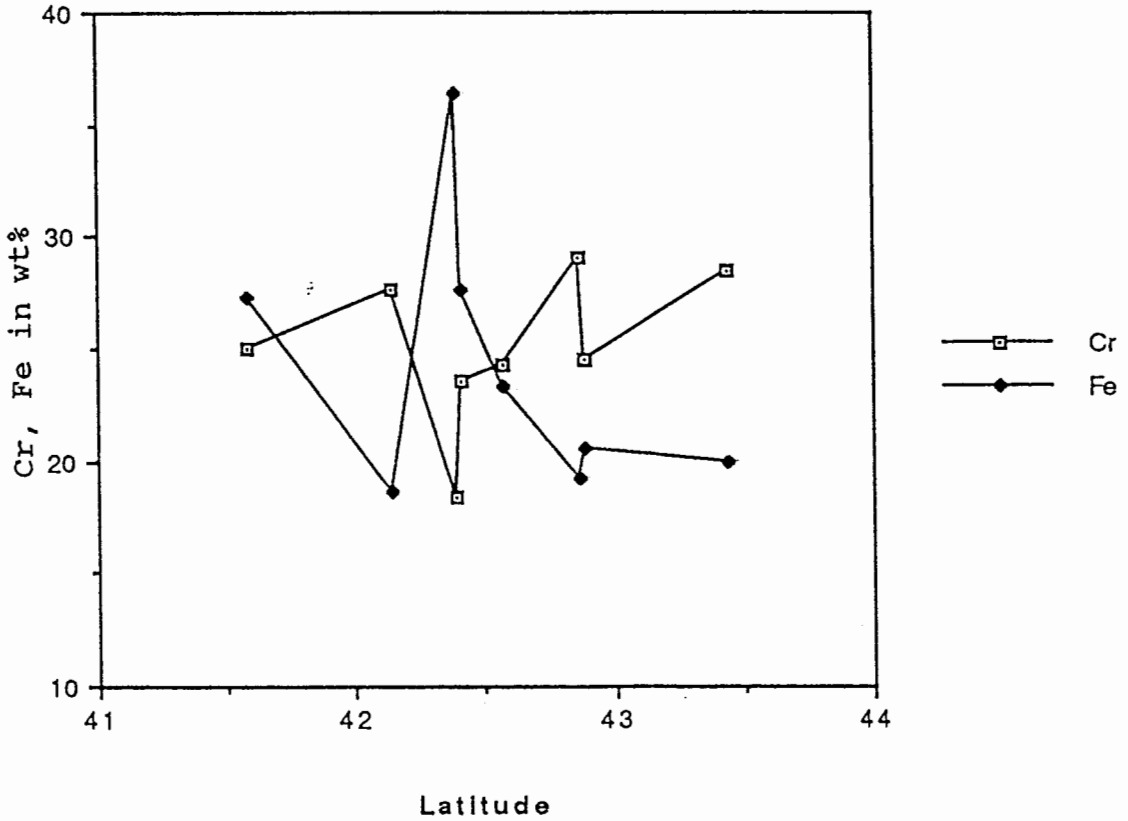


Figure 37. Major Elemental (Cr, Fe) Distributions in the Chromite Phase as a Function of Latitude.

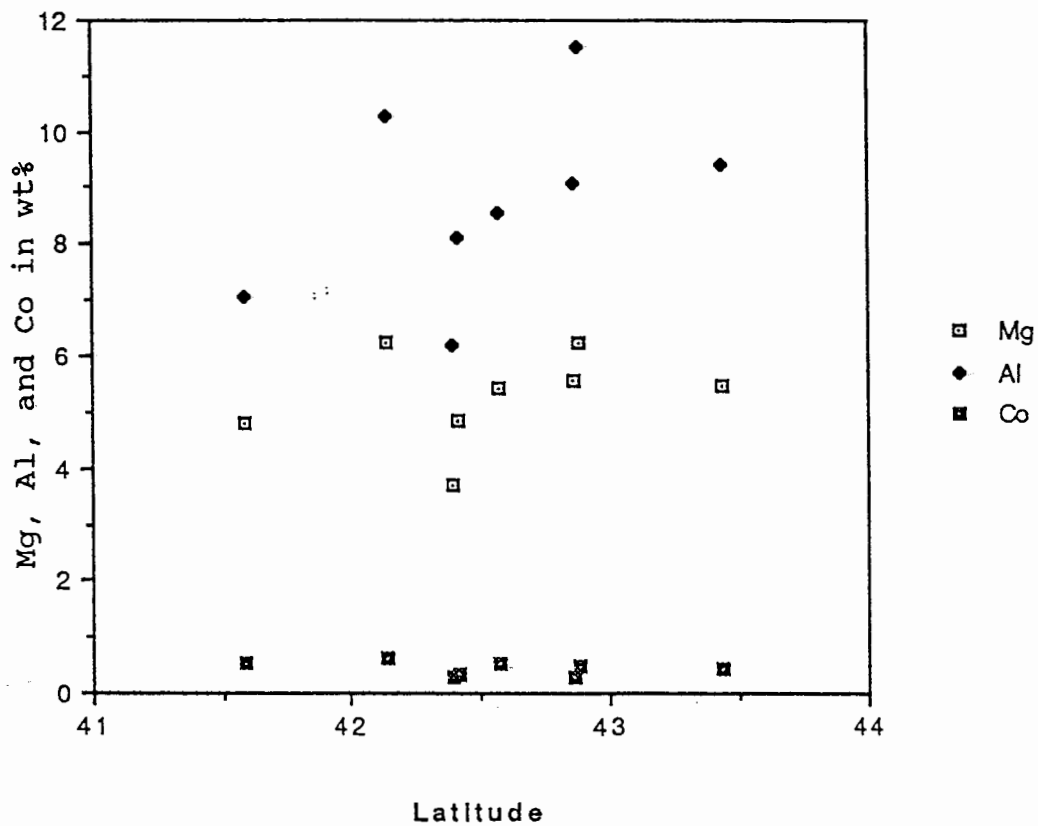


Figure 38. Trace Element Contaminants in the Shelf Chromite Grains as a Function of Latitude.

TABLE VIII

MICROPROBE ANALYSIS OF AVERAGED ELEMENTAL COMPOSITONS OF
MAGNETITE FROM THE SELECTED SHELF PLACER MINERALS

	Sample	Latitude	Longitude	Mg	Al	Si	Ca
1	S68Mag	43.440	124.41	0.46	0.59	0.06	0.157
2	S17Mag	42.860	124.57	0.42	0.47	0.05	0.021
3	S51Mag	42.420	124.58	0.86	0.81	0.11	0.015
4	S48Mag	42.400	124.44	0.68	0.85	0.24	0.037

	Ti	V	Cr	Mn	Fe	Co	Ni
1	4.820	0.650	0.123	0.300	60.107	0.141	0.073
2	4.638	0.000	0.306	0.160	61.478	0.129	0.138
3	3.625	0.000	0.120	0.290	62.295	0.100	0.122
4	1.886	0.430	0.276	0.160	62.638	0.117	0.107

	Zn	O	Total
1	0.073	22.065	94.417
2	0.049	21.736	89.417
3	0.039	21.892	90.275
4	1.598	21.659	89.249

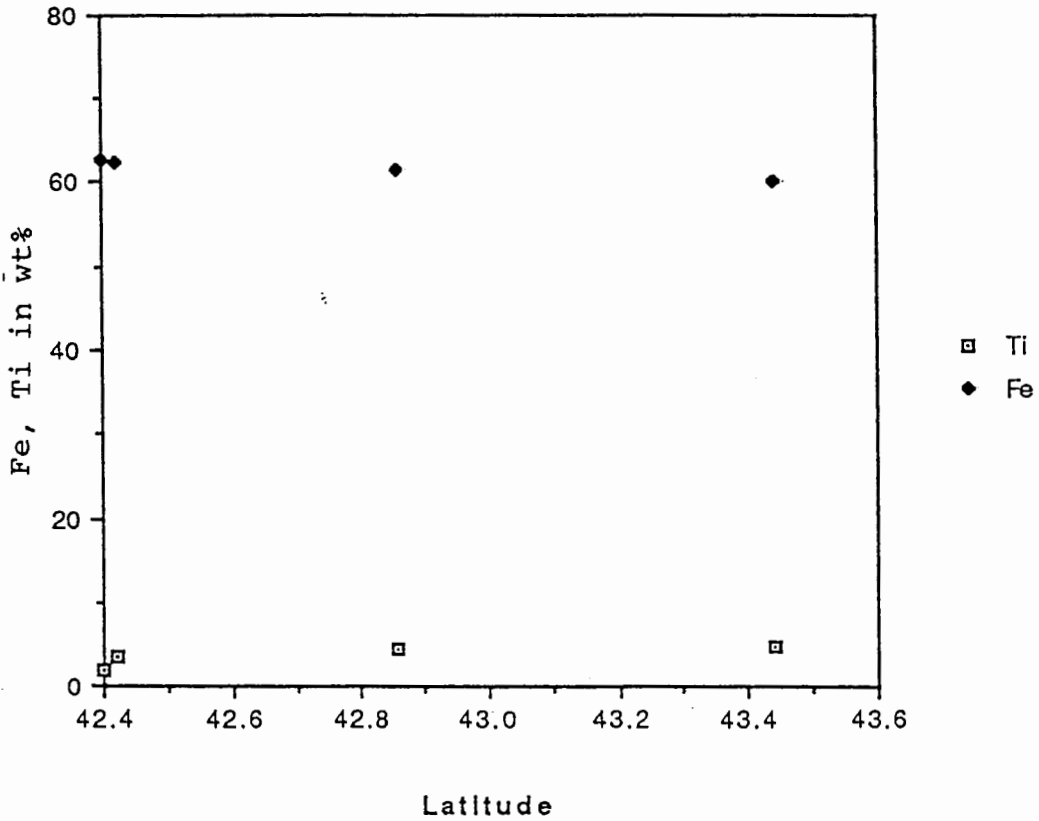


Figure 39. Major Elemental (Fe, Ti), Distributions in the Magnetite Phase as a Function of Latitude.

CHAPTER VII

DISCUSSION

SHELF OPAQUE DISPERSAL PATTERNS (Q-MODE FACTOR ANALYSIS)

In order to establish shelf opaque oxide dispersal patterns elemental compositions (INAA analysis) of 125 opaque mineral splits from the Oregon shelf, river, and beach sites have been analyzed by multivariate analysis. Q-mode factor analysis was performed on the compositional data using the extended CABFAC program to identify potential end-member sources (Klovan and Meisch, 1976). Element abundances were normalized by their corresponding range of values so that major and trace elements are not underrepresented in the factor analysis. Multivariate (Q-mode) was performed on the shelf opaque oxide geochemical data, as well as on a combined shelf-beach-river data set. Table IX shows the general statistics of the opaque oxide compositions, including the average relative abundances of 21 various elements. Analysis of the combined shelf-river-beach data set yielded four factors accounting for 99% of

TABLE IX

GENERAL STATISTICS FOR ELEMENT ABUNDANCES IN SHELF OPAQUE SEPARATES

	VARIABLE	AVERAGE	STANDARD DEVIATION	MINIMUM VALUE	MAXIMUM VALUE
1					
2	Na	1753.85	1131.58	205.00	4980.20
3	Mg	46987.34	25648.04	3500.00	144350.00
4	Al	20145.96	7157.06	2364.00	38053.00
5	Ca	21045.86	14341.98	1821.00	72635.00
6	Sc	47.96	17.76	3.80	76.70
7	Ti	101940.55	66757.67	110804.00	266139.00
8	V	1468.70	1288.20	520.80	15150.00
9	Cr	27319.36	26798.33	606.00	129498.00
10	Mn	6373.38	2526.22	2560.40	16787.40
11	Fe	344806.88	61305.32	192957.00	510830.00
12	Co	123.84	54.04	42.90	366.90
13	As	6.47	4.08	1.66	38.56
14	Sb	1.19	0.77	0.23	5.61
15	La	13.55	9.14	1.36	55.97
16	Ce	25.26	17.93	3.66	112.67
17	Sm	2.94	1.62	0.48	9.59
18	Eu	0.70	0.37	0.09	1.84
19	Yb	4.39	3.73	0.41	23.42
20	Lu	0.76	1.01	0.09	9.57
21	Hf	8.94	6.74	0.66	29.60
22	Ta	8.31	6.98	0.31	30.82

the element composition variance. Initial model runs based on additional factors did not produce significantly different results from the four factor models. The specific element contributions (factor scores) to the four factors are presented in Table X.

The sample factor scores and factor loadings for the combined onshore/offshore data set are presented in Table XI. The first factor (28.8% of the variance) contains high scores for Cr, Al, Co, Fe and Sb. The second factor (33.4% of the variance) includes high scores for Ti, Hf, Sc, Ta and Fe. The third factor (14.3% of the variance) contains high scores for Na, Mg, Al, Ca and Sc. The fourth factor (19.7% of the variance) includes high scores for Na, and LREE- La, Ce, Sm and Eu (light rare earth-elements).

The factor loadings are plotted as a function of sample latitude to portray the regional variation in the contribution of each end-member source (dispersal patterns on the shelf). The first factor shows maximum loadings south of 43° and probably represents a Klamath Mountain source, because it is uniquely enriched in Cr, Co, Al and Sb (Figure 34). The second factor shows maximum loadings between 42.50° and 45.50° and it is uniquely enriched in Ti, Hf, Sc and Ta (Figure 41), and probably represents a Coast Range source. The second factor loadings in northern Oregon reach a minimum at 46° , reflecting the dilution to the north by the continental Columbia River drainage which supplies

ELEMENT FACTOR SCORES FOR THE COMBINED RIVER, BEACH, AND SHELF SAMPLE SET

	Sample	Latitude	Longitude	Factor 1	Factor 2	Factor 3	Factor 4
1	S-1	41.00	124.18	0.330	0.201	0.605	0.559
2	S-2	41.20	124.18	0.609	0.487	0.417	0.406
3	S-3	41.42	124.17	0.476	0.226	0.725	0.421
4	S-4	41.59	124.36	0.491	0.205	0.766	0.345
5	S-5	41.59	124.31	0.537	0.231	0.736	0.313
6	S-6	41.59	124.16	0.551	0.228	0.734	0.305
7	S-7	42.08	124.39	0.379	0.196	0.804	0.379
8	S-8	42.29	124.50	0.394	0.840	0.233	0.269
9	S-9	42.28	124.43	0.828	0.367	0.307	0.272
10	S-10	42.58	124.41	0.580	0.324	0.579	0.455
11	S-11	42.56	124.38	0.560	0.269	0.621	0.445
12	S-12	42.57	124.55	0.535	0.283	0.594	0.508
13	S-13	42.57	124.48	0.565	0.260	0.644	0.425
14	S-14	42.53	124.71	0.522	0.431	0.531	0.498
15	S-15	42.87	124.61	0.346	0.867	0.231	0.239
16	S-16	42.88	124.58	0.388	0.857	0.239	0.219
17	S-17	42.86	124.57	0.452	0.840	0.225	0.183
18	S-18	43.16	124.70	0.471	0.480	0.567	0.463
19	S-19	43.20	124.45	0.483	0.726	0.280	0.390
20	S-20	43.35	124.41	0.532	0.649	0.355	0.403
21	S-21	43.56	124.51	0.485	0.516	0.477	0.515
22	S-22	43.56	124.37	0.458	0.587	0.404	0.524
23	S-23	43.56	124.14	0.298	0.813	0.288	0.383
24	S-24	44.20	124.41	0.321	0.650	0.425	0.498
25	S-25	44.39	124.60	0.422	0.652	0.408	0.472
26	S-26	44.38	124.27	0.304	0.762	0.262	0.472
27	S-27	44.58	124.17	0.244	0.937	0.146	0.177
28	S-28	45.11	124.22	0.389	0.564	0.379	0.613
29	S-29	45.35	124.40	0.334	0.553	0.390	0.643
30	S-30	45.35	124.26	0.330	0.605	0.331	0.640
31	S-31	45.35	124.12	0.307	0.628	0.353	0.609
32	S-32	45.35	123.97	0.277	0.764	0.341	0.448
33	S-33	45.56	124.28	0.292	0.415	0.246	0.806
34	S-34	46.20	124.26	0.329	0.556	0.196	0.719
35	S-35	46.20	124.29	0.205	0.383	0.255	0.844
36	S-37	42.10	124.37	0.787	0.331	0.436	0.268
37	S-38	42.15	124.39	0.428	0.249	0.776	0.370
38	S-39	42.15	124.37	0.873	0.381	0.167	0.204
39	S-40	42.21	124.41	0.692	0.286	0.344	0.264
40	S-41	42.35	124.44	0.828	0.350	0.347	0.261
41	S-43	42.35	124.46	0.777	0.306	0.439	0.321
42	S-44	42.36	124.46	0.780	0.323	0.437	0.303
43	S-45	42.39	124.46	0.810	0.326	0.358	0.305
44	S-46	42.39	124.56	0.678	0.347	0.464	0.424
45	S-47	42.23	124.56	0.580	0.409	0.405	0.410
46	S-48	42.40	124.44	0.677	0.311	0.535	0.386
47	S-49	42.40	124.44	0.684	0.339	0.441	0.460
48	S-50	42.42	124.58	0.675	0.327	0.469	0.441
49	S-51	42.42	124.54	0.656	0.381	0.403	0.465
50	S-52	42.25	124.54	0.648	0.361	0.446	0.469
51	S-53	42.47	124.65	0.575	0.338	0.531	0.510
52	S-54	42.47	124.65	0.615	0.353	0.485	0.506
53	S-55	42.57	124.48	0.685	0.146	0.492	0.455
54	S-56	42.58	124.41	0.595	0.298	0.596	0.428
55	S-57	42.38	124.55	0.559	0.328	0.515	0.551
56	S-58	42.38	124.42	0.743	0.462	0.323	0.265

TABLE X

ELEMENT FACTOR SCORES FOR THE COMBINED RIVER, BEACH, AND
SHELF SAMPLE SET
(continued)

	Sample	Latitude	Longitude	Factor 1	Factor 2	Factor 3	Factor 4
57	S-59	42.41	124.33	0.501	0.586	0.384	0.501
58	S-60	42.44	124.66	0.524	0.595	0.394	0.453
59	S-61	42.76	124.56	0.392	0.815	0.255	0.307
60	S-62	43.11	124.68	0.522	0.608	0.427	0.408
61	S-63	43.11	124.48	0.317	0.706	0.202	0.548
62	S-65	43.12	124.43	0.403	0.802	0.211	0.343
63	S-66	43.29	124.59	0.549	0.317	0.486	0.594
64	S-67	43.35	124.28	0.429	0.454	0.421	0.645
65	S-68	43.44	124.41	0.369	0.689	0.253	0.551
66	S-69	44.20	124.14	0.297	0.870	0.172	0.283
67	S-70	44.59	124.47	0.430	0.474	0.400	0.622
68	S-71	44.59	124.20	0.337	0.641	0.313	0.592
69	S-72	44.59	124.05	0.234	0.944	0.141	0.175
70	S-73	45.14	124.99	0.226	0.935	0.152	0.210
71	OR-1	43.41	124.54	0.500	0.591	0.387	0.492
72	OR-2	43.50	124.20	0.304	0.655	0.385	0.563
73	OR-3	44.05	124.16	0.273	0.876	0.185	0.322
74	OR-4	44.05	124.43	0.400	0.760	0.314	0.389
75	OR-5	44.72	124.10	0.279	0.701	0.382	0.496
76	OR-6	44.72	124.24	0.266	0.790	0.212	0.488
77	OR-7	44.72	124.38	0.346	0.618	0.454	0.534
78	OR-7A	45.20	124.02	0.263	0.896	0.188	0.285
79	OR-8	45.29	124.01	0.296	0.667	0.391	0.547
80	OR-9	45.29	124.09	0.277	0.807	0.234	0.459
81	OR-10	45.29	123.99	0.301	0.672	0.335	0.575
82	OR-11	45.29	124.06	0.262	0.414	0.417	0.751
83	OR-12	45.47	124.21	0.312	0.482	0.341	0.740
84	OR-13	45.47	124.42	0.244	0.624	0.211	0.672
85	OR-14	45.53	123.99	0.297	0.721	0.337	0.517
86	OR-15	45.56	124.07	0.278	0.472	0.320	0.763
87	OR-16	46.02	124.05	0.327	0.512	0.339	0.708
88	B-11	40.70	124.20	0.829	0.344	0.176	0.234
89	B-12	41.04	124.08	0.704	0.527	0.214	0.324
90	B-13	41.36	124.06	0.771	0.440	0.231	0.313
91	B-14	41.47	124.07	0.826	0.458	0.053	0.235
92	B-15	41.73	124.16	0.849	0.410	0.242	0.140
93	B-16	41.86	124.13	0.800	0.312	0.413	0.220
94	B-17	42.02	124.16	0.914	0.281	0.130	0.156
95	TB-3	42.32	124.24	0.894	0.365	0.072	0.166
96	B-18	42.37	124.24	0.876	0.329	0.234	0.201
97	B-19	42.50	124.22	0.882	0.342	0.170	0.172
98	TB-8	42.73	124.26	0.408	0.830	0.172	0.244
99	B-20	42.84	124.30	0.608	0.732	0.157	0.167
100	B-21	43.21	124.20	0.440	0.837	0.149	0.192
101	B-22	44.03	124.10	0.225	0.887	0.078	0.221
102	B-23	44.67	124.04	0.254	0.934	0.125	0.095
103	B-24	45.01	124.04	0.206	0.957	0.157	0.077
104	TB-5	45.31	124.02	0.324	0.864	0.085	0.203
105	TB-4	45.72	123.59	0.347	0.811	0.028	0.152
106	B-25	45.91	123.58	0.420	0.797	0.131	0.327
107	B-26	46.22	124.00	0.458	0.579	0.204	0.581
108	R-11	40.62	124.14	0.716	0.286	0.381	0.469
109	R-12	40.93	124.05	0.828	0.304	0.164	0.287
110	R-13	41.54	124.04	0.884	0.327	0.194	0.243
111	R-14	41.93	124.10	0.905	0.128	0.247	0.119
112	R-15	42.05	124.15	0.451	0.246	0.803	0.243

TABLE X

ELEMENT FACTOR SCORES FOR THE COMBINED RIVER, BEACH, AND
SHELF SAMPLE SET
(continued)

	Sample	Latitude	Longitude	Factor 1	Factor 2	Factor 3	Factor 4
113	R-16	42.27	124.25	0.798	0.183	0.209	0.443
114	R-17	42.42	124.20	0.813	0.359	0.302	0.315
115	R-18	42.79	124.28	0.578	0.320	0.276	0.648
116	R-19	42.85	124.30	0.883	0.218	0.210	0.217
117	R-20	43.12	124.22	0.576	0.622	0.236	0.358
118	R-21	43.67	124.02	0.423	0.590	0.288	0.603
119	R-22	44.01	123.58	0.202	0.924	0.045	0.297
120	R-23	44.42	123.59	0.211	0.913	0.138	0.289
121	R-24	44.92	124.00	0.155	0.949	0.115	0.115
122	R-25	45.15	123.58	0.309	0.585	0.245	0.640
123	R-26	45.45	123.47	0.255	0.461	0.421	0.681
124	R-27	45.65	123.51	0.366	0.560	0.346	0.611
125	R-28	46.25	123.58	0.334	0.403	0.262	0.623

FACTOR LOADINGS FOR FOUR FACTORS OF ELEMENTAL COMPOSITION

VARIABLE		1	2	3	4
1	Na	-0.237	-0.348	1.114	2.052
2	Mg	0.469	-0.198	2.543	-0.281
3	Al	1.972	-0.254	1.172	0.433
4	Ca	-0.162	-0.255	2.620	0.218
5	Sc	-0.314	2.220	1.806	-0.099
6	Ti	-0.188	2.241	-0.140	-0.224
7	V	0.435	0.101	-0.092	0.051
8	Cr	2.118	-0.256	-0.440	-0.444
9	Mn	0.652	1.236	-0.039	0.032
10	Fe	2.632	1.036	-0.473	0.276
11	Co	2.055	-0.014	-0.177	-0.090
12	As	0.194	-0.042	0.341	0.590
13	Sb	0.165	0.127	0.277	0.736
14	La	-0.137	0.362	-0.627	1.672
15	Ce	-0.074	0.192	-0.600	1.689
16	Sm	-0.075	0.167	-0.286	1.996
17	Eu	0.134	-0.024	-0.152	2.357
18	Yb	-0.223	0.993	0.056	0.049
19	Lu	-0.105	0.376	-0.102	0.187
20	Hf	-0.098	1.827	-0.494	-0.035
21	Ta	-0.492	1.845	-0.084	-0.124
22					
23	VARIANCE	28.774	33.417	14.335	19.679

Total variance = 96.205

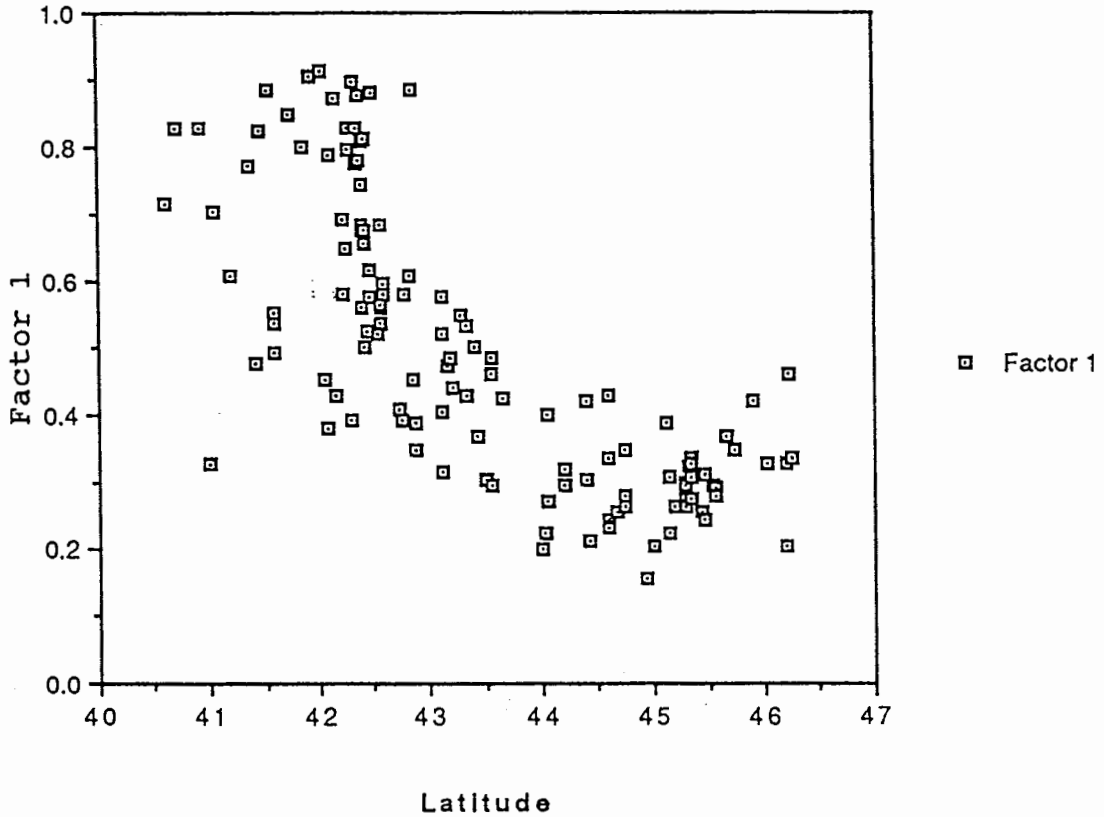


Figure 40. Plot of Combined Shelf and Onshore Factor 1 Loadings as a Function of Latitude.

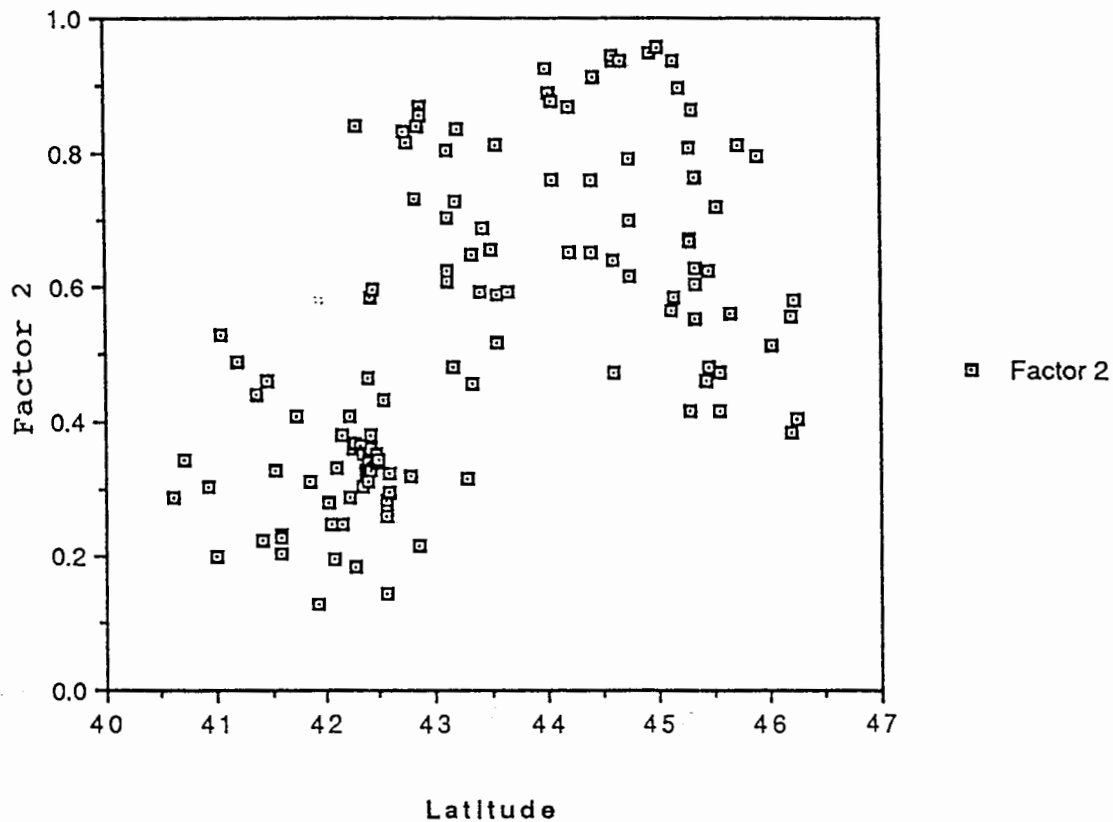


Figure 41. Plot of Combined Shelf and Onshore Factor 2 Loadings as a Function of Latitude.

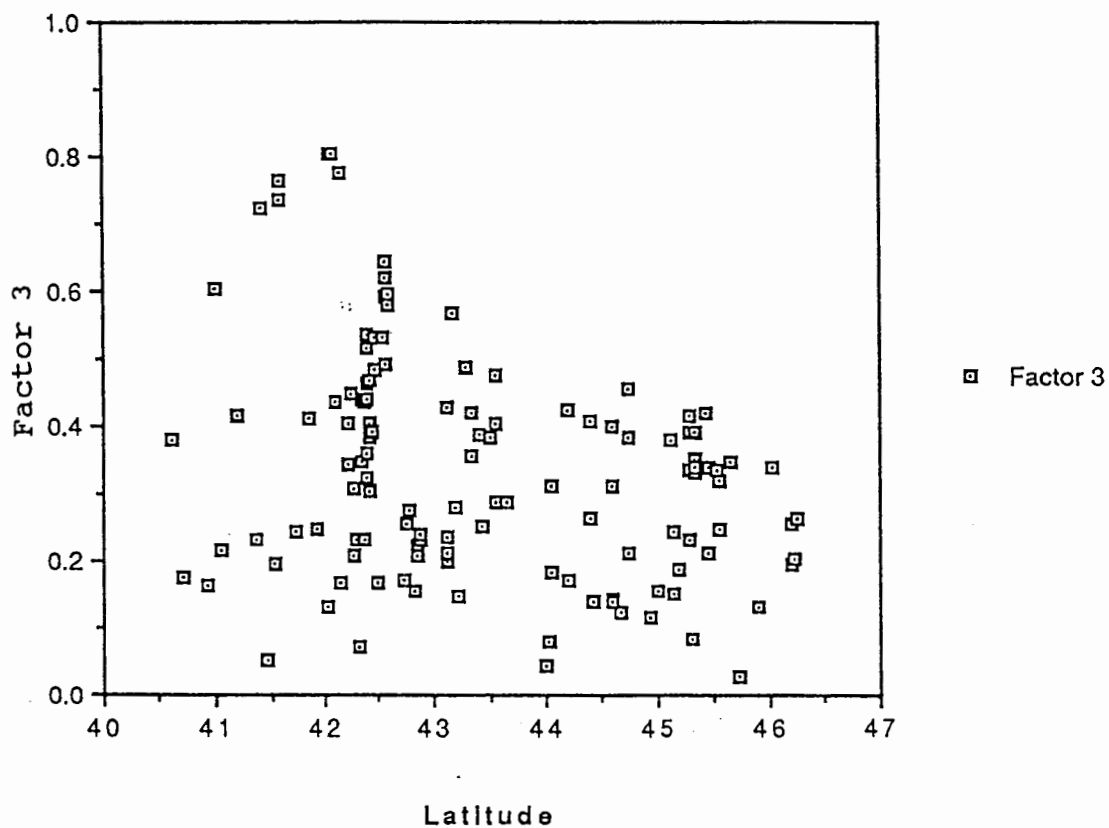


Figure 42. Plot of Combined Shelf and Onshore Factor 3 Loadings as a Function of Latitude.

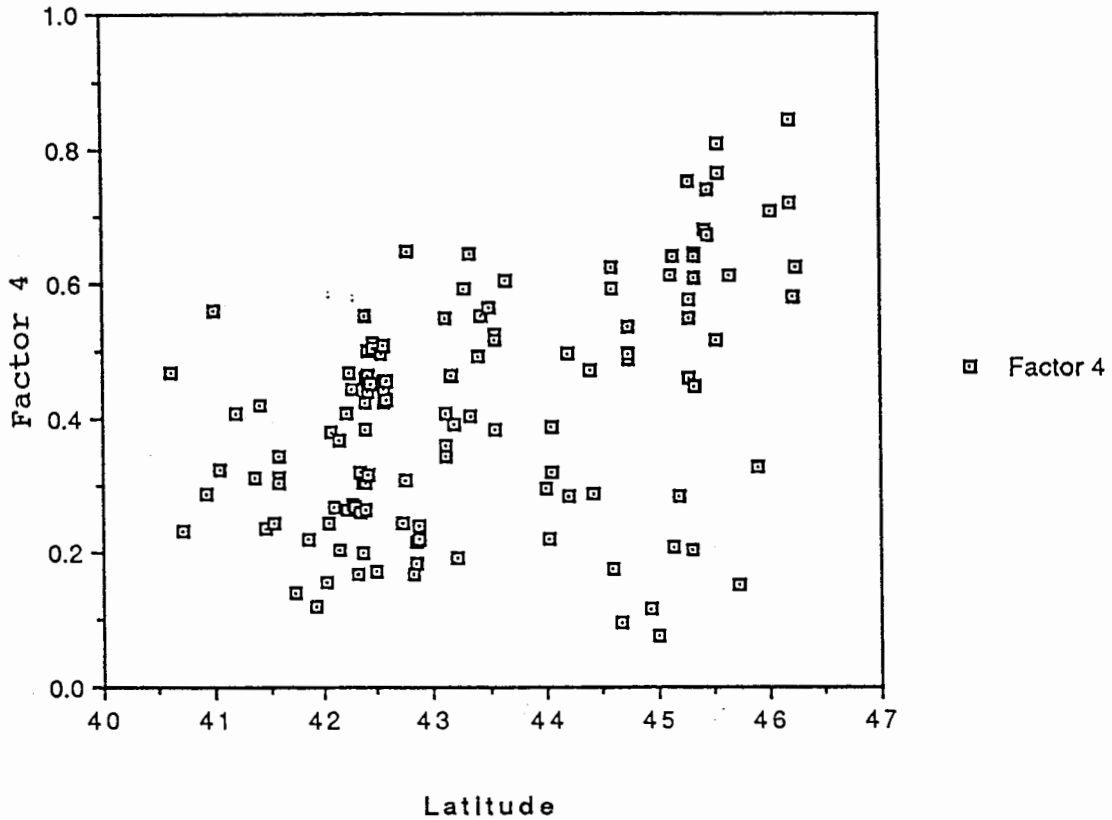


Figure 43. Plot of Combined Shelf and Onshore Factor 4 Loadings as a Function of Latitude.

less Ti-rich oxides. The third factor is dominated by Na, Al, Mg, Ca and Sc (Figure 42) appears to represent a northern Klamath source terrain. The fourth factor is high in Na, La, Ce, Sm and Eu (Figure 43), and displays maximum loadings between north of 45.5° . The maximum loadings of this factor appear to correspond to the Columbia River source.

Q-mode factor analysis of the oxide compositional data delineates four end-member sources as discussed in the earlier section. The multivariate analysis apparently breaks the two accreted terrains (Klamath Mountain and Coast Range) into two potential source areas, and indicates a fourth factor associated with the Columbia River mouth (source). This analysis addresses the along margin/shelf variability but not the across-shelf variability as discussed earlier.

CONTOUR MAPS COMPRISING DISPERSAL OF OPAQUE OXIDE-, NON- OPAQUE MINERALS AND QUARTZ GRAIN ROUNDING

Contour maps were created from the factor loadings of opaque oxide composition, and from previously reported heavy non-opaque mineral dispersal and Fourier grain-shape analysis of quartz grains. These maps (see Appendix C) are used to compare dispersal patterns produced by opaque oxide, non-opaque and quartz minerals. This allows a test of three

independent techniques widely used to constrain (1) dispersal patterns, (2) provenance of opaque oxides in the continental shelf, and (3) site specific geochemical models of exploration. Scheidegger et al. (1971) investigated the sediment sources and heavy mineral dispersal patterns of the continental shelf sands using diagnostic (non-opaque) heavy minerals. Factor one represents Klamath Mountain provenance and it is rich in glaucophane. Factor two is typical of Coast Range provenance and is characterized with the presence of clinopyroxenes. Factor three contains orthopyroxene rich sediments off the mouths of Umpqua and Columbia Rivers. The distribution of these factor loadings indicate a net northward transport of shelf sand. Factor four is dominated by garnet rich sediments and probably derived from several of the central Oregon coast rivers.

Swilley (1986) studied the continental shelf area located directly offshore of the northern coastal area of Oregon, 44-46°. Vector analysis of the shape of quartz (Fourier grain-shape) sand grains yielded four distinct types of sediments. End-member one represents grains derived from unconsolidated dune and beach sands (grains with well rounded shape). End-member two is characterized by grains, probably derived from Columbia River detritus (grains are very angular in shape). End-member three is dominated by sediments fluvially derived from the erosion of sedimentary rocks (mixed to well rounded grains). End-

member four represents detritus fluviially derived from volcanic rocks (grains mixed to angular shape).

O'Neal (1986) examined the shape characteristics of quartz grains from the southern Oregon continental shelf between 41.5 and 44.5° N. latitude. End-member one represents fluviially transported sediments derived primarily from the Klamath Mountain terrain. End-member two is representative of the numerous marine coastal terrace deposits and the Coast Range of southern Oregon. End-member three represents sands derived from the extensive beach and dune deposits located along the coast.

This study on the geochemistry and dispersal of opaque oxides from the continental shelf deposits yields four end member sources. The multivariate analysis (Q-mode factor analysis) was used to delineate similar source terrains. Factor one is high in Al, Cr, Co and Fe (is dominant in the southern shelf and corresponds to the Klamath source terrain). Factor two is high in Sc, Ti and Ta (and is dominant in the northern shelf and corresponds to the Coast Range terrain). Factor three is high in Na, Al, Mg, Ca and Sc (appears to represent a north Klamath source terrain). Factor four is high in Na, La, Ce, Sm and Eu (indicates maximum loadings off the Columbia River source).

Consequently, the resulting interpretation will compare the inferred transport mechanisms for heavy non-opaque- and opaque minerals as well as their differentiated

source rocks. These factor loadings established a dominant west-east (across-shelf) and south-north (along-shelf) dispersal pattern for the opaque- and non-opaque minerals respectively. Furthermore, the quartz rounding also implies largely across-shelf dispersal. In summary, the sole use of non-opaque heavy mineral analysis suggests much greater northward shelf transport than is indicated by the quartz and opaque mineral tracers.

RELATIONSHIPS OF THE VARIOUS HYDRODYNAMIC MODELS

Placer mineral concentrations within beaches and rivers have been studied for quite some time, but the physical processes responsible for the grain- and shear selective sorting leading to offshore concentration of opaque minerals remain poorly studied. Recent investigations by Slingerland (1977, 1984), Komar and Wang (1984), and Komar (1989) have focussed on the role of selective grain entrainment in the formation of beach placers. The formation of the placer involves processes of (1) initial hydraulic settling equivalence and (2) subsequent selective entrainment based on contrasting grain densities and sizes of the different minerals (Figures 38a). In a sand deposit of mixed grains the heavy minerals are denser and finer grained than quartz and feldspar grains. A bottom current can more easily entrain and transport the

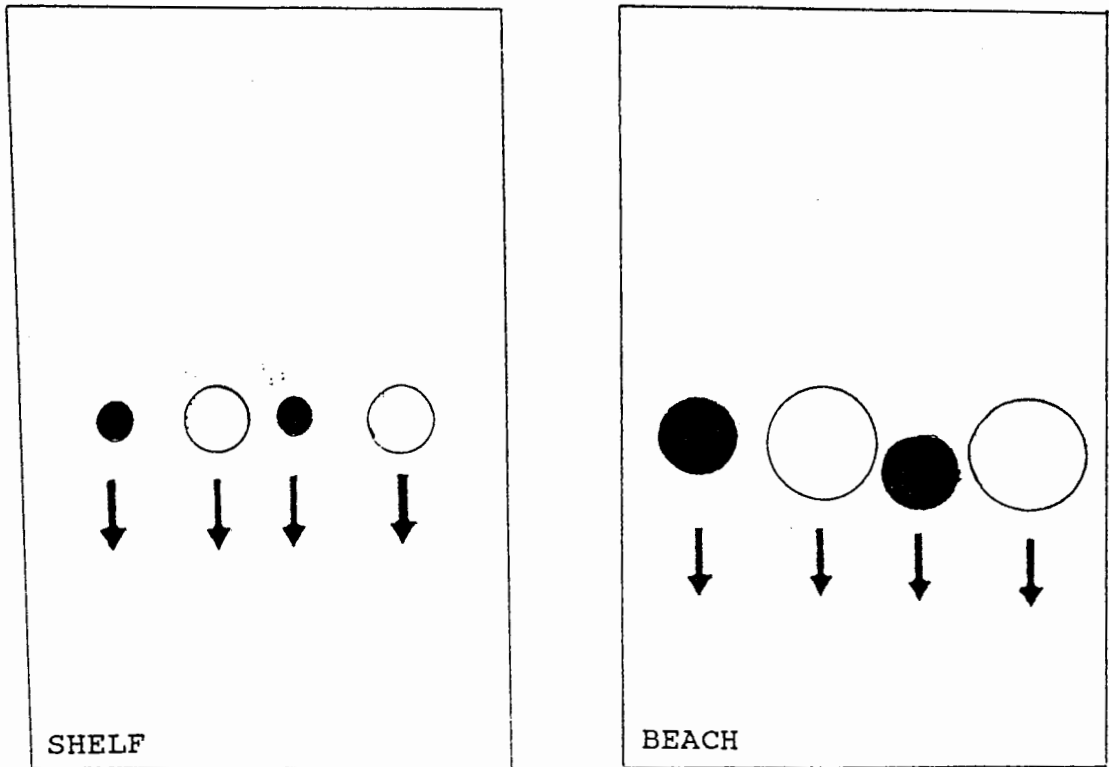


Figure 44. Hydraulic Settling Equivalence Model (Komar and Wang, 1984; Komar, 1988) for the formation of heavy minerals involves process of selective entrainment and sorting according to their contrasting grain densities and sizes. The opaque- and non-opaque minerals are denoted by closed and open circles respectively.

larger light minerals leaving behind a lag containing heavy minerals. The heavy minerals with high densities and small diameter are more resistant to shear stress, having lower exposures to the flow and greater pivoting angles.

Komar and Wang (1984) have found that among the heavy minerals, hornblende is relatively easily entrained. By comparison the opaque oxides are less easily entrained due to their high density and smaller sizes. The shear sorting leading to heavy mineral deposits occur due to the initial differences in grain size settling equivalence. The sorting processes generally leave the denser opaque minerals (ilmenite, chromite and magnetite) in the placer.

Heavy minerals (10-50% by weight) in surface sands of the continental shelf have been identified offshore of the Rogue River and shelf sands off Cape Blanco (Kulm et al., 1968a; Kulm, 1988). The heavy mineral (HM) concentrations (mineral halos up to 56 percent heavies) in the continental shelf surface sediments, suggest that anomalous concentrations of economic placers might form at a shallow subsurface depth on the shelf. Kulm (1988) suggests that offshore heavy mineral concentrations might be derived from placer mineral accumulations on the beach faces with the subsequent reworking of the beach face placers during the Holocene marine transgression. He found deep water to shallow water foraminiferal assemblages, downcore increases in heavy mineral abundances, and early Holocene C¹⁴ dates

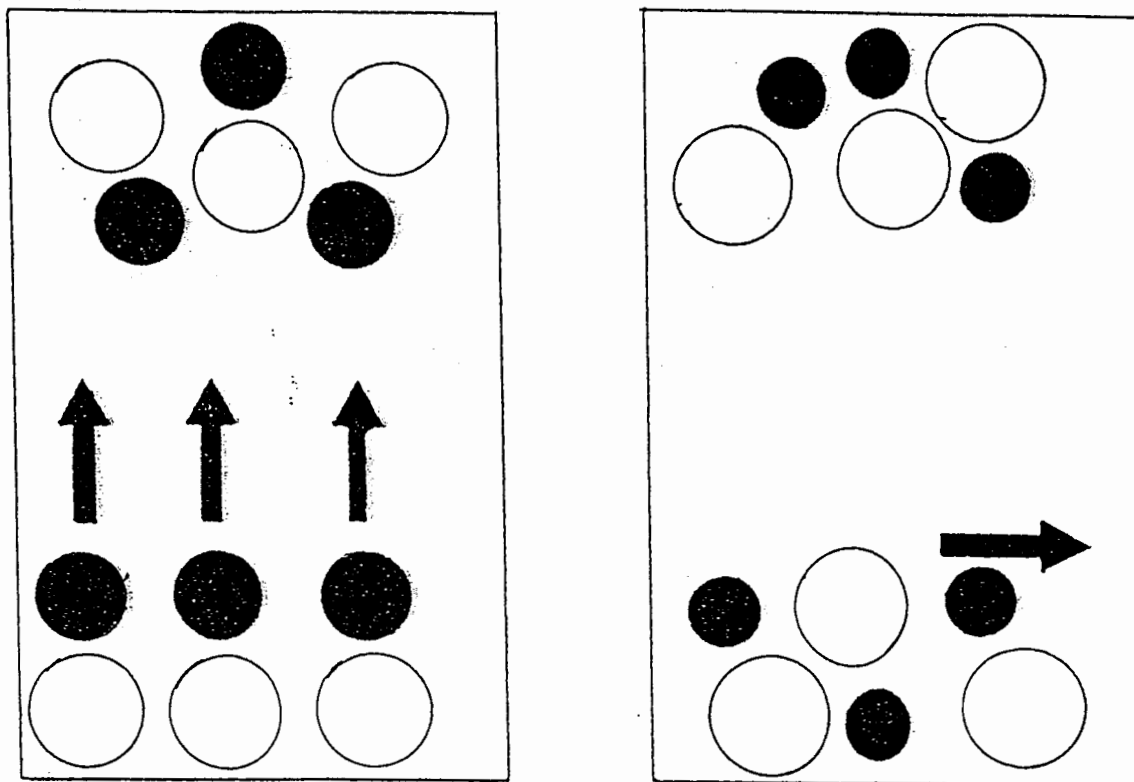


Figure 45. Kulm's hypothesis (1988) and Phillip's hypothesis (1979) relating to the formation of beach placers. Kulm (left) suggests that offshore HM concentrations can be derived from the subsequent reworking of beach placer concentrations during marine transgression, while Phillip (right) suggests the potential for a shelf winnowing process coupled with local entrainment shear stress, rather than a vertical mixing of a coarser beach placer.

from the shallow box cores (0.4 m penetration).

Alternatively, the shelf HM accumulations might have formed from the winnowing of fine grained shelf deposits by offshore currents (Phillips, 1979; Figure 45). The latter hypothesis would suggest hydraulic settling equivalence but unequivalent entrainment shear stress of light and heavy placer minerals.

The results (refer to Table 5) from grain-size statistics, settling velocity equivalence and entrainment shear stress for quartz and magnetite are used, in order to constrain the origin (offshore vs onshore) for anomalous placer minerals off the continental shelf. A prevalent view for the formation of the shelf HM concentrations is heavy mineral concentrations in basal (beach) placer deposits are mixed with overlying, fine-grained shelf deposits during or after the Holocene transgression (Chambers, 1969; Kulm, 1988). In this case, the opaque minerals would not be in settling velocity equivalence with light minerals, and would be present in large-grain fractions (> 140 microns). By contrast, the results from grain-size statistics demonstrated approximate settling velocity equivalence, but widely different shear stress values. The current study results are, however, consistent with Phillip's work (1979) and suggest the potential for a shelf winnowing process, by local entrainment shear stress, rather than a vertical mixing of a coarser basal placer. The shelf winnowing

process, possibly forced by the focussing of storm geostrophic currents around headlands could account for the association of shelf HM concentrations around prominent headlands.

The wave and storm generated currents, shelf currents and bio-geochemical mixing can affect the surficial heavy mineral distribution on the continental shelf. The lack of a three dimensional study (deep penetration vibra cores) of opaque mineral enrichments precludes one from further constraining the models for continental shelf placers.

MINERAL ECONOMIC GRADE AND SILICATE CONTAMINANTS

The INAA analysis of the opaque mineral fractions indicate the relative latitudinal variation of the chromium and titanium bearing iron oxides. A total of 20 shelf samples were analyzed for opaque oxide chemistry by electron microprobe (Mumford, 1991; personal communication). Chromite is relatively abundant in the shelf sands southern Oregon and it has an average chromium oxide content of >28% in the samples analyzed. The average ratios of chromium to iron in these samples are 1.07 (Blanco) and 1.43 (Umpqua; Table XII).

Ilmenite is abundant offshore of northern Oregon. The average titanium oxide content of ilmenite (defined as >20% Ti) is 26% Ti from one sample. Trace element contaminants

(Ca, Mg and Mn) in the shelf ilmenite grains totalled less than 3%. The chromite grade (% Cr) and ilmenite grade (% Ti) was determined in order to evaluate the economic and strategic resource potential for the shelf deposits. In summary, the chromite on the southern Oregon shelf appears to be of commercial grade. While, the ilmenite would require economic upgrading in order to be used for commercial interests (Kulm and Peterson, 1989).

TABLE XII

SUMMARY OF AVERAGE SHELF MICROPROBE ANALYSIS

SHELF	Average	Average	Cr:Fe ratio	Ti Grains	Cr
Grains	Ti	Cr			
Umpqua S68	26.307	28.473	1.43	40	24
123 m					
Blanco S17	25.977	29.046	1.07	46	39
21 m					
Blanco S16	26.716	24.466	1.19	22	21
27 m					
Rogue S48	28.364	18.425	0.51	13	25
17 m					
Rogue S51	25.084	23.596	0.85	17	33
70 m					
Klamath S5	27.469	25.053	0.92	8	30
50 m					

Note: Titanium oxide values: Ti content >20%
 Chromium oxide values: Cr content >5%

CHAPTER VIII

CONCLUSIONS

The following conclusions have been reached concerning the mineralogy, geochemistry, and provenance of opaque oxides derived from the continental shelf placer deposits.

1) Elemental analyses of the bulk opaque mineral fractions have resulted in delineation of potential offshore mineral resources representing discrete provenances on the shelf. High values of Ti (exceeding 20 wt%) are found in the northern shelf between latitudes 42.5° and 46.0°. By contrast, the elevated Cr values (4-6 wt%) are restricted to the southern shelf between latitudes 40.5° and 42.5°. The shelf opaque mineral geochemistry reflects an across-shelf mineral dispersal pattern, rather than a south-north (along-shelf) dispersal pattern as indicated by non-opaque heavy mineral analysis (Scheidegger et al., 1971). The contrasting distributions of chromium-rich oxides (south of 43°) and titanium-rich oxides (north of 43°) delineated different source rocks from the Klamath Mountains (south) and the Coast Range (north).

- 2) Linear regressions of specific major and trace element pairs have established trace-element partitioning into the dominant opaque oxide phases. Strong correlations between the relative abundances of some trace and major element pairs (Co-Cr, Ta-Ti, Hf-Ti, Sc-Ti and V-Fe) indicated that these trace elements are selectively partitioned into the dominant mineral phases based on valence and ionic radii constraints. The local and regional variations in abundance of the non-partitioned LREE (La, Ce, and Sm) discriminated the different source rocks associated with a Klamath Mountain source and a Columbia River source respectively.
- 3) Initial investigations of the mineral-grain size relations of the Sixes River do not support the hypothesis that apparent elevated relative abundances of chromite in beach deposits results from coarse grained chromite in source rocks.
- 4) Grain-mineral and -size distributions from the six box core samples representing the inner-shelf near Cape Blanco (S. Oregon) established possible origins for placers on the shelf. The results demonstrate approximate settling velocity equivalence, but widely different shear stress values. These results suggest the potential for a shelf winnowing process, by local entrainment shear stress, rather than a vertical mixing of a coarser basal placer.
- 5) The microprobe analyses of the opaque minerals have determined accurate mineral economic grade within the

specific oxide mineral phases ilmenite, chromite and magnetite from the shelf placers. Average titanium oxide values for the ilmenite (defined as 20% Ti) range from 25.08 to 27.47% Ti for the samples derived from the inner-shelf and mid-shelf regions offshore of the Rogue River. Trace element contaminants (Ca, Mg and Mn) in the shelf ilmenite grains totalled less than 3%. The average chromium values for chromite (defined as >5% Cr) from the shelf samples range from 18 to 29% Cr based on the eight averaged chromite analyses. Silicate contaminants Al, Mg accounted for 15% in the analyzed chromites. The average iron oxide values for magnetite from the shelf samples range from 60 to 62% (%Fe) in magnetites. Whereas, silicate contaminants V, Mn and Al in the shelf magnetite grains generally totalled less than 2%.

6) Multivariate (Q-mode) analysis on the combined shelf-beach-river geochemical data have resulted in four factors accounting for over 95% of the data variance. Factor 1 is high in Al, Cr, Co and Fe; Factor 2 is high in Sc, Ti and Ta; Factor 3 is high in Na, Al, Mg, Ca and Sc; while Factor 4 is high in Na, La, Ce, Sm and Eu. Combined shelf/onshore Factor 1 is dominant in the southern shelf and corresponds to the Klamath source terrain. Factor 2 is dominant in the northern shelf and corresponds to the Coast Range terrain. Factor 3 appears to represent a north Klamath source terrain, and Factor 4 shows maximum loadings off the

Columbia River mouth. These factors demonstrate dominant across-shelf dispersal rather than along-shelf dispersal as previously reported.

REFERENCES

- Baldwin, E.W., 1964, Geology of Oregon: University of Oregon, Eugene, Oregon, 165 p.
- Beiersdorf, H., Kudrass, H.R., and von Stackelberg, U., 1980, Placer deposits of ilmenite and zircon on the Zambezi shelf: *Geologisches Jahrbuch, Reihe D, Heft 36*, Hannover, p.5-85.
- Chambers, D.M., 1969, Holocene sedimentation and potential placer deposits on the continental shelf off the Rogue River, Oregon: Corvallis, Oregon, Oregon State-University unpublished M.S.thesis, 83 p.
- Darby, D.A., 1984, Trace elements in ilmenite: A way to discriminate provenance or age in coastal sands: *Geological Society of America Bulletin*, v.95, p.1208-1218.
- Day, D.T., and Richards, R.H., 1906, Useful minerals in the black sands of the Pacific slope: U.S. Geological Survey, *Mineral Resources of the United States 1905*, p.1175-1246.
- Everts, C.H., 1972, Exploration for high energy marine placer sites: Part 1-Field and flume tests, North Carolina coast: Madison, Wisconsin, The University of Wisconsin Sea Grant Program Report WIS-SG-72-210, 179 p.
- Gibbs, R.J., Matthews, M.D., and Link, D.A., 1971, The relationship between sphere size and settling velocity: *Journal of Sedimentary Petrology*, v.41, p.7-18.
- Griggs, A.B., 1945, Chromite-bearing sands of the southern part of the coast of Oregon: U.S. Geological Survey Bulletin 945-E, p.113-150.
- Gross, M.G., and Nelson, J.L., 1966, Sediment movement on the continental shelf near Washington and Oregon: *Science*, v.151, p.1-3.

- Hevesy, G., and Levi, H., 1936, The use of neutrons in analytical chemistry: *Mathematical Physics Medicine*, v.14, no 5, 34 p.
- Horner, R.R., 1918, Notes on the black sand deposits of southern Oregon and northern California: U.S. Bureau of Mines Technical Paper 196, 42 p.
- Irwin, W.P., 1966, Geology of the Klamath Mountains Province: California Division of Mines and Geology Bulletin, v.190, p.19-38.
- Irwin, W.P., 1981, Tectonic accretion of the Klamath Mountains, in Ernst, W.G., ed., *The geotectonic development of California*: Englewood Cliffs, New-Jersey, Prentice-Hall, p.29-49.
- Kelly, J.V., 1947, Columbia River magnetite sands, Clatsop County, Oregon, and Pacific County, Washington, Hammond and McGowan deposits: U.S. Bureau of Mines Report of Investigations 4011, 7 p.
- Klovan, J.E., and Meisch, A.T., 1976, Extended CABFAC and Q-model computer programs for Q-mode factor analysis of compositional data: *Computers and Geosciences*, v.1, p.161-178.
- Knoll, G.F., 1979, Radiation Detection and Measurement: John Wiley and Sons, New York, NY, p.313-316.
- Komar, P.D., 1981, The applicability of the Gibbs equation for grain settling velocities to conditions other than quartz in water: *Journal of Sedimentary Petrology*, v.51, p.1125-1132.
- Komar, P.D., and Wang, C., 1984, Processes of selective grain transport and formation of placers on beaches: *Journal of Geology*, v.92, p.637-655.
- Komar, P.D., and Clemens, K.E., 1986, The relationship between a grain's settling velocity and threshold of motion under unidirectional currents: *Journal of Sedimentary Petrology*, v.56, p.258-266.
- Komar, P.D., 1988, Physical processes of waves and currents and the formation of marine placers: *Aquatic Sciences*, v.1, n.3, p.393-423.

- Kudrass, H.R., 1987, Sedimentary models to estimate the heavy mineral potential of shelf sediments, in Marine Minerals: Advances in Research and Resource Assessment, Teleki, P.G. et al., Eds., NATO Advanced Study Institutes Series C, Mathematical and Physical Sciences.
- Kulm, L.D., Heinrichs, D.F., Buerhrig, R.M., and Chambers, D.M., 1968, Evidence for possible placer accumulations on the southern Oregon continental shelf: Oregon Geology, v.30, p.165-184.
- Kulm, L.D., Rouse, R.C., Harlett, J.C., Neudeck, R.H., Chambers, D.M., and Runge, E.J., 1975, Oregon continental shelf sedimentation: Interrelationships of facies distribution and sedimentary processes: Journal of Geology, v.83, p.145-175.
- Kulm, L.D., 1988, Potential heavy mineral and metal placers on the southern Oregon continental shelf: Marine Mining, v.7, p.361-395.
- Kulm, L.D., and Peterson, C.D., 1989, Preliminary economic evaluation of continental shelf placer deposits off Cape Blanco, Rogue River, and Umpqua River: Oregon Department of Geology and Mineral Industries Open File Report x-xx-x, Portland, Oregon, 25 p.
- Laul, J.A., 1979, Neutron activation analysis of geological materials: Atomic Energy Review, v.17, no 3, p.603-695.
- Lupeke, G., 1980, Opaque minerals as aids in distinguishing between source and sorting effects on beach-sand mineralogy in southwestern Oregon: Journal of Sedimentary Petrology, v.50, p. 489-496.
- Mallik, T.K., 1986, Micromorphology of some placer minerals from Kerala beach, India: Marine Geology, v.71, p. 371-381.
- Mooney, W.D., and Weaver, C.S., 1989, Regional crustal structure and tectonics of the Pacific Coastal States; California, Oregon, and Washington, in Pakiser, L.C., and Mooney, W.D., Geophysical framework of the continental United States: Boulder, Colorado, Geological Society of America Memoir 172, p.129-161.
- Moore, G.W., and Silver, E.A., 1968, Gold distribution on the sea floor off the Klamath Mountains, California: U.S. Geological Survey Circular 605, 9 p.

- Mumford, D.F., 1988, Geology of the Elsie-lower Nehalem River area, south-central Clatsop and northern Tillamook counties, northwestern Oregon: Corvallis, Oregon, Oregon State University unpublished M.S.thesis, 392 p.
- O'Neal, M.A., 1986, Sources, transport, and dispersal history of southern Oregon continental shelf sediments: Fourier grain-shape analysis: Wichita, Kansas, Wichita State University unpublished M.S. thesis, 107 p.
- Page, B.M., 1966, Geology of the coast ranges of California: California Division of Mines and Geology Bulletin, v.190, p.255-276.
- Pardee, J.T., 1934, Beach placers of the Oregon coast: U.S. Geological Survey Circular 8, 41 p.
- Peck, D.L., Griggs, A.B., Schlicker, H.G., Wells, F.G., and Dole, H.M., 1964, Geology of the central and northern parts of the western Cascade Range in Oregon: U.S. Geological Survey Professional Paper 449, 56 p.
- Peterson, C.D., Komar, P.D., and Scheidegger, K.F., 1986, Distribution, geometry, and origin of heavy mineral placer deposits on Oregon beaches: Journal of Sedimentary Petrology, v.56, no.1, p.67-77.
- Peterson, C.D., Gleeson, G.W., and Wetzel, N., 1987, Stratigraphic development, mineral sources and preservation of marine placers from Pleistocene terraces in southern Oregon, U.S.A: Sedimentary Geology, v.53, p.203-229.
- Peterson, C.D., and Binney, S.E., 1988, Compositional variations of coastal placers in the Pacific Northwest, U.S.A: Marine Mining, v.7, p.397-416.
- Peterson, C.D., and Kulm, L.D., 1989, An investigation of heavy mineral placers on the Oregon continental shelf: Oregon Division of State Lands.
- Peterson, C.D., Binney, S.E., and Kulm, L.D., (in prep), Elemental composition of economic opaque mineral fractions from river sources and coastal placers of the Pacific Northwest, U.S.A.

- Phillips, R.L., 1979, Heavy minerals and bedrock minerals on the continental shelf of Washington, Oregon, and California, in Outer Continental Shelf Mining Policy Phase II Task Force, Feasibility Document: Outer Continental Shelf Hard Minerals Leasing, U.S. Geological Survey, Appendix 8, 56 p.
- Ramp, L., 1961, Chromite in southwestern Oregon: Oregon Department of Geology and Mineral Resources Bulletin, v.52, 169 p.
- Rubey, W.W., 1933, The size distribution of heavy minerals within a waterlaid sandstone: Journal of Sedimentary Petrology, v.3, p.3.
- Sallenger, A.H., 1979, Inverse grading and hydraulic equivalence in grain flow deposits: Journal of Sedimentary Petrology, v.49, p.553-562.
- Scheidegger, K.F., Kulm, L.D., and Runge, E.J., 1971, Sediment sources and dispersal patterns of Oregon continental shelf sands: Journal of Sedimentary Petrology, v.71, p.1112-1120.
- Slingerland, R.L., 1977, The effects of entrainment on the hydraulic equivalence relationships of light and heavy minerals in sands: Journal of Sedimentary Petrology, v.47, p.753-770.
- Smith, J.D., and Hopkins, T.S., 1972, Sediment transport on the continental shelf off of Washington and Oregon in light of recent current measurements, in D.J.P. Swift, D.B. Duane, and O.H. Pilkey, eds., Shelf sediment transport-Process and pattern: Stroudsburg, Pennsylvania, Dowden, Hutchinson, and Ross, Inc., chapter 7, p.143-180.
- Snavely, P.D., McLeod, N.S., and Wagner, H.C., 1968, Tholeiitic and alkalic basalts of the Eocene Siletz River Volcanics, Oregon Coast Range: American Journal of Science, v.266, p.454-481.
- Spigai, J.J., 1971, Marine geology of the continental margin off southern Oregon: Corvallis, Oregon, Oregon State University unpublished Ph.D. thesis, 214 p.
- Stapor, F.W., 1973, Heavy mineral concentration processes and density/shape/size equilibria of marine and coastal dune sands from the Apalachicola, Florida, region: Journal of Sedimentary Petrology, v.43, p.396-407.

- Swilley, G.K., 1986, Fourier grain shape analysis of sediments from the continental shelf off the coast of northern Oregon: Wichita, Kansas, Wichita State University unpublished M.S. thesis, 109 p.
- Taylor, S.R., and McLennan, S.M., 1985, The Continental Crust: Its Composition and Evolution: Blackwell, Oxford, 312 p.
- Twenhofel, W.H., 1946, Mineralogical and physical composition of the sands of the Oregon coast from Coos Bay to the mouth of the Columbia River: Oregon Department of Geology and Mineral Industries Bulletin 30, 64 p.
- Venkatarathnam, K., and McNamus, D.A., 1973, Origin and distribution of sands and gravels on the northern continental shelf off Washington: Journal of Sedimentary Petrology, v.43, p.799-811.
- Wells, R.E., Engebretson, P.D., Snavely, Jr., and Coe, R.S., 1984, Cenozoic plate motions and the volcano-tectonic evolution of western Oregon and Washington: Tectonics, v.3, p.275-294.
- Whetten, J.T., Kelley, J.C., and Hanson, L.G., 1969, Characteristics of Columbia River sediment and sediment transport: Journal of Sedimentary Petrology, v.39, p.1149-1186.
- White, S.M., 1967, Mineralogy and geochemistry of continental shelf sediments off Washington-Oregon coast: Journal of Sedimentary Petrology, v.40, p.38-54.

	Sample	Longitude	Latitude	Na	Mg	Al	Ca
1	S-1	124.18	41.00	3175.90	113388.00	25951.00	72635.00
2	S-2	124.18	41.20	1411.30	40477.00	22447.00	36244.00
3	S-3	124.17	41.42	2320.60	123557.00	25095.00	44432.00
4	S-4	124.36	41.59	2190.30	100433.00	26369.00	57632.00
5	S-5	124.31	41.59	1869.30	92481.00	27098.00	57438.00
6	S-6	124.16	41.59	1697.10	106004.00	25023.00	50357.00
7	S-7	124.39	42.08	2363.80	144350.00	22775.00	63616.00
8	S-8	124.50	42.29	613.60	28138.00	15877.00	8333.00
9	S-9	124.43	42.28	878.80	49376.00	22081.00	12072.00
10	S-10	124.41	42.58	2903.00	74980.00	24589.00	30002.00
11	S-11	124.38	42.56	3348.20	96056.00	35214.00	33297.00
12	S-12	124.55	42.57	3285.20	65508.00	26214.00	35145.00
13	S-13	124.48	42.57	2535.30	105352.00	26292.00	37205.00
14	S-14	124.71	42.53	2877.40	65633.00	25361.00	30134.00
15	S-15	124.61	42.87	486.20	26341.00	13824.00	8565.00
16	S-16	124.58	42.88	461.70	36641.00	13298.00	6022.00
17	S-17	124.57	42.86	426.20	28751.00	15816.00	7166.00
18	S-18	124.70	43.16	2737.90	68594.00	23723.00	36558.00
19	S-19	124.45	43.20	1436.90	32116.00	18437.00	12913.00
20	S-20	124.41	43.35	1763.50	44160.00	21238.00	17474.00
21	S-21	124.51	43.56	2434.90	72318.00	23572.00	31361.00
22	S-22	124.37	43.56	2335.40	50671.00	22388.00	23817.00
23	S-23	124.14	43.56	1245.30	41632.00	15479.00	11225.00
24	S-24	124.41	44.20	2566.90	66301.00	19840.00	21859.00
25	S-25	124.60	44.39	2476.70	50662.00	20775.00	25705.00
26	S-26	124.27	44.38	1519.40	32731.00	16960.00	19284.00
27	S-27	124.17	44.58	294.30	26501.00	8847.00	4164.00
28	S-28	124.22	45.11	3175.30	40340.00	21172.00	27946.00
29	S-29	124.40	45.35	3760.30	33262.00	21230.00	27579.00
30	S-30	124.26	45.35	3148.20	33522.00	18613.00	24233.00
31	S-31	124.12	45.35	2689.50	46637.00	18362.00	32723.00
32	S-32	123.97	45.35	2691.30	35547.00	15240.00	20608.00
33	S-33	124.28	45.56	3586.50	34406.00	19115.00	28895.00
34	S-34	124.26	46.20	2697.70	26090.00	16253.00	19417.00
35	S-35	124.29	46.20	4799.00	47858.00	22526.00	33736.00
36	S-37	124.37	42.10	1157.50	65874.00	27436.00	22435.00
37	S-38	124.39	42.15	2218.90	111129.00	29201.00	59305.00
38	S-39	124.37	42.15	383.90	29385.00	21206.00	8054.00
39	S-40	124.41	42.21	1126.90	57686.00	26085.00	22739.00
40	S-41	124.44	42.35	872.30	47288.00	25479.00	16615.00
41	S-43	124.46	42.35	1245.30	60338.00	25624.00	21328.00
42	S-44	124.46	42.36	1212.70	52523.00	26688.00	24344.00
43	S-45	124.46	42.39	1065.40	53446.00	22595.00	19676.00
44	S-46	124.56	42.39	2267.30	56122.00	23149.00	21479.00
45	S-47	124.56	42.23	2078.00	66995.00	2364.00	23102.00
46	S-48	124.44	42.40	1679.00	74702.00	24297.00	30196.00
47	S-49	124.44	42.40	1853.70	57783.00	23712.00	20074.00
48	S-50	124.58	42.42	2178.90	60847.00	22419.00	22654.00
49	S-51	124.54	42.42	2303.00	49113.00	18934.00	15983.00
50	S-52	124.54	42.25	2298.40	59304.00	21013.00	20713.00
51	S-53	124.65	42.47	2731.00	65563.00	22422.00	31206.00
52	S-54	124.65	42.47	2335.50	71424.00	24354.00	25306.00
53	S-55	124.48	42.57	2087.10	76634.00	25649.00	33909.00
54	S-56	124.41	42.58	2688.80	83372.00	23726.00	27044.00
55	S-57	124.55	42.38	2713.50	63141.00	23860.00	26162.00
56	S-58	124.42	42.38	700.30	50318.00	29425.00	17651.00

	Sample	Longitude	Latitude	Na	Mg	Al	Ca
57	S-59	124.33	42.41	1887.90	53786.00	20841.00	24773.00
58	S-60	124.66	42.44	1566.00	42747.00	22591.00	25205.00
59	S-61	124.56	42.76	759.90	32547.00	15738.00	9155.00
60	S-62	124.68	43.11	1757.10	62671.00	21527.00	18120.00
61	S-63	124.48	43.11	1109.50	37277.00	17772.00	15335.00
62	S-65	124.43	43.12	650.80	29646.00	18938.00	10548.00
63	S-66	124.59	43.29	2899.90	61966.00	28988.00	29435.00
64	S-67	124.28	43.35	3111.10	53905.00	28020.00	33954.00
65	S-68	124.41	43.44	1529.30	40542.00	20386.00	10859.00
66	S-69	124.14	44.20	562.80	33246.00	13788.00	6545.00
67	S-70	124.47	44.59	3889.10	57916.00	23589.00	20143.00
68	S-71	124.20	44.59	1937.10	48613.00	19065.00	20598.00
69	S-72	124.05	44.59	435.30	13898.00	8068.00	4586.00
70	S-73	124.99	45.14	594.30	18304.00	7926.00	6129.00
71	OR-1	124.54	43.41	1727.20	41396.00	20086.00	25283.00
72	OR-2	124.20	43.50	2185.30	45065.00	17935.00	27852.00
73	OR-3	124.16	44.05	688.10	16313.00	12154.00	11696.00
74	OR-4	124.43	44.05	996.50	42733.00	17619.00	20680.00
75	OR-5	124.10	44.72	1913.90	75260.00	16689.00	21014.00
76	OR-6	124.24	44.72	1169.70	30986.00	13855.00	15990.00
77	OR-7	124.38	44.72	2388.00	49050.00	19641.00	35808.00
78	OR-7A	124.02	45.20	1077.10	20903.00	10231.00	6512.00
79	OR-8	124.01	45.29	2605.50	55727.00	17076.00	27865.00
80	OR-9	124.09	45.29	1369.30	28505.00	12329.00	14884.00
81	OR-10	123.99	45.29	2784.70	33498.00	16026.00	25352.00
82	OR-11	124.06	45.29	4980.20	45779.00	24258.00	39197.00
83	OR-12	124.21	45.47	3819.30	37804.00	20191.00	27791.00
84	OR-13	124.42	45.47	2350.90	35978.00	13236.00	14988.00
85	OR-14	123.99	45.53	2346.00	33060.00	14757.00	26380.00
86	OR-15	124.07	45.56	3560.10	49710.00	19195.00	30757.00
87	OR-16	124.05	46.02	3777.30	34303.00	17924.00	22515.00

	Sc	Ti	V	Cr	Mn	Fe	Co
1	46.90	35571.00	648.50	20894.00	5045.30	213551.00	113.20
2	35.70	102892.00	1254.70	41534.00	9092.80	334271.00	134.40
3	41.30	21826.00	635.60	22066.00	3442.00	210242.00	120.00
4	42.50	15097.00	849.00	25068.00	2919.00	221349.00	113.90
5	44.10	21194.00	802.10	34622.00	3099.20	237744.00	130.90
6	39.80	21750.00	863.00	31780.00	3043.50	243085.00	127.80
7	49.10	11804.00	520.80	14703.00	2560.40	192957.00	106.90
8	76.20	189361.00	1357.20	26844.00	9059.20	360133.00	115.70
9	23.70	45050.00	2056.90	45470.00	4772.50	432265.00	161.20
10	39.20	40314.00	1271.20	28771.00	4044.70	303340.00	123.80
11	42.10	45100.00	1466.90	24015.00	4043.50	307336.00	117.40
12	37.80	34854.00	1229.30	20193.00	3851.00	293002.00	109.90
13	37.60	29122.00	1180.00	25324.00	3666.10	309705.00	124.40
14	52.60	61329.00	1236.20	26525.00	5324.20	315971.00	118.30
15	74.90	203994.00	1264.60	22843.00	10526.10	331172.00	100.20
16	72.50	190171.00	1346.60	24821.00	9092.50	357023.00	112.50
17	69.30	178102.00	1396.90	34137.00	8939.50	378069.00	131.50
18	59.50	83223.00	1281.50	25203.00	5798.00	301051.00	107.30
19	59.40	138874.00	1297.60	30015.00	8513.30	363146.00	125.00
20	56.90	117312.00	1408.80	31631.00	6937.30	375584.00	126.90
21	56.50	92738.00	1193.60	30310.00	6422.40	331380.00	125.90
22	57.60	104445.00	1284.50	26655.00	7344.30	314829.00	109.00
23	76.10	176993.00	1045.50	11178.00	10629.30	299356.00	79.20
24	70.10	126382.00	1106.50	11109.00	9049.10	270644.00	87.30
25	64.10	115570.00	1324.50	19191.00	7316.20	353973.00	107.40
26	69.50	149018.00	1286.50	10976.00	10916.90	328099.00	78.40
27	75.20	226027.00	1427.80	4143.00	10495.70	390776.00	66.50
28	58.50	105783.00	1458.50	14355.00	6319.10	347389.00	97.00
29	57.50	107425.00	1208.40	8615.00	6143.20	298428.00	80.70
30	58.70	126180.00	1373.80	7819.00	5840.30	329891.00	84.20
31	64.40	137372.00	1336.40	10657.00	7135.90	316342.00	85.50
32	62.60	173823.00	1207.70	1823.00	7293.50	301666.00	72.90
33	43.00	60631.00	1276.50	1548.00	4667.40	351907.00	59.80
34	45.90	117620.00	1564.60	6654.00	5764.70	379509.00	75.30
35	57.20	77912.00	1419.70	985.00	4323.70	274720.00	74.90
36	31.90	52578.00	1804.50	51720.00	4304.00	402908.00	176.20
37	58.50	16420.00	578.90	19857.00	3322.10	201994.00	104.10
38	22.70	49270.00	2170.30	52594.00	4961.60	510830.00	193.20
39	31.50	36418.00	1515.00	46838.00	4665.80	388495.00	164.80
40	26.70	44180.00	1756.30	50582.00	4695.30	411683.00	167.40
41	28.70	32791.00	1570.70	42776.00	4180.30	378230.00	156.40
42	29.90	38400.00	1491.40	46195.00	4577.50	375226.00	161.20
43	25.70	34464.00	1795.00	43417.00	4447.30	446895.00	171.90
44	35.10	36561.00	1580.20	29002.00	4117.70	384400.00	129.90
45	35.80	40001.00	1654.00	32224.00	4269.80	413127.00	138.10
46	30.70	36151.00	1386.60	28319.00	3728.10	354986.00	140.30
47	32.80	38111.00	1335.30	29490.00	4174.70	365107.00	143.70
48	33.20	32758.00	1683.80	27154.00	3883.80	395443.00	131.40
49	35.20	39439.00	1518.20	20315.00	3962.00	406612.00	131.00
50	34.30	44907.00	1587.20	21494.00	4085.70	394322.00	129.70
51	42.30	40772.00	1240.00	27960.00	4526.30	338789.00	130.40
52	37.10	48314.00	1433.40	29723.00	4799.40	355625.00	130.40
53	3.80	24688.00	1218.00	26379.00	3750.10	343583.00	138.70
54	35.60	34695.00	1236.90	25843.00	4266.90	294078.00	127.90
55	40.90	31642.00	1125.60	20354.00	4212.00	314103.00	125.30
56	40.60	80261.00	1082.20	72440.00	9174.40	345656.00	233.50

	Sc	Ti	V	Cr	Mn	Fe	Co
57	52.40	91791.00	1319.10	25093.00	6200.80	363490.00	125.60
58	56.00	86100.00	1183.10	31277.00	6946.20	326471.00	126.10
59	76.20	184369.00	1238.80	24847.00	9573.20	349149.00	115.80
60	56.70	101982.00	1231.20	27852.00	6244.60	334839.00	120.90
61	71.10	151093.00	1081.70	19653.00	10605.30	323751.00	103.80
62	65.40	154744.00	1170.10	27277.00	11713.50	347140.00	116.60
63	38.20	46283.00	1443.10	25865.00	4615.60	310960.00	114.90
64	51.30	79872.00	1119.30	26010.00	8065.90	274905.00	115.40
65	60.90	137058.00	1237.80	2258.00	8070.20	335435.00	105.60
66	64.10	196223.00	1413.60	5464.00	12426.30	372356.00	80.20
67	47.30	91935.00	1405.00	11058.00	5752.30	354875.00	108.30
68	65.40	127812.00	1128.80	14238.00	8691.50	307240.00	91.50
69	71.50	233899.00	1196.10	3337.00	9230.10	367176.00	64.20
70	70.40	242831.00	1142.50	2320.00	8178.30	361059.00	61.80
71	51.00	104127.00	1295.50	26975.00	6795.10	321497.00	116.50
72	64.20	130453.00	1134.50	5693.00	7896.30	276904.00	74.60
73	69.60	199461.00	1245.00	6772.00	11573.10	338184.00	76.30
74	62.30	164397.00	1234.60	23532.00	8399.70	319038.00	103.90
75	64.10	140045.00	918.50	3830.00	10129.20	269054.00	70.10
76	67.50	172262.00	1182.50	7409.00	9494.30	312917.00	73.20
77	63.00	123398.00	1075.80	11777.00	6771.30	282749.00	88.20
78	61.00	209897.00	1130.20	2026.00	7500.60	328662.00	68.50
79	56.10	147004.00	1052.60	1413.00	8028.90	288909.00	73.50
80	64.30	180858.00	1120.90	7583.00	8250.50	308851.00	78.10
81	52.30	144338.00	1175.50	2864.00	5829.40	297845.00	78.80
82	53.80	96431.00	1119.90	3871.00	4755.00	243768.00	72.70
83	51.40	100463.00	1414.40	6119.00	5021.20	300527.00	82.50
84	64.30	169894.00	1398.30	3730.00	6290.70	325282.00	80.50
85	57.60	165683.00	1411.70	3269.00	6554.40	307314.00	78.60
86	48.90	92866.00	1281.40	2406.00	5250.20	294314.00	74.90
87	49.60	103474.00	1727.80	3306.00	5099.60	309595.00	81.20

	As	Sb	La	Ce	Sm	Eu	Yb
1	38.56	5.61	11.85	30.38	3.98	1.48	4.46
2	6.46	1.82	6.50	15.14	2.58	0.72	3.15
3	8.07	1.33	8.58	14.96	2.79	0.59	1.82
4	6.68	0.97	5.71	9.80	1.72	0.41	1.14
5	5.77	0.58	4.22	7.34	1.53	0.48	1.32
6	7.15	0.76	4.14	8.46	1.50	0.43	0.96
7	9.19	1.33	5.81	13.55	2.08	0.76	1.25
8	4.06	0.97	15.42	24.66	2.33	0.48	5.95
9	5.01	0.88	3.33	9.41	1.13	0.40	1.26
10	4.77	0.96	7.01	16.36	2.00	0.56	1.46
11	6.54	1.06	6.57	16.21	2.33	0.61	1.63
12	9.70	1.23	7.36	15.50	2.59	0.55	1.95
13	12.34	1.58	7.43	14.45	2.22	0.53	1.72
14	6.82	0.79	11.79	20.92	2.78	0.76	2.33
15	3.94	1.13	12.45	17.54	2.12	0.53	7.45
16	3.66	1.13	11.01	16.35	2.21	0.40	6.39
17	5.40	0.92	9.06	14.84	1.64	0.29	6.20
18	4.24	1.01	9.62	18.42	2.69	0.80	2.71
19	5.69	1.14	14.12	27.41	2.83	0.60	4.58
20	4.35	1.04	13.80	24.69	2.74	0.56	3.82
21	5.38	1.48	15.14	30.31	3.46	0.98	4.37
22	5.72	1.54	17.43	36.79	3.79	0.75	4.62
23	7.64	1.23	17.74	30.62	3.71	0.69	9.81
24	7.03	3.39	14.92	37.28	3.92	0.81	8.48
25	6.82	1.78	15.61	31.41	3.14	0.71	4.71
26	7.51	2.40	26.49	47.03	4.47	0.66	11.09
27	5.28	0.84	14.20	21.51	2.01	0.26	11.86
28	11.07	2.23	20.60	44.27	4.34	0.96	3.81
29	8.72	2.08	21.38	38.94	4.50	0.95	4.98
30	8.57	1.52	20.99	44.74	4.70	1.21	4.46
31	8.88	2.27	24.69	65.55	4.78	1.05	5.11
32	5.24	0.51	12.00	21.35	3.38	0.82	8.05
33	8.32	1.28	41.79	84.61	7.38	1.28	5.88
34	13.26	2.02	32.22	82.89	5.42	1.18	3.87
35	8.20	1.45	55.97	112.67	9.59	1.84	6.22
36	6.07	1.21	5.26	9.25	1.67	0.25	1.38
37	6.50	0.77	6.02	13.17	2.31	0.65	1.72
38	3.64	0.57	4.52	13.00	1.02	0.26	0.99
39	6.13	1.08	4.93	8.46	1.53	0.47	1.39
40	5.23	0.82	4.04	6.49	1.27	0.37	1.39
41	6.91	0.88	4.86	13.25	1.63	0.36	1.02
42	6.31	0.82	4.66	8.77	1.40	0.40	1.25
43	4.95	0.58	4.51	9.02	1.37	0.51	0.96
44	4.49	0.68	6.99	13.74	2.06	0.48	1.26
45	4.53	0.72	6.76	16.26	1.89	0.58	1.50
46	6.02	0.89	7.13	12.57	2.11	0.46	1.45
47	7.73	0.94	7.40	13.39	2.30	0.72	1.81
48	6.98	1.05	7.11	9.44	1.97	0.62	1.53
49	5.24	0.71	7.00	15.09	2.43	0.54	1.48
50	4.54	0.79	9.35	16.95	2.50	0.54	1.24
51	5.31	1.27	7.68	16.11	2.60	0.85	1.90
52	6.93	1.49	10.04	23.29	2.60	0.77	2.19
53	10.16	1.40	6.37	10.64	2.01	0.62	1.00
54	6.92	0.72	5.76	8.00	1.96	0.56	1.49
55	9.74	1.35	9.50	23.88	3.16	0.71	2.15
56	5.16	2.38	8.20	18.00	1.80	0.39	4.63

	As	Sb	La	Ce	Sm	Eu	Yb
57	5.68	1.02	15.68	25.63	3.55	0.93	3.38
58	5.66	1.03	15.45	28.80	2.83	0.71	3.85
59	4.26	1.67	14.47	23.69	2.65	0.61	3.84
60	5.19	0.79	11.24	22.42	2.70	0.64	3.84
61	5.20	0.94	38.43	62.25	5.43	1.18	12.38
62	6.06	1.29	18.32	28.56	3.30	0.65	12.28
63	7.21	1.85	15.23	28.96	3.30	0.91	1.90
64	7.19	1.83	23.01	45.73	4.90	1.18	5.39
65	4.11	1.31	25.07	49.30	4.04	1.10	5.75
66	4.40	1.23	16.27	25.94	2.84	0.57	16.76
67	6.95	3.04	15.35	27.76	4.08	1.08	3.81
68	6.99	2.66	26.64	51.66	4.93	1.17	7.52
69	2.72	0.79	12.00	14.57	2.02	0.27	10.50
70	2.33	0.47	12.66	17.97	1.78	0.49	9.66
71	5.04	1.34	13.56	31.10	3.29	0.75	3.19
72	10.43	2.29	19.22	34.50	4.60	1.04	6.38
73	5.85	1.43	19.11	30.10	3.23	0.51	10.89
74	4.38	1.18	14.10	31.80	3.36	0.73	4.94
75	7.97	1.57	19.56	32.80	4.84	0.97	11.59
76	6.93	1.36	31.33	51.90	4.44	0.82	9.92
77	7.16	1.77	17.76	33.60	4.03	0.86	4.69
78	3.93	0.65	9.45	16.20	2.63	0.54	8.90
79	6.73	1.80	16.82	29.50	4.30	1.05	9.06
80	5.42	1.64	20.73	36.40	4.07	0.83	7.18
81	6.45	0.92	16.40	31.30	4.36	1.03	5.99
82	9.06	1.45	21.96	48.20	6.41	1.67	4.93
83	11.69	2.15	24.80	54.90	5.74	1.40	3.85
84	6.77	4.21	30.57	66.90	6.62	1.55	4.68
85	6.58	1.03	16.37	27.00	4.13	0.93	5.82
86	8.22	1.07	34.62	66.30	7.31	1.35	4.92
87	12.31	1.29	22.14	44.10	5.09	1.15	4.30

	Lu	Hf	Ta
1	0.43	2.01	1.52
2	0.36	4.37	4.45
3	0.24	1.30	0.77
4	0.17	0.83	0.31
5	0.16	1.20	0.92
6	0.12	1.70	0.51
7	0.11	1.43	1.10
8	1.05	13.85	16.11
9	0.19	3.06	1.85
10	0.21	2.65	2.34
11	0.27	2.24	1.48
12	0.17	2.12	1.06
13	0.14	2.51	0.83
14	0.29	4.48	4.58
15	1.17	12.23	19.06
16	0.85	13.33	17.22
17	0.90	15.48	15.63
18	0.45	4.76	5.60
19	0.91	9.38	13.24
20	0.49	8.10	10.45
21	0.50	6.04	8.51
22	0.65	7.42	8.90
23	1.34	12.50	16.34
24	1.40	10.02	12.68
25	0.77	11.19	12.51
26	1.88	14.26	15.98
27	2.09	25.14	22.24
28	0.47	9.77	10.30
29	1.10	8.84	9.79
30	0.78	10.78	12.09
31	0.80	12.90	13.08
32	1.20	14.64	15.23
33	0.85	8.99	5.55
34	0.59	10.93	11.27
35	0.84	10.87	7.46
36	0.18	1.79	1.16
37	0.23	1.19	0.72
38	0.37	3.02	1.46
39	0.15	2.40	1.32
40	0.17	2.74	1.54
41	0.17	1.67	0.91
42	0.12	1.84	1.55
43	0.16	2.37	1.13
44	0.21	2.17	1.25
45	0.21	2.98	1.38
46	0.21	2.46	1.22
47	0.17	1.98	1.48
48	0.17	2.26	0.85
49	0.14	3.09	0.61
50	0.11	2.73	0.59
51	0.29	1.75	1.75
52	0.24	2.60	2.08
53	0.16	1.58	0.45
54	0.18	1.77	1.88
55	0.14	2.44	1.14
56	0.70	4.39	5.92

	Lu	Hf	Ta
57	0.85	10.12	9.27
58	0.70	8.84	7.80
59	0.95	12.97	15.64
60	0.54	8.47	7.70
61	1.87	11.44	13.56
62	1.80	16.25	15.11
63	0.30	2.49	2.12
64	0.81	6.40	6.77
65	0.80	11.42	12.47
66	2.43	18.66	19.10
67	0.43	9.61	6.56
68	1.13	9.60	12.35
69	1.95	20.18	22.22
70	1.69	20.06	21.88
71	0.54	6.46	8.31
72	1.13	11.01	11.76
73	2.15	14.58	20.37
74	0.88	12.37	14.45
75	1.97	10.99	14.92
76	1.46	14.80	16.81
77	0.81	8.61	11.21
78	1.46	17.34	18.28
79	1.49	12.18	11.95
80	1.14	14.07	17.66
81	0.98	13.34	12.92
82	0.71	9.51	7.62
83	0.53	9.29	8.72
84	0.78	11.75	15.10
85	1.03	12.65	13.97
86	0.68	9.53	8.99
87	0.75	8.59	7.52

APPENDIX B

DETAILED FACTOR LOADINGS

	Sample	Latitude	Longitude	Factor 1	Factor 2	Factor 3	Factor 4
1	S-1	46.20	124.13	0.15	0.17	0.10	0.59
2	S-15	46.14	124.23	0.31	0.15	0.09	0.45
3	S-19	46.11	124.62	0.11	0.19	0.32	0.38
4	S-23	46.11	124.34	0.29	0.11	0.40	0.21
5	S-39	46.05	124.38	0.03	0.31	0.40	0.27
6	S-41	46.05	124.23	0.14	0.54	0.21	0.11
7	S-43	46.05	124.08	0.08	0.20	0.37	0.34
8	S-44	46.02	123.59	0.15	0.17	0.54	0.14
9	S-63	45.59	124.29	0.16	0.39	0.26	0.19
10	S-65	45.59	124.14	0.12	0.23	0.20	0.45
11	S-67	45.59	124.00	0.27	0.14	0.30	0.29
12	S-87	45.53	124.28	0.18	0.22	0.30	0.30
13	S-89	45.53	124.13	0.00	0.13	0.42	0.45
14	S-91	45.53	123.99	0.29	0.16	0.46	0.09
15	S-95	45.50	124.18	0.12	0.24	0.30	0.33
16	S-110	45.47	124.28	0.01	0.21	0.45	0.32
17	S-112	45.47	124.14	0.17	0.11	0.41	0.30
18	S-114	45.47	123.99	0.21	0.14	0.47	0.18
19	S-135	45.41	124.15	0.18	0.31	0.06	0.45
20	S-137	45.41	124.01	0.35	0.12	0.33	0.21
21	S-153	45.35	124.26	0.28	0.15	0.43	0.14
22	S-155	45.35	124.12	0.19	0.11	0.36	0.33
23	S-157	45.35	124.97	0.16	0.01	0.29	0.53
24	S-169	45.29	124.37	0.43	0.03	0.47	0.07
25	S-171	45.29	124.23	0.28	0.12	0.26	0.34
26	S-173	45.29	124.09	0.45	0.14	0.42	0.00
27	S-175	45.29	123.99	0.35	0.11	0.37	0.18
28	S-184	45.23	124.34	0.42	0.03	0.32	0.23
29	S-187	45.23	124.12	0.24	0.09	0.30	0.36
30	S-189	45.23	123.99	0.34	0.00	0.17	0.54
31	S-197	45.28	124.30	0.72	0.00	0.16	0.16
32	S-200	45.17	124.09	0.32	0.00	0.22	0.47
33	S-202	45.17	123.59	0.41	0.00	0.42	0.17
34	S-216	45.11	124.08	0.35	0.08	0.46	0.11
35	S-218	45.11	123.99	0.40	0.02	0.13	0.45
36	S-234	45.05	124.16	0.44	0.10	0.24	0.21
37	S-236	45.05	124.02	0.24	0.10	0.41	0.24
38	S-249	44.59	124.20	0.19	0.23	0.14	0.44
39	S-251	44.59	124.05	0.24	0.04	0.53	0.18
40	S-270	44.88	124.24	0.22	0.26	0.37	0.15
41	S-272	44.88	124.60	0.37	0.10	0.26	0.26
42	S-290	44.78	124.31	0.19	0.26	0.20	0.35
43	S-291	44.78	124.24	0.24	0.15	0.27	0.34
44	S-08-4	44.39	124.36	0.24	0.16	0.46	0.15
45	S-330	44.58	124.31	0.33	0.03	0.20	0.44
46	S-332	44.58	124.17	0.45	0.11	0.33	0.11
47	S-348	44.48	124.45	0.40	0.11	0.30	0.19
48	S-351	44.47	124.23	0.38	0.26	0.12	0.24
49	S-353	44.48	124.11	0.37	0.00	0.22	0.41
50	S-357	44.43	124.31	0.22	0.00	0.35	0.43
51	S-374	44.20	124.14	0.29	0.07	0.37	0.27
52	S-376	44.33	124.26	0.35	0.09	0.34	0.22
53	S-378	44.20	124.41	0.33	0.13	0.31	0.23
54	S-392	44.17	124.35	0.19	0.04	0.41	0.36
55	S-395	44.17	124.14	0.31	0.15	0.35	0.18
56	Umpqua R.	43.67	124.02	0.00	0.43	0.26	0.31

	Sample	Latitude	Longitude	Factor 1	Factor 2	Factor 3	Factor 4
57	Klamath R.	41.54	124.04	0.07	0.67	0.15	0.11
58	Rogue R.	42.42	124.20	0.08	0.48	0.20	0.24
59	Columbia R.	46.25	123.58	0.05	0.33	0.25	0.37
60	Smith R.	41.93	124.10	0.10	0.36	0.16	0.37
61	Alsea R.	44.42	123.59	0.04	0.37	0.08	0.51
62	Coquille R.	43.12	124.22	0.00	0.35	0.31	0.36
63	Agate Beach	44.67	124.04	0.38	0.02	0.28	0.32

	Sample	Latitude	Longitude	Factor 1	Factor 2	Factor 3
1	O-1	44.19	124.19	0.05	0.31	0.64
2	O-2	44.19	124.46	0.20	0.42	0.38
3	O-3	44.13	124.93	0.08	0.34	0.58
4	O-4	44.08	124.64	0.08	0.52	0.41
5	O-5	44.08	124.43	0.07	0.30	0.63
6	O-6	44.08	124.30	0.08	0.43	0.49
7	O-7	44.08	124.16	0.03	0.33	0.64
8	O-8	43.98	124.24	0.00	0.25	0.75
9	O-9	43.98	124.38	0.24	0.44	0.32
10	O-10	43.98	124.51	-0.01	0.62	0.39
11	O-11	43.93	124.86	0.18	0.47	0.36
12	O-12	43.84	124.52	0.13	0.13	0.74
13	O-13	43.82	124.45	0.13	0.45	0.42
14	O-14	43.81	124.30	0.06	0.62	0.32
15	O-15	43.82	124.23	0.05	0.29	0.66
16	O-16	43.82	124.20	0.10	0.41	0.49
17	O-17	43.68	124.27	0.18	0.56	0.27
18	O-18	43.68	124.41	0.18	0.64	0.18
19	O-19	43.68	124.54	0.54	0.36	0.10
20	O-20	43.58	124.48	0.06	0.38	0.56
21	O-21	43.58	124.41	0.48	0.30	0.22
22	O-22	43.58	124.25	0.17	0.20	0.63
23	O-23	43.48	124.31	0.32	0.25	0.43
24	O-24	43.48	124.45	0.31	0.49	0.20
25	O-25	43.38	124.57	0.21	0.62	0.17
26	O-26	43.38	124.43	0.33	0.54	0.13
27	O-27	43.27	124.41	0.20	0.63	0.17
28	O-28	43.27	124.43	0.33	0.54	0.13
29	O-29	43.23	124.46	0.20	0.63	0.17
30	O-30	43.23	124.42	-0.03	0.69	0.34
31	O-31	43.13	124.48	0.19	0.30	0.51
32	O-32	43.03	124.74	0.08	0.54	0.37
33	O-33	43.03	124.56	0.10	0.46	0.45
34	O-34	43.03	124.47	0.21	0.40	0.39
35	O-35	42.93	124.51	0.08	0.63	0.29
36	O-36	42.93	124.60	0.13	0.35	0.52
37	O-37	42.83	124.71	0.27	0.33	0.41
38	O-38	42.83	124.62	0.46	0.17	0.36
39	O-39	42.73	124.50	0.26	0.35	0.39
40	O-40	42.73	124.66	0.29	0.48	0.23
41	O-41	42.73	124.71	0.08	0.49	0.43
42	O-42	42.63	124.42	-0.01	0.44	0.57
43	O-43	42.56	124.56	0.17	0.44	0.40
44	O-44	42.59	124.68	0.35	0.51	0.14
45	O-45	42.50	124.64	0.29	0.54	0.16
46	O-46	42.47	124.65	0.52	0.33	0.16
47	O-47	42.47	124.58	0.34	0.50	0.15
48	O-48	42.47	124.53	0.24	0.34	0.42
49	O-49	42.38	124.51	0.31	0.43	0.26
50	O-50	42.39	124.67	0.48	0.42	0.10
51	O-51	42.33	124.45	0.17	0.64	0.19
52	O-52	42.29	124.46	0.20	0.51	0.29
53	O-53	42.28	124.58	0.13	0.38	0.49
54	O-54	42.23	124.42	0.32	0.28	0.41
55	O-55	42.18	124.37	0.31	0.28	0.41
56	O-56	42.13	124.37	0.21	0.40	0.39

	Sample	Latitude	Longitude	Factor 1	Factor 2	Factor 3
57	O-57	42.10	124.37	0.05	0.69	0.27
58	O-58	41.98	124.33	0.60	0.34	0.06
59	O-59	41.98	124.24	0.49	0.35	0.15
60	Agate Beach	44.67	124.04	0.06	0.20	0.74
61	Alsea R.	44.42	123.59	0.37	0.51	0.12
62	Columbia R.	46.25	123.58	0.25	0.57	0.18
63	Coquille R.	43.12	124.22	0.16	0.72	0.12
64	Klamath R.	41.54	124.04	0.74	0.26	0.00
65	Rogue R.	42.42	124.20	0.54	0.13	0.32
66	Siletz R.	44.92	124.00	0.52	0.42	0.07
67	Smith R.	41.93	124.10	0.42	0.38	0.19
68	Umpqua R.	43.67	124.02	0.37	0.48	0.15

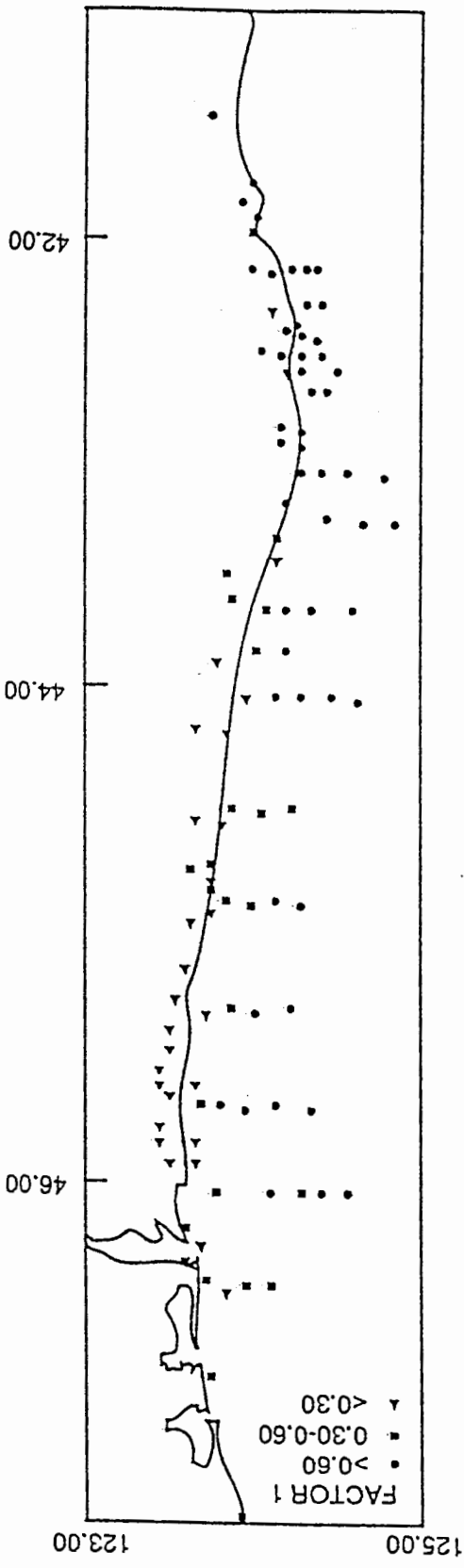
	Sample	Latitude	Comm.	Factor 1	Factor 2	Factor 3	Factor 4
1	S-1	41.00	0.83	0.33	0.20	0.60	0.56
2	S-2	41.20	0.95	0.61	0.49	0.42	0.41
3	S-3	41.42	0.98	0.48	0.23	0.72	0.42
4	S-4	41.59	0.99	0.49	0.20	0.77	0.34
5	S-5	41.59	0.98	0.54	0.23	0.74	0.31
6	S-6	41.59	0.99	0.55	0.23	0.73	0.30
7	S-7	42.08	0.97	0.38	0.20	0.80	0.38
8	S-8	42.29	0.99	0.39	0.84	0.23	0.27
9	S-9	42.28	0.99	0.83	0.37	0.31	0.27
10	S-10	42.58	0.98	0.58	0.32	0.58	0.46
11	S-11	42.56	0.97	0.56	0.27	0.62	0.45
12	S-12	42.57	0.98	0.54	0.28	0.59	0.51
13	S-13	42.57	0.98	0.56	0.26	0.64	0.42
14	S-14	42.53	0.99	0.52	0.43	0.53	0.50
15	S-15	42.87	0.98	0.35	0.87	0.23	0.24
16	S-16	42.88	0.99	0.39	0.86	0.24	0.22
17	S-17	42.86	0.99	0.45	0.84	0.23	0.18
18	S-18	43.16	0.99	0.47	0.48	0.57	0.46
19	S-19	43.20	0.99	0.48	0.73	0.28	0.39
20	S-20	43.35	0.99	0.53	0.65	0.35	0.40
21	S-21	43.56	0.99	0.48	0.52	0.48	0.52
22	S-22	43.56	0.99	0.46	0.59	0.40	0.52
23	S-23	43.56	0.98	0.30	0.81	0.29	0.38
24	S-24	44.20	0.95	0.32	0.65	0.42	0.50
25	S-25	44.39	0.99	0.42	0.65	0.41	0.47
26	S-26	44.38	0.97	0.30	0.76	0.26	0.47
27	S-27	44.58	0.99	0.24	0.94	0.15	0.18
28	S-28	45.11	0.99	0.39	0.56	0.38	0.61
29	S-29	45.35	0.98	0.33	0.55	0.39	0.64
30	S-30	45.35	0.99	0.33	0.60	0.33	0.64
31	S-31	45.35	0.98	0.31	0.63	0.35	0.61
32	S-32	45.35	0.98	0.28	0.76	0.34	0.45
33	S-33	45.56	0.97	0.29	0.41	0.25	0.81
34	S-34	46.20	0.97	0.33	0.56	0.20	0.72
35	S-35	46.20	0.97	0.20	0.38	0.26	0.84
36	S-37	42.10	0.99	0.79	0.33	0.44	0.27
37	S-38	42.15	0.98	0.43	0.25	0.78	0.37
38	S-39	42.15	0.98	0.87	0.38	0.17	0.20
39	S-40	42.21	0.75	0.69	0.29	0.34	0.26
40	S-41	42.35	1.00	0.83	0.35	0.35	0.26
41	S-43	42.35	0.99	0.78	0.31	0.44	0.32
42	S-44	42.36	0.99	0.78	0.32	0.44	0.30
43	S-45	42.39	0.98	0.81	0.33	0.36	0.30
44	S-46	42.39	0.97	0.68	0.35	0.46	0.42
45	S-47	42.23	0.83	0.58	0.41	0.41	0.41
46	S-48	42.40	0.99	0.68	0.31	0.54	0.39
47	S-49	42.40	0.99	0.68	0.34	0.44	0.46
48	S-50	42.42	0.98	0.68	0.33	0.47	0.44
49	S-51	42.42	0.95	0.66	0.38	0.40	0.47
50	S-52	42.25	0.97	0.65	0.36	0.45	0.47
51	S-53	42.47	0.99	0.57	0.34	0.53	0.51
52	S-54	42.47	0.99	0.61	0.35	0.48	0.51
53	S-55	42.57	0.94	0.69	0.15	0.49	0.46
54	S-56	42.58	0.98	0.59	0.30	0.60	0.43
55	S-57	42.38	0.99	0.56	0.33	0.52	0.55
56	S-58	42.38	0.94	0.74	0.46	0.32	0.27

	Sample	Latitude	Comm.	Factor 1	Factor 2	Factor 3	Factor 4
57	S-59	42.41	0.99	0.50	0.59	0.38	0.50
58	S-60	42.44	0.99	0.52	0.59	0.39	0.45
59	S-61	42.76	0.98	0.39	0.81	0.26	0.31
60	S-62	43.11	0.99	0.52	0.61	0.43	0.41
61	S-63	43.11	0.94	0.32	0.71	0.20	0.55
62	S-65	43.12	0.97	0.40	0.80	0.21	0.34
63	S-66	43.29	0.99	0.55	0.32	0.49	0.59
64	S-67	43.35	0.98	0.43	0.45	0.42	0.65
65	S-68	43.44	0.98	0.37	0.69	0.25	0.55
66	S-69	44.20	0.95	0.30	0.87	0.17	0.28
67	S-70	44.59	0.96	0.43	0.47	0.40	0.62
68	S-71	44.59	0.97	0.34	0.64	0.31	0.59
69	S-72	44.59	1.00	0.23	0.94	0.14	0.17
70	S-73	45.14	0.99	0.23	0.94	0.15	0.21
71	OR-1	43.41	0.99	0.50	0.59	0.39	0.49
72	OR-2	43.50	0.99	0.30	0.66	0.39	0.56
73	OR-3	44.05	0.98	0.27	0.88	0.18	0.32
74	OR-4	44.05	0.99	0.40	0.76	0.31	0.39
75	OR-5	44.72	0.96	0.28	0.70	0.38	0.50
76	OR-6	44.72	0.98	0.27	0.79	0.21	0.49
77	OR-7	44.72	0.99	0.35	0.62	0.45	0.53
78	OR-7A	45.20	0.99	0.26	0.90	0.19	0.28
79	OR-8	45.29	0.90	0.30	0.67	0.39	0.55
80	OR-9	45.29	0.99	0.28	0.81	0.23	0.46
81	OR-10	45.29	0.99	0.30	0.67	0.34	0.57
82	OR-11	45.29	0.98	0.26	0.41	0.42	0.75
83	OR-12	45.47	0.99	0.31	0.48	0.34	0.74
84	OR-13	45.47	0.94	0.24	0.62	0.21	0.67
85	OR-14	45.53	0.99	0.30	0.72	0.34	0.52
86	OR-15	45.56	0.98	0.28	0.47	0.32	0.76
87	OR-16	46.02	0.99	0.33	0.51	0.34	0.71
88	B-11	40.70	0.89	0.83	0.34	0.18	0.23
89	B-12	41.04	0.92	0.70	0.53	0.21	0.32
90	B-13	41.36	0.94	0.77	0.44	0.23	0.31
91	B-14	41.47	0.95	0.83	0.46	0.05	0.23
92	B-15	41.73	0.97	0.85	0.41	0.24	0.14
93	B-16	41.86	0.96	0.80	0.31	0.41	0.22
94	B-17	42.02	0.95	0.91	0.28	0.13	0.16
95	TB-3	42.32	0.96	0.89	0.36	0.07	0.17
96	B-18	42.37	0.97	0.88	0.33	0.23	0.20
97	B-19	42.50	0.95	0.88	0.34	0.17	0.17
98	TB-8	42.73	0.94	0.41	0.83	0.17	0.24
99	B-20	42.84	0.96	0.61	0.73	0.16	0.17
100	B-21	43.21	0.95	0.44	0.84	0.15	0.19
101	B-22	44.03	0.89	0.23	0.89	0.08	0.22
102	B-23	44.67	0.96	0.25	0.93	0.12	0.10
103	B-24	45.01	0.99	0.21	0.96	0.16	0.08
104	TB-5	45.31	0.90	0.32	0.86	0.09	0.20
105	TB-4	45.72	0.80	0.35	0.81	0.03	0.15
106	B-25	45.91	0.94	0.42	0.80	0.13	0.33
107	B-26	46.22	0.92	0.46	0.58	0.20	0.58
108	R-11	40.62	0.96	0.72	0.29	0.38	0.47
109	R-12	40.93	0.89	0.83	0.30	0.16	0.29
110	R-13	41.54	0.98	0.88	0.33	0.19	0.24
111	R-14	41.93	0.91	0.91	0.13	0.25	0.12
112	R-15	42.05	0.97	0.45	0.25	0.80	0.24

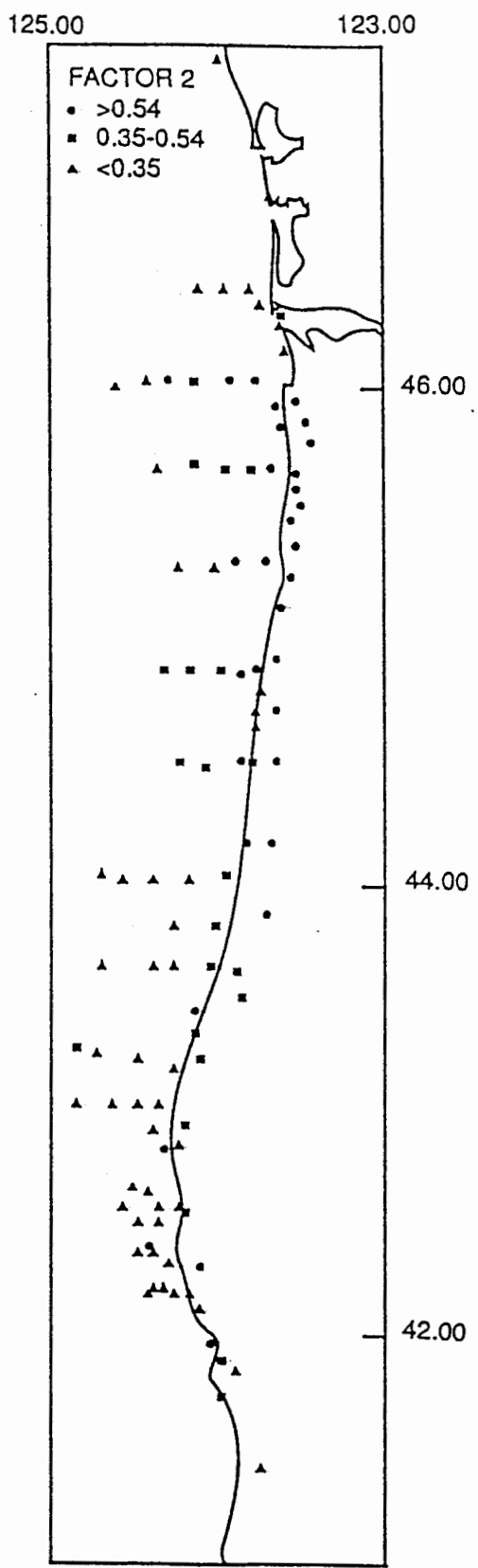
	Sample	Latitude	Comm.	Factor 1	Factor 2	Factor 3	Factor 4
113	R-16	42.27	0.91	0.80	0.18	0.21	0.44
114	R-17	42.42	0.98	0.81	0.36	0.30	0.32
115	R-18	42.79	0.93	0.58	0.32	0.28	0.65
116	R-19	42.85	0.92	0.88	0.22	0.21	0.22
117	R-20	43.12	0.90	0.58	0.62	0.24	0.36
118	R-21	43.67	0.97	0.42	0.59	0.29	0.60
119	R-22	44.01	0.98	0.20	0.92	0.04	0.30
120	R-23	44.42	0.98	0.21	0.91	0.14	0.29
121	R-24	44.92	0.95	0.15	0.95	0.12	0.12
122	R-25	45.15	0.91	0.31	0.58	0.24	0.64
123	R-26	45.45	0.92	0.26	0.46	0.42	0.68
124	R-27	45.65	0.94	0.37	0.56	0.35	0.61
125	R-28	46.25	0.73	0.33	0.40	0.26	0.62

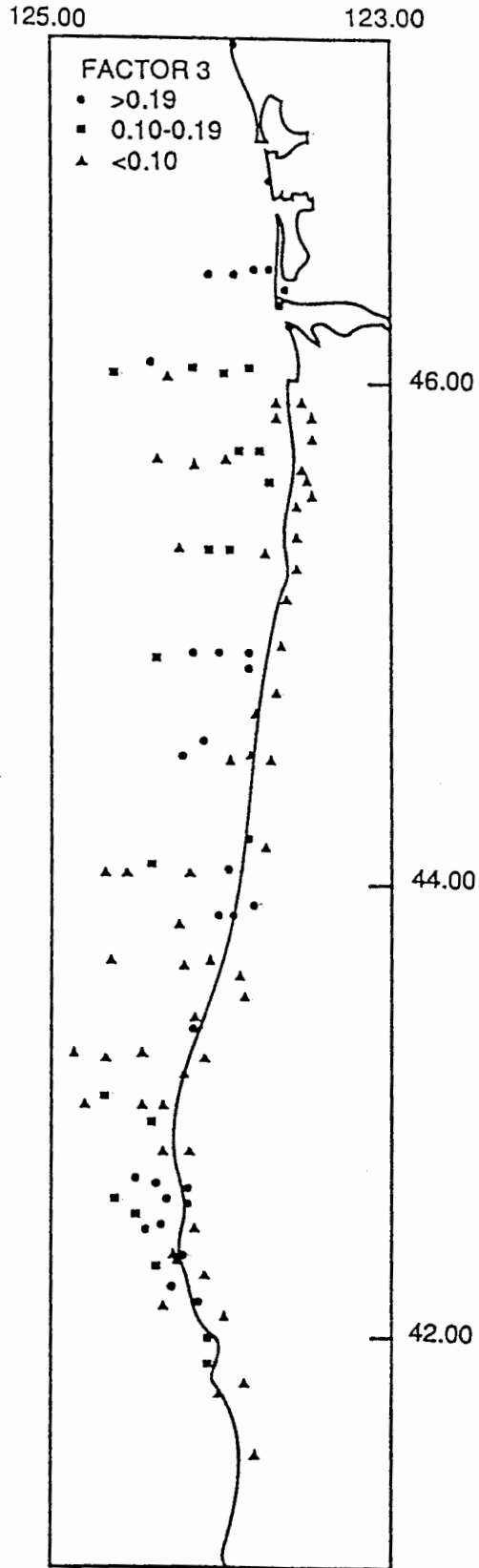
APPENDIX C

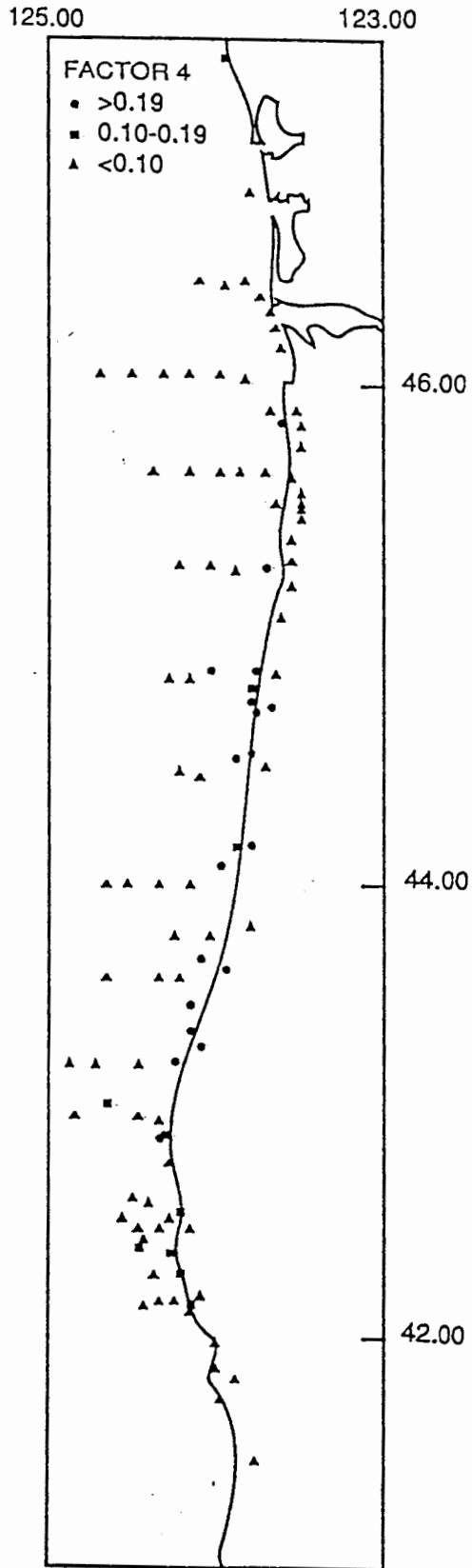
CONTOUR MAPS



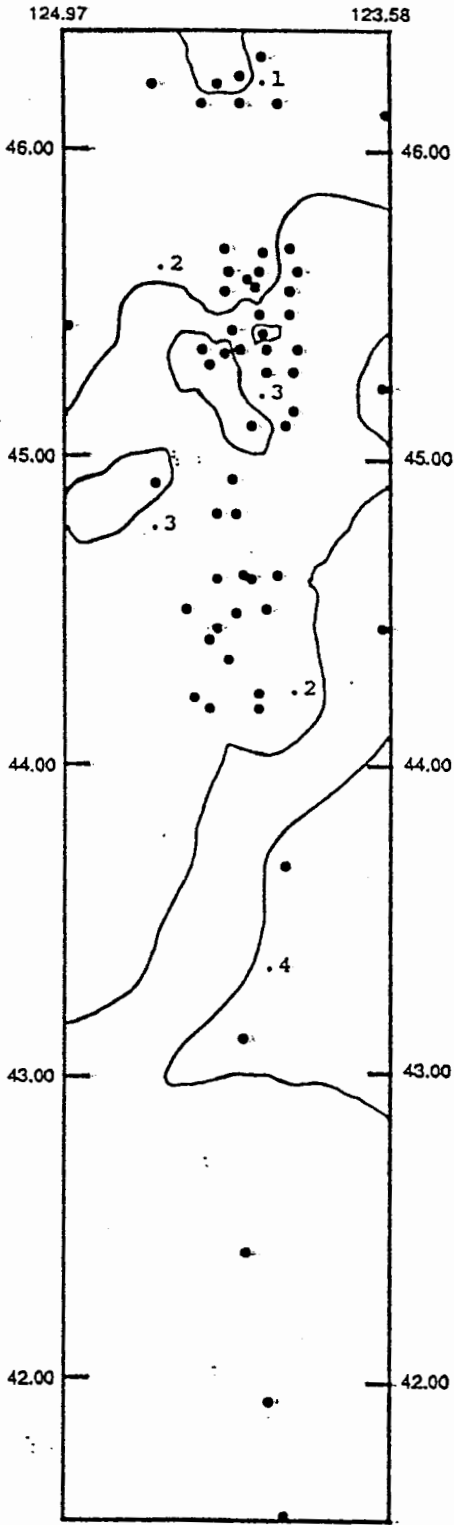
NON-OPAQUE HEAVY MINERAL ANALYSIS (SCHEIDEGGER ET AL., 1971)





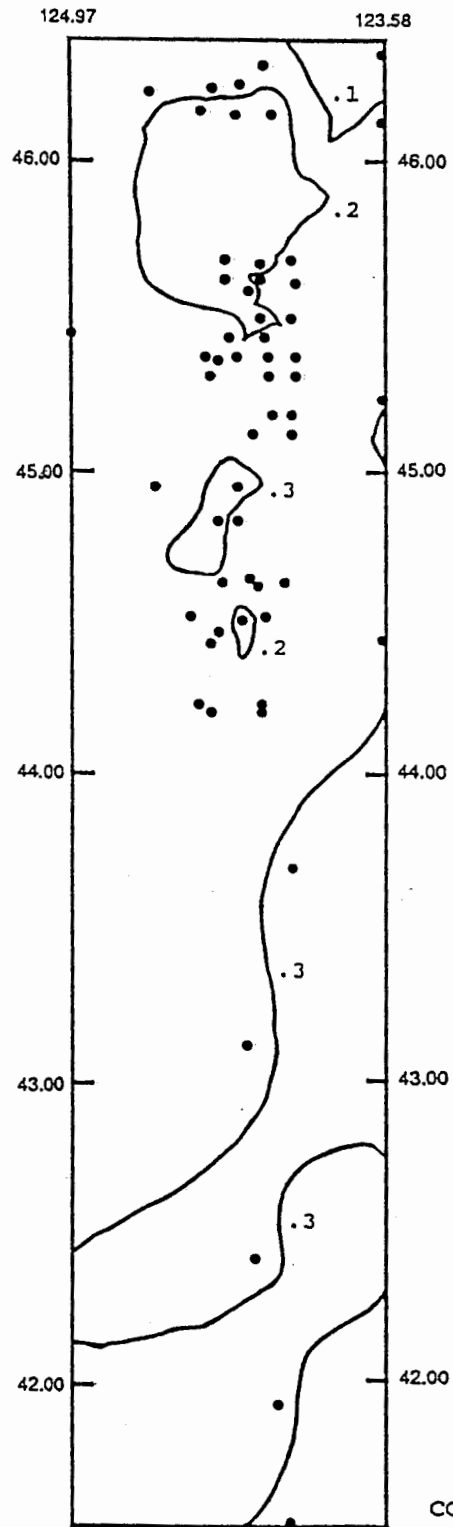


END-MEMBER ONE DISTRIBUTION (G. K. SWILLEY, 1986)

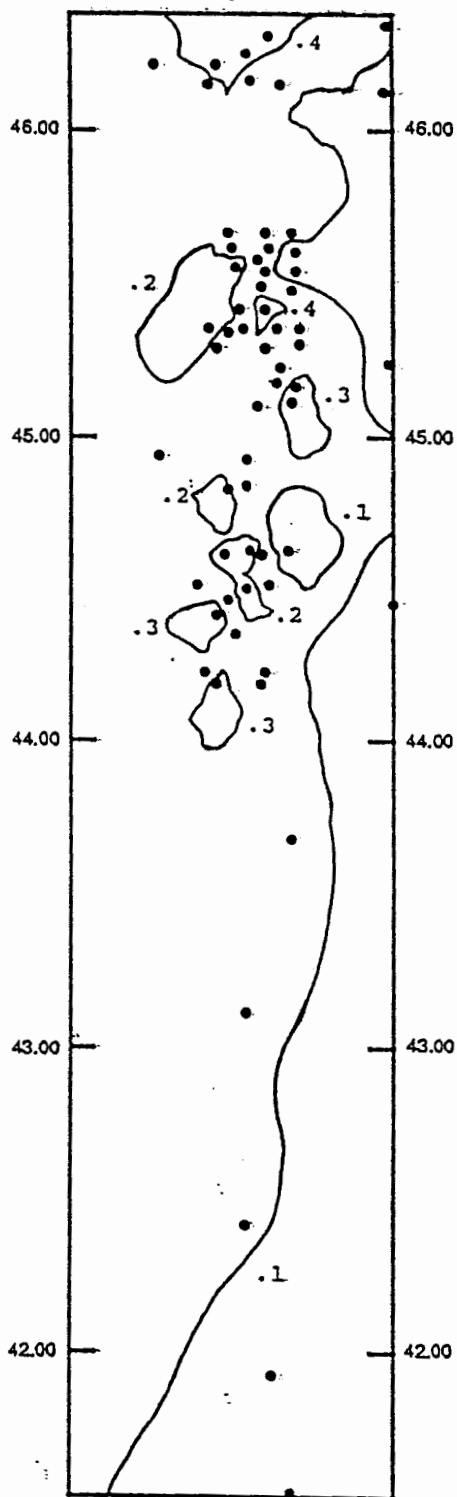


CONTOUR INTERVAL .1

END-MEMBER TWO DISTRIBUTION (G. K. SWILLEY, 1986)

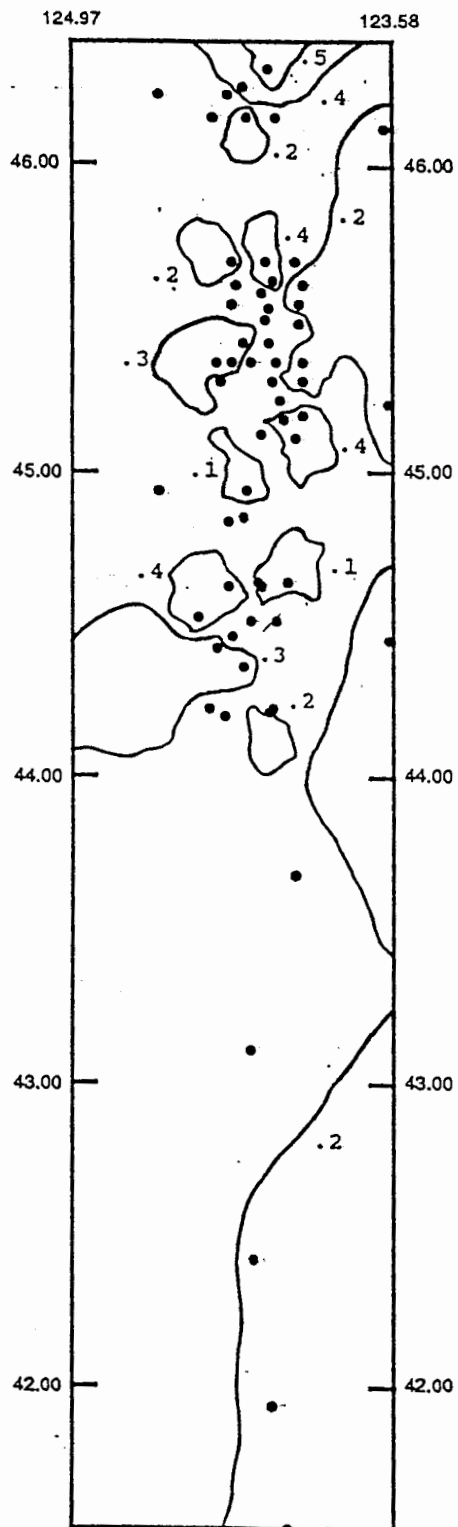


END-MEMBER THREE DISTRIBUTION (G. K. SWILLEY, 1986)

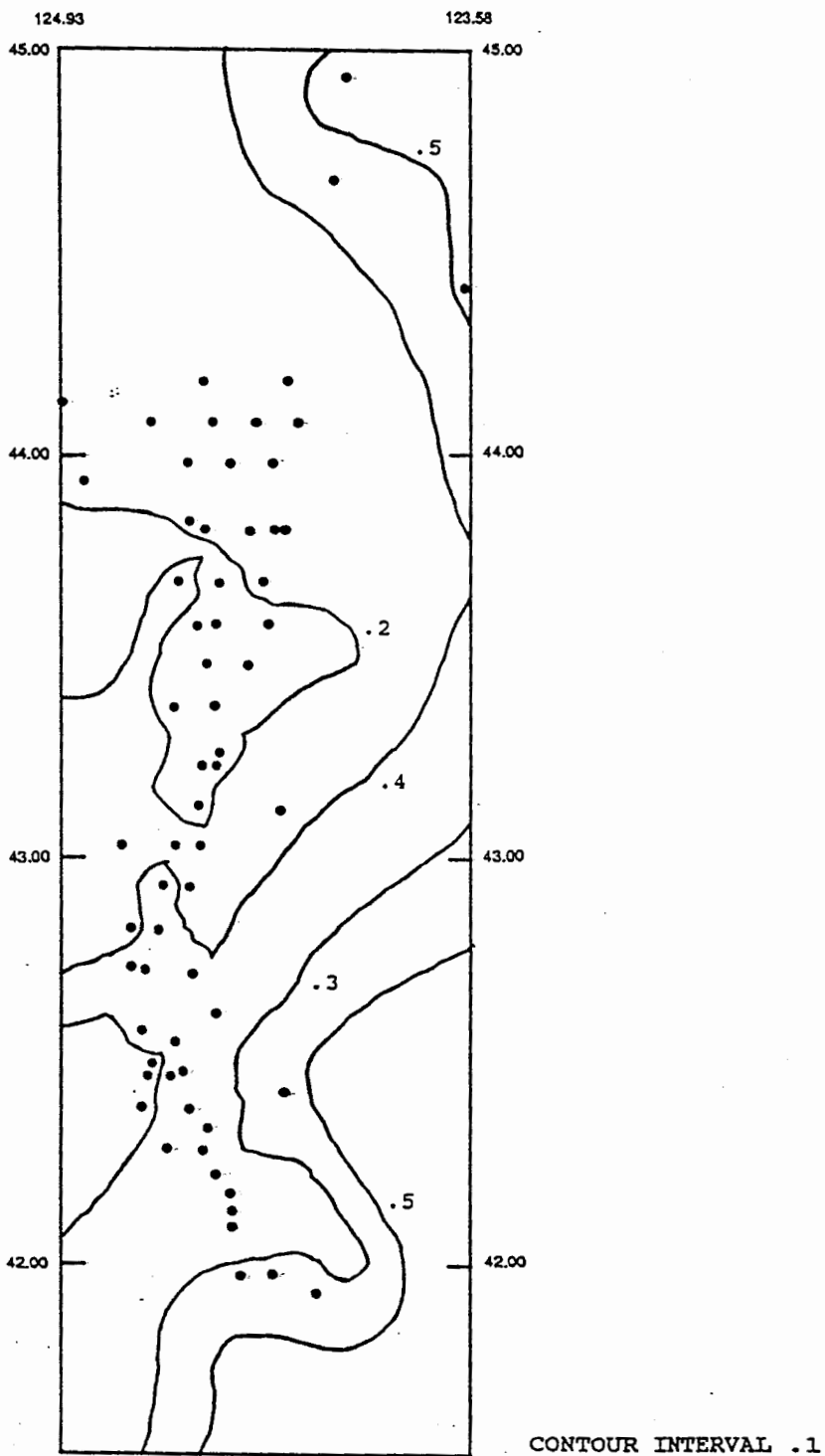


CONTOUR INTERVAL .1

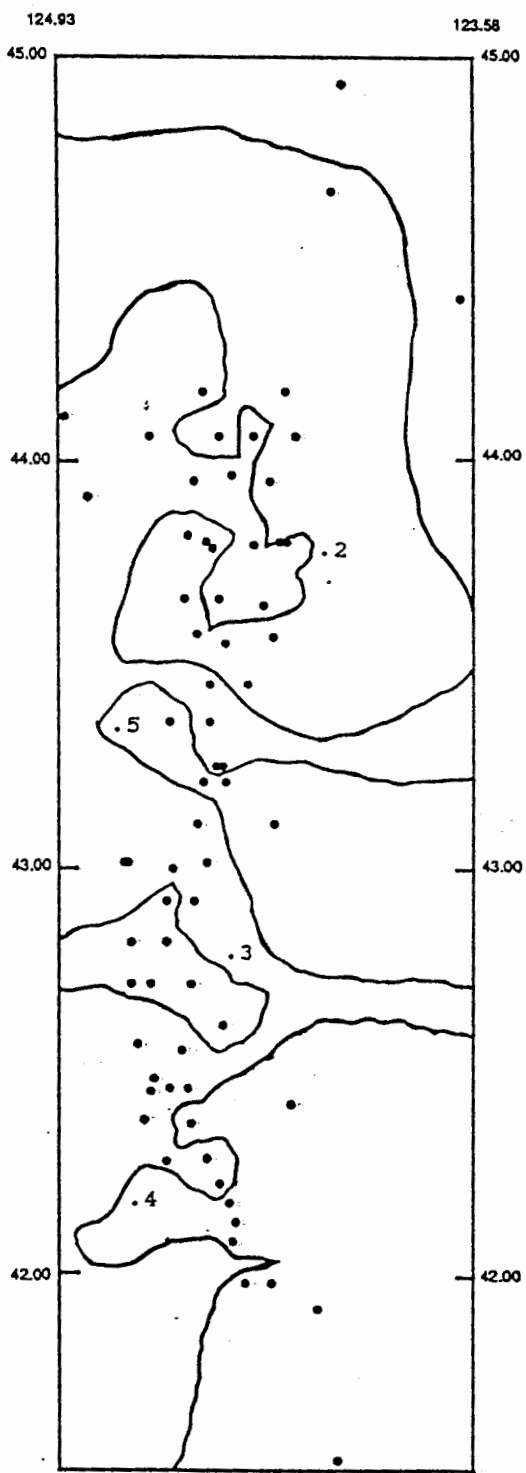
END-MEMBER FOUR DISTRIBUTION (G. K. SWILLEY, 1986)



FOURIER GRAIN-SHAPE ANALYSIS OF QUARTZ GRAINS
END-MEMBER ONE DISTRIBUTION (M. A. O'NEAL, 1986)

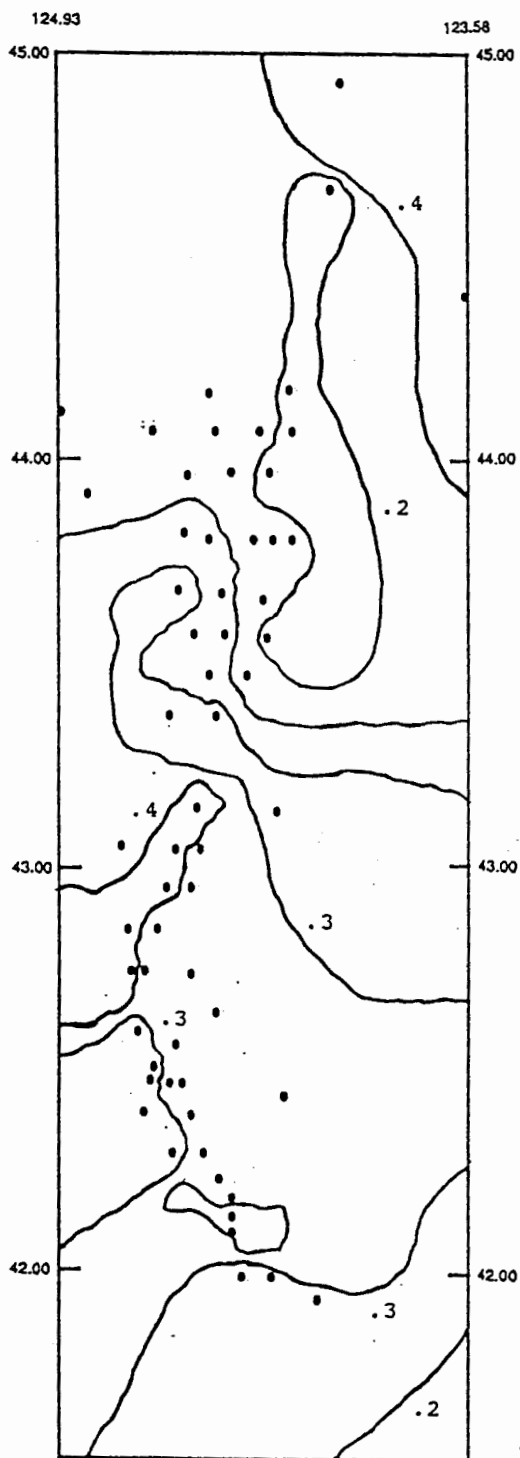


END-MEMBER TWO DISTRIBUTION (M. A. O'NEAL, 1986)



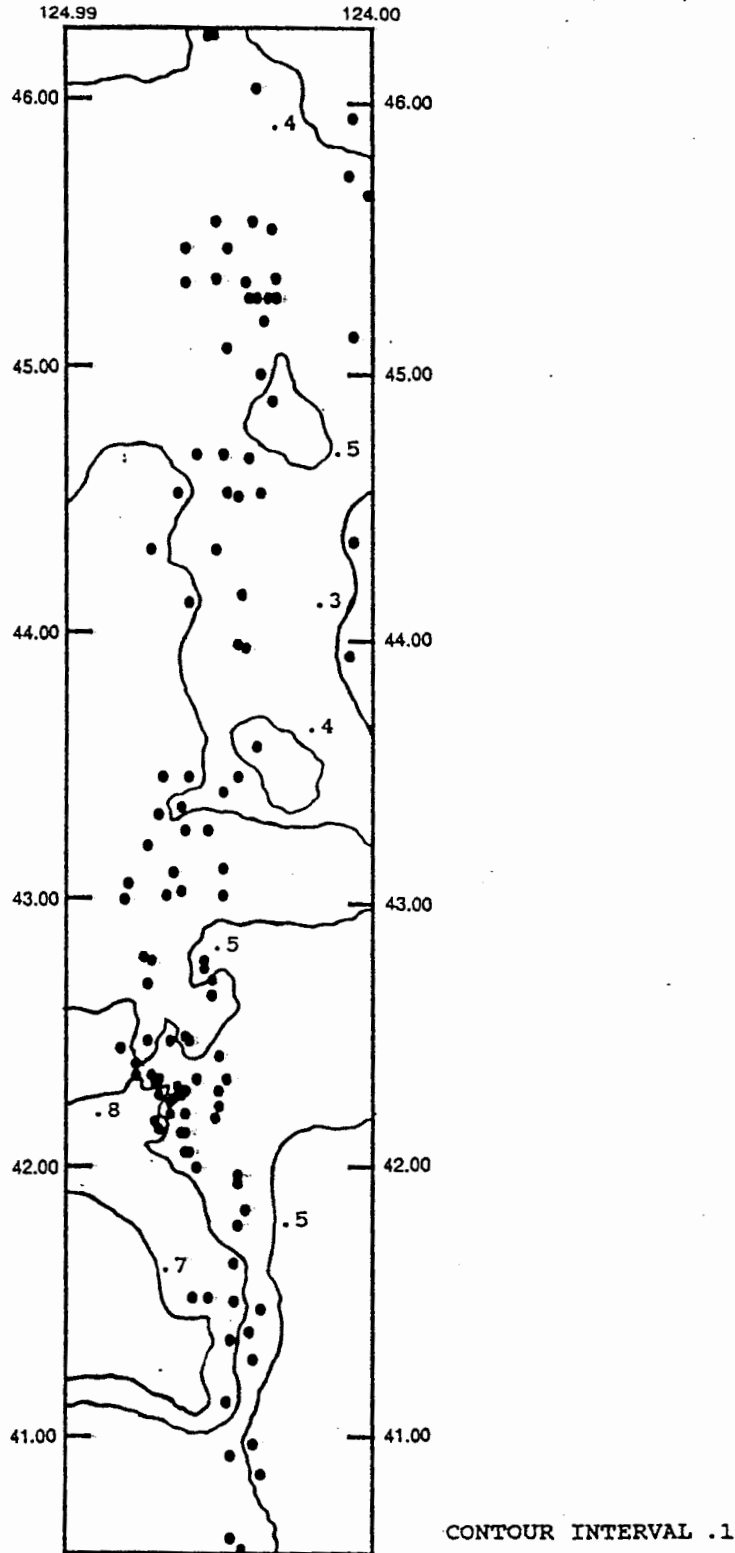
CONTOUR INTERVAL .1

END-MEMBER THREE DISTRIBUTION (M. A. O'NEAL, 1986)

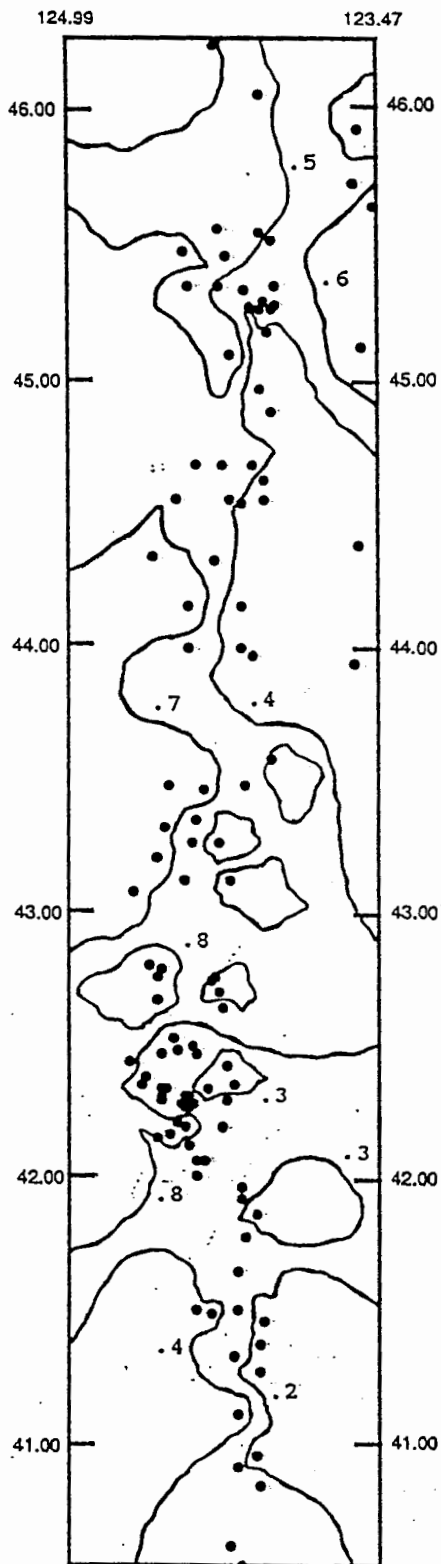


CONTOUR INTERVAL .1

SHELF-BEACH-RIVER COMBINED GEOCHEMICAL ANALYSIS OF OPAQUE OXIDES
END-MEMBER ONE DISTRIBUTION (K. S. RAVI, 1992)

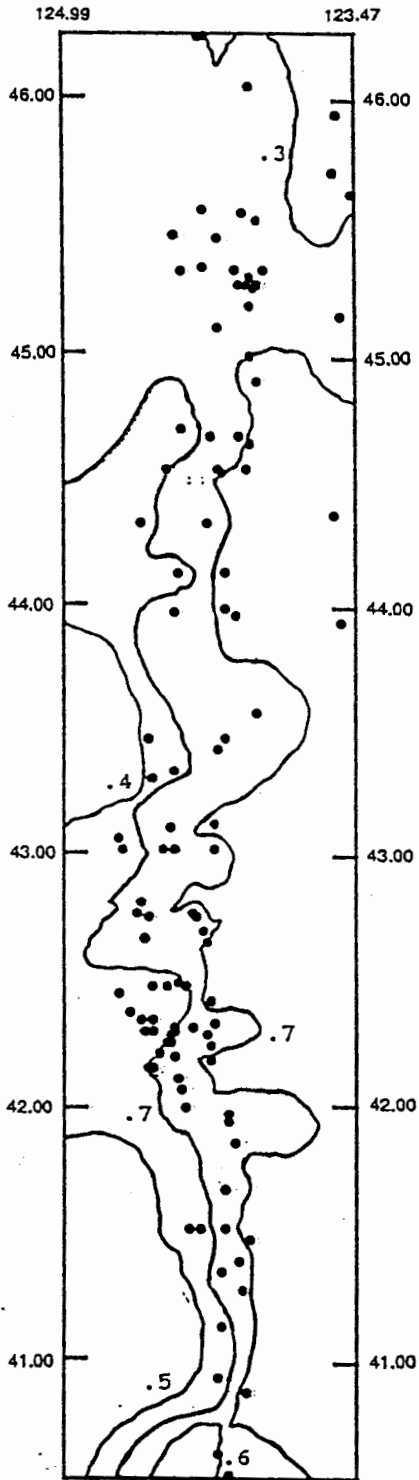


END-MEMBER TWO DISTRIBUTION (K. S. RAVI, 1992)



CONTOUR INTERVAL .1

END-MEMBER THREE DISTRIBUTION (K. S. RAVI, 1992)



CONTOUR INTERVAL .1

END-MEMBER FOUR DISTRIBUTION (K. S. RAVI, 1992)

